# Neuromuscular Analysis of Haptic Gas Pedal Feedback during Car Following

David A. Abbink

# Neuromuscular Analysis of Haptic Gas Pedal Feedback during Car Following

# **Proefschrift**

ter verkrijging van de graad van doctor aan de Technische Universiteit Delft, op gezag van de Rector Magnificus prof. dr ir J.T. Fokkema, voorzitter van het College voor Promoties, in het openbaar te verdedigen op maandag 11 december 2006 om 12:30 uur door

# David Alexander ABBINK

werktuigkundig ingenieur geboren te Purmerend, Nederland.

Dit proefschrift is goedgekeurd door de promotor:

Prof. dr F.C.T. van der Helm

Toegevoegd promotor:

Dr. ir M. Mulder

Samenstelling promotiecommissie:

Rector Magnificus, Technische Universiteit Delft, voorzitter Prof. dr F.C.T. van der Helm, Technische Universiteit Delft, promotor

Dr. ir M. Mulder, Technische Universiteit Delft, toegevoegd promotor

Prof. dr ir M.H.G. Verhaegen,
Prof. dr ir M. Steinbuch,
Prof. dr ir J.S.A.M. Wismans,
Prof. dr ir J.A. Mulder,
Technische Universiteit Eindhoven
Technische Universiteit Eindhoven
Technische Universiteit Delft

Dr. ir E.R. Boer, LUEBEC

Prof. dr ir H.G. Stassen, Technische Universiteit Delft, reservelid

The research described in this thesis has been made possible by the financial and scientific support of Nissan Motor Company and LUEBEC.

Title: Neuromuscular Analysis of Haptic Gas Pedal Feedback during Car Following

Author: David A. Abbink Cover Design: Balázs Huszthy

Print Optima Grafische Communicatie

Copyright 2006, D.A. Abbink, Delft, The Netherlands

All rights reserved. No part of this book may be reproduced by any means, or transmitted without the written permission of the author. Any use or application of data, methods and/or results etc., occurring in this report will be at the user's own risk.

ISBN-10: 90-8559-253-4 ISBN-13: 978-90-8559-253-2

# **Contents in brief**

1	Introduction	1
2	The Motivation for a Continuous Haptic Driver Support System	17
3	Force Perception Measurements at the Foot	33
4	<b>EMG Measurements of Lower Leg Muscles during Isometric Gas Pedal Manipulation</b>	41
5	Measuring the Effects of Haptic Feedback on Neuromuscular Control and Car-Following Behaviour.	53
6	Modeling the Effects of Haptic Feedback on Neuromuscular Control and Car-Following Behaviour.	73
7	Do Gas Pedal Feedback Torques Influence Driver's Response to a Braking Lead Vehicle?	95
R	General Discussion of the Results	111

# **Contents**

Co	onten	ts in brief	iii	
C	onten	ts	v	
1	Intro	oduction		
	1.1	The Price of Mobility	2	
	1.2	Improving Driving Safety and Comfort	2	
		1.2.1 Driving Tasks	3	
		1.2.2 Advanced Driver Assistance Systems	3	
	1.3	The Nissan Haptic Driver Support System Project	5	
		1.3.1 Architecture of the Nissan Haptic Driver Support System	6	
		1.3.2 Research Challenges	7	
	1.4	A brief introduction to Human Motion Control	9	
		1.4.1 The Central Nervous System (Controller)	9	
		1.4.2 Muscles (Actuators)	10	
		1.4.3 Proprioceptors (Sensors)	10	
		1.4.4 Measuring neuromuscular dynamics	12	
		1.4.5 Implications for haptic feedback	13	
		Goal of the thesis	13	
		Research Approach	14	
	1.7	Thesis Outline	15	
2		Motivation for a Continuous Haptic Driver Support System	17	
		Introduction	18	
		Car following	18	
	2.3	Existing Driver Assistance Systems	21	
		2.3.1 ADAS that automate longitudinal tasks	21	
		2.3.2 ADAS that support longitudinal tasks	23	
	2.4	· ····································	24	
		2.4.1 Available Sensory Channels	26	
		2.4.2 Continuous Haptic Feedback on Gas Pedal	26	
		2.4.3 Expected Benefits	27	
	2.5	Discussion	28	
		2.5.1 Properties of the Haptic Feedback	28	
		2.5.2 Future Applications	30	
	2.6	Conclusions	30	

3	Ford		ception Measurements at the Foot	33
	3.1	Introd	uction	34
	3.2	Metho	od	34
		3.2.1	Subjects	34
		3.2.2	Apparatus	35
			Signals	35
		3.2.4	Task Instruction	36
		3.2.5	Analysis	36
	3.3	Resul		37
		3.3.1	Effect of Force Amplitude	38
		3.3.2	Effect of Frequency	39
		3.3.3	Effect of Footwear	39
	3.4	Discu	ssion	39
			Inter-Subject Variability	39
		3.4.2	Effect of frequency and footwear	40
	3.5	Concl	usions	40
4			surements of Lower Leg Muscles during Isometric Gas Pedal N	
	•	ılation		41
		Introd		42
	4.2	Metho		43
			Subjects	43
			Experimental Setup	43
			Measured Signals	43
			Experiment description	45
			Analysis	45
	_	Resul		46
	4.4	Discu		49
			Implications for gas pedal use and design	49
	4.5	Concl	usions	51
5		_	the Effects of Haptic Feedback on Neuromuscular Control a	
			ving Behaviour.	53
	-	Introd		54
	5.2	Metho		56
			Subjects	56
			Apparatus	56
			Experiment Protocol	57
			Data Analysis	61
	5.3	Resul		64
		5.3.1	FRFs of the Admittance	65
		5.3.2	FRFs of $H_{control}$	67
		5.3.3	Time Domain Analysis	67
	5.4	Discu		68
		5.4.1	Effect of DSS on Car Following	69

		5.4.2	Effect of DSS on Admittance	70		
	5.5	Concl	usions	72		
6	Mod	leling t	he Effects of Haptic Feedback on Neuromuscular Control an	d		
	Car-		ing Behaviour.	73		
	6.1	Introd	uction	74		
	6.2	Metho	d	76		
			Summary of Used Data	77		
			Admittance Parameterization	77		
		6.2.3	Visual Controller Parameterization	83		
	6.3	Result		84		
		6.3.1	NMS parameters	84		
		6.3.2	Visual Parameters	85		
		6.3.3	Total Driver Model Validation	89		
	6.4	Discus		90		
			NMS model structure and parameter fit procedure	90		
			Effects of the haptic DSS on car-following behaviour	91		
			Model Assumptions	92		
	6.5	Concl	usions	93		
7	Do Gas Pedal Feedback Torques Influence Driver's Response to a Braking					
	Lea	d Vehic	cle?	95		
		Introd		96		
	7.2	Metho		97		
			Subjects and Setup	97		
			Experiment Protocol	97		
			Signals	99		
			Analysis	100		
	7.3	Result		102		
			Transient Perturbations	102		
			Continuous Perturbations	104		
	7.4	Discus		106		
			Transient Response	106		
			Continuous Response	107		
	7.5	Concl	usions	108		
8	Gen		scussion of the Results	111		
	8.1	Introd		112		
	8.2		s and Conclusions	113		
		8.2.1	Driver's physical control effort decreases when the DSS is active Driver's car-following performance increases or remains similar	113		
		8.2.2	with the DSS	114		
		8.2.3	Haptic feedback can temporarily replace visual feedback	115		
		8.2.4	The DSS evokes a force task	116		

	8.2.5	Golgi Tendon Organ reflex is a main contributor to admittance	
		adaptation	117
	8.2.6	The DSS allows control actions to be done partly on a spinal level	117
	8.2.7	The design of the DSS is essential for the measured benefits	118
	8.2.8	Summarized Conclusions	119
8.3	Limitat	tions and Recommendations	119
	8.3.1	Analysis Limitations: Used System Identification Techniques	119
	8.3.2	Analysis Limitations: Used Experimental Conditions	119
	8.3.3	Application Limitations: Operational domain	121
	8.3.4	Recommendations: Improve Analysis Cycle	121
	8.3.5	Recommendations: Use the Analysis to Improve the DSS	122
8.4	Future	Directions	123
Refere	nces		125
Summa	ary		131
Samen	vatting		135
Dankw	oord		139
Curricu	ılum vit	tae	143

#### List of abbreviations

ADAS advanced driver assistance system

ANOVA analysis of variance
BWS binary warning system
CNS central nervous system
DSS driver support system
EMG electromyography
FFT fast Fourier transform

FRF frequency response function

FT classical force task
GL Gastrocnemius Lateralis
GM Gastrocnemius Medialis
GTO Golgi tendon organ

H driving condition with only haptic feedback

IEMG integrated rectified EMG
iTTC inverse time-to-contact
NMS neuromusculoskeletal
PT classical position task
RT classical relax task

SO Soleus

STD standard deviation
TA Tibialis Anterior
THW time headway

VAF variance accounted for

V driving condition with visual feedback

VH driving condition with visual and haptic feedback

#### Introduction

"Begin at the beginning," the king said, very gravely "and go on till you come to the end: then stop." — Lewis Carroll

Over the last decades, the increase in road mobility has stimulated both governmental organizations and the automotive industry to come up with various measures to reduce the number of traffic accidents and their impact on human lives. A fairly recent direction is that of designing intelligent systems that aim to aid drivers in the execution of their driving tasks.

In spring 2002 Nissan Motor Company initiated a three-year research project, with the goal to design and evaluate a driver support system based on continuous haptic feedback. The system was designed to support the car-following task on highways, by mapping the separation to the lead vehicle to forces on the gas pedal. A thorough understanding of the neuromuscular properties of the ankle-foot complex while manipulating the gas pedal is important, which is why the BioMechanical Engineering department of Delft University of Technology was asked to participate.

The thesis presents the contributions made to the design and evaluation of a successful prototype, which are based on neuromuscular experiments and modeling.

Besides explaining the relevance of this work, the proposed driver support system is explained, and a short introduction on human motion control is given. The last sections describe the goal, research approach and outline of the thesis.

# 1.1 The Price of Mobility

They're funny things, Accidents. You never have them till you're having them. – Eeyore

The crash of Nicolas-Joseph Cugnot's steam-powered automobile into a brick wall marked the first automobile accident in 1771. Almost a century later, in Ireland, the first automobile fatality was reported. During the 20th century, with the development of the internal combustion engine, vehicle mass-production and an exponential increase in the need for mobility, cars have become indispensable, and accidents seemingly inevitable. Today, approximately 1.4 million road accidents<sup>1</sup> occur every year in Europe alone, leaving 1.7 million people injured, and 40 thousand people killed (Commission of European Communities, 2001). When expressed in monetary terms the direct and indirect costs of all road accidents in Europe have been estimated at 160 billion euro. Although there have been many improvements in traffic safety (in the last 30 years traffic volume has tripled, while road deaths have halved), the price of our mobility is still very high.

# 1.2 Improving Driving Safety and Comfort

The best car safety device is a rear-view mirror with a cop in it. – Dudley Moore (actor, musician)

Governmental organizations continuously aim to improve driving safety by a variety of measures: improvements in road infrastructure, encouraging drivers to drive more responsibly through campaigns and legislation (use seat belts, don't speed, don't drink and drive, don't use cellphones), and by stimulating the development of safer vehicles. Over the past years, the automotive industry has invented many systems that improve car safety. In the past, the main direction of innovation has been 'passive vehicle safety' systems, which aim to reduce the effect of a collision for all those involved. Safety belts, crumple zones, cage constructions and airbags all have substantially contributed to increased passive safety. Another way to improve safety is use 'active safety' that aim to reduce the chance of an accident occurring in the first place. Active safety systems have been designed to increase detection (brake lights and other lights) and vehicle control (anti-lock braking systems (ABS), traction control, electronic stability control).

Apart from safety issues, the automotive industry always has to consider the customer's comfort and driving pleasure. Sound systems, cell phones, on-board navigation and even entertainment systems have become increasingly more common. In some cases such systems do not only provide comfort or pleasure to drivers, but may also distract them from their primary task: interacting safely with the road and other road users (Srinivasan and Jovanis, 1997). Driver inattention is one of the main causes of traffic accidents (Knipling et al., 1993), and recent research has focused on a new class

<sup>&</sup>lt;sup>1</sup>Counting only the accidents involving human injury

of systems usually called Advanced Driver Assistance Systems (ADAS), which aim to comfortably aid the drivers in their driving tasks.

#### 1.2.1 Driving Tasks

In order to understand when drivers can benefit from ADAS, it is helpful to analyze the tasks that drivers need to perform to drive safely and comfortably. Several approaches to order the many driving tasks have been reported in literature (for a good overview, see Hoedemaeker, 1999), of which three are used in this thesis.

The first is a division in the direction of movement:

- Longitudinal: speed control, car following, braking and accelerating
- Lateral: lane keeping, changing lanes, curve negotiation
- · Combined: swerving, overtaking

The second is a division according to criticality, which can be defined as the time left to respond in order to avoid an unwanted situation. A coarse division could look like:

- Low criticality: speed control, lane keeping
- Medium criticality: car following, curve negotiation
- High criticality: emergency braking, regaining control of a slipping vehicle

The third – and perhaps the most well-known – approach is based on the level of cognition of the task (Michon, 1985), and decomposes driving tasks in the following three hierarchical levels:

- Strategical or navigational: route planning, desired trip time and speed
- · Tactical: interaction with traffic and road
- Operational: vehicle control through pedals and steering wheel

#### 1.2.2 Advanced Driver Assistance Systems

An ADAS can either assist drivers with their tasks by informing or aiding the driver (supporting the task) or by taking over control (automating the task). In either case the ADAS rely on sensors that detect relevant information about the vehicle, the surroundings and sometimes the driver state. Although sensor technology is a necessary part in the design of a successful ADAS, it is generally acknowledged that the main design challenges lie in human-machine interfacing. Beneficial effects of an ADAS on one driving task are often accompanied by reduced performance in another. If there is one thing that the past decades of ADAS research has shown, it's that driver behaviour is complex and therefore hard to predict (Carsten and Nilsson, 2001; Fancher and Ervin, 1998; Hoedemaeker, 1999; Lee et al., 2002).

In the past two decades several European research programs have been initiated which

have studied practical and fundamental issues of ADAS, starting with the Prometheus project in 1986, followed shortly after by DRIVE (Dedicated Road Infrastructure for Vehicle safety in Europe). One of the largest projects in the DRIVE program was the GIDS (Generic Intelligent Driver Support) project, which already explored the use of a haptic gas pedal. See Michon, 1993 for more information. More recent projects (e.g., PROSPER and TRAIL) investigated longitudinal and lateral assistance and provided a lot of insight in their impact on behavioral aspects such as adaptation and acceptance.

The research efforts of the automotive industry and governmental organizations have led to several relatively well-known examples of ADAS, of which some will be discussed briefly here. The list is far from complete, but will rather serve to illustrate some of the issues, limitations and beneficial effects associated with currently available ADAS.

**ADAS for the Navigation Task** Navigation support systems belong to a class of ADAS usually called In-Vehicle Information Systems (IVIS). They aid drivers in their route planning by providing information and suggestions. The system provides support at a non-critical, strategical level. However, literature has reported they may be a source of distraction for tactical and operational tasks (Srinivasan and Jovanis, 1997).

**ADAS** for the Speed Control Task Cruise Control is one of the best known ADAS, and is widely available on the market through a variety of car manufacturers. Cruise Control automates the vehicle's speed control, a longitudinal, non-critical task at the operational level. The system is designed to automatically maintain a constant speed, which the driver can set and overrule.

Supporting speed control (as opposed to automating it) has also been investigated in a number of projects. In the GIDS project a continuous counter-force was applied to the gas pedal, proportional to the deviation from a target speed, reducing the speed errors compared with unsupported driving or feedback through other modalities (Godthelp and Schumann, 1993; Verwey et al., 1993).

In the PROSPER project a gas pedal was developed that produces a counter force *and* reduces fuel injection into the engine whenever the driver exceeds a certain speed limit. Prototypes were evaluated on a large scale on Swedish roads and studied with respect to speed, traffic safety, driver behaviour and acceptance. The variance of speed decreased (Hjälmdahl et al., 2002) which was hypothesized to positively impact traffic safety (Várhelyi, 2002).

**ADAS** for the Car-following Task Assisting free speed control may have a positive effect on traffic flow, but it will not assist in the interaction with other road users. To that effect, ADAS's have been developed that measure distance and relative velocity to lead vehicles with a radar, and when the separation<sup>3</sup> becomes too small either act independently (task automated by ADAS), or inform the driver to act (task supported by ADAS).

<sup>&</sup>lt;sup>2</sup>'Haptic' is derived from the Greek 'haptesthai': to touch

<sup>&</sup>lt;sup>3</sup>Separation is used in this thesis to denote either a spatial or temporal separation to a lead vehicle, without assuming the correct representation beforehand.

A well-known ADAS that automates the car-following task is the Adaptive Cruise Control (ACC), which is available on the market through several car manufacturers. It provides support at low and medium levels of criticality, by automating the operational task of longitudinal control. ACC functions as a normal Cruise Control when the road ahead is free, but when a vehicle is in front of the car, it will maintain a constant separation to it. If the separation becomes too small the ACC automatically brakes, within certain limits: when the necessary deceleration is too large, an auditory warning informs the driver to take over again. As with the Cruise Control system, drivers can provide set points and overrule the ACC. There are several limitations of using ACC, such as over-reliance on the system, reduced driver attention and problems of handing back control in case the systems operational boundaries are reached. See Hoedemaeker, 1999 for an overview of the benefits and issues associated with ACC.

Another class of ADAS is designed to *support* the longitudinal task, aiming to avoid the issues that accompany automation of the car-following task. The ADAS monitors the separation and if it exceeds a boundary value, the driver is provided with a binary warning through auditory, visual or haptic signals. Several studies on collision avoidance warning systems are available in literature (Lee et al., 2002, 2004).

Another such system has been described in literature (Janssen, 1995), where a powerful but overruleable counter-force was generated on the gas pedal whenever the time-to-contact <sup>4</sup> reached 4 seconds. Both studies mention the issues of reliability, nuisance and false alarms, and stated that near-future deployment seems unlikely.

Another haptic supporting ADAS was announced by Continental Automotive Systems on their website<sup>5</sup>. The system, still announced to appear at the end of 2005, will provide a counterforce on the gas pedal when the time headway (THW)<sup>6</sup> exceeds a certain limit, and increases the counterforce with increasing deviation from a safe THW.

So far the haptic channel has been used to provide binary support, but haptics also offer the possibility of continuous communication of separation, analogous to visual feedback. Such continuous haptic feedback could support drivers in their car-following task, while hopefully avoiding the issues associated with both automation and binary warnings. In spring 2002 Nissan Motor Company initiated an international research project to explore the possibilities of continuous haptic feedback during car following.

## 1.3 The Nissan Haptic Driver Support System Project

It is very sobering to be up in space and realize that one's safety is determined by the lowest bidder on a government contract.

- Alan Shepherd (astronaut)

The goal of Nissan's 3-year project was to design and evaluate a prototype<sup>7</sup> of a

<sup>&</sup>lt;sup>4</sup>Time-to-contact or TTC is a measure of how long it will take for two cars to collide, provided they won't change their speed

<sup>&</sup>lt;sup>5</sup>http://www.conti-online.com

<sup>&</sup>lt;sup>6</sup>Time headway is the relative distance to the lead vehicle, scaled by the own vehicle's velocity

<sup>&</sup>lt;sup>7</sup>The final system design – which should optimize the total system (low cost, low weight, optimize required

haptic driver support system (DSS). The proposed DSS keeps the driver in the direct loop and uses continuous haptic information to inform the driver about separation to the lead vehicle. The system is aimed to support the driver with car following on highways (an operational and tactical longitudinal tasks of mainly medium criticality).

The main expected benefits are that drivers will always be in control, that during short periods of visual inattention they will still be aware of the separation due to the haptic feedback, and that faster responses may be possible because spinal reflexes can be used to react. Expected challenges are the correct information transfer from separation to haptics, the prevention of nuisance and fatigue, and understanding how the system influences driving behaviour.

In order to address the many research questions associated with the project, Nissan Research Center (NRC) cooperated with the Delft University of Technology (DUT) and several universities in the United States and Canada, bringing together a team of research engineers, behavioral scientists, mathematicians and psychologists.

The project was human-centered, meaning that the capabilities, limitations and preferences of drivers were taken into account in the design process. Drivers should intuitively understand how the DSS functions and how to use its information, and the system should never be a nuisance. Before research questions are discussed in more detail, the general architecture of the proposed DSS is explained, along with information about car following.

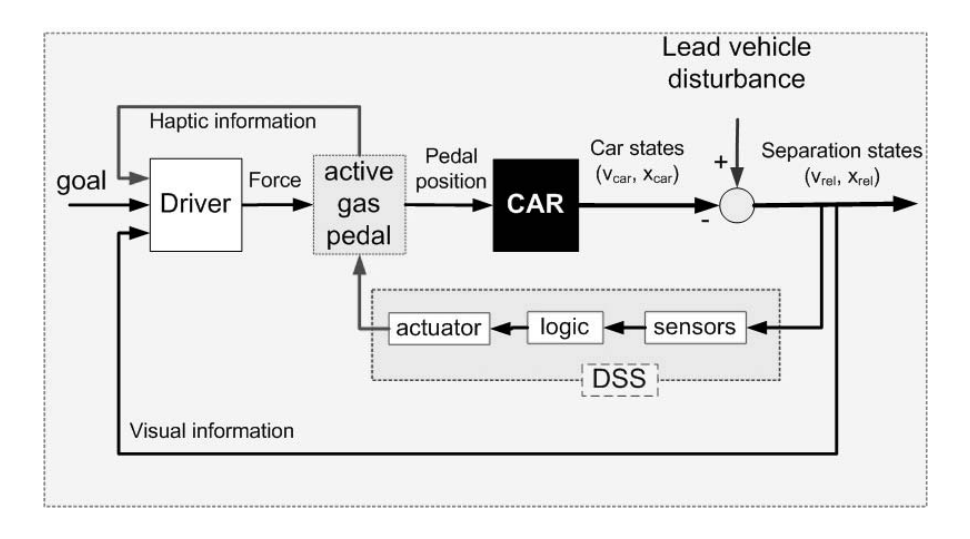
#### 1.3.1 Architecture of the Nissan Haptic Driver Support System

Figure 1.1 shows a schematic representation of a car-following situation. Control engineers will immediately recognize a closed-loop system, with the driver controlling the separation, which is perturbed by changes in the lead vehicle velocity. In this scheme, the goal of the driver is to keep the separation states (e.g., relative position  $x_{rel}$  and relative velocity  $v_{rel}$ ) at acceptable values. What is deemed acceptable may vary between drivers and within a driver: drivers are not optimal controllers (Boer, 2000), but tend to prefer a low control effort to a high performance. Moreover, many factors influence how much attention the car following receives such as the driver's goals for the trip, experience, additional tasks, and emotional state.

In order to successfully control the separation states, feedback about them is necessary. Years of driver assessment studies have not resulted in consensus on what variables the driver uses to maintain longitudinal separation, but they include relative distance, relative velocity, time-to-contact and time headway (for a good overview of the abundance of lateral and longitudinal metrics in driver assessment, see de Winter et al., accepted). Normally, feedback on the separation is available only visually, but the DSS additionally provides the driver with haptic feedback (e.g., pedal force or stiffness, and the pedal position). Simply put, when the separation to a lead vehicle changes, the driver cannot only see it, but also feel it. Note that the authority for longitudinal control actions always remains with the driver.

There are three essential technical components that allow the DSS to provide meaning-

space in a variety of vehicles) – was out of the scope of the project.



**Figure 1.1:** Simplified control-theoretic representation of a driver following a lead vehicle, while being aided by a haptic driver support system (DSS). The driver receives visual and haptic feedback of the separation to the lead vehicle and – if deemed necessary – can change the car's speed by releasing or depressing the gas pedal.

ful haptic feedback (see Figure 1.1). The first component contains the sensor system, which should capture the separation states accurately and fast. The second contains the control logic, which describes the translation from separation states to continuous haptic information. The third is an actuator, which realizes the required changes in gas pedal force or stiffness, that are in addition to those resulting from the normal dynamics of a passive gas pedal (a pre-loaded spring).

## 1.3.2 Research Challenges

The project presented the research team with many challenges, which are shown schematically in Figure 1.2. The three most important research areas are discussed in the following section. Note that the research areas will interact in a good design process: fundamental analysis is needed to base a first design on, which after evaluation will result in new knowledge in each area.

#### **Prototype Design Challenges**

The design of a prototype of haptic feedback system can be separated in several challenges. First of all it needs to be decided what variables are relevant to be communicated haptically, called the DSS logic. An abundance of metrics can be uses, such as relative distance, relative velocity, time headway (THW) or time-to-contact (TTC). A wrong mapping will lead to an unrealistic representation of the changes in the separation state, and will cause a mismatch between visual and haptic feedback. The choice of the cor-

rect (combination of) variables, and the formula to describe their relation to a hazard level formed an important part of the research done at DUT. This design challenge was mainly investigated by Mark Mulder (Mulder, 2007). The final mapping described in that thesis was used in the experiments contained in this thesis, and will described in Chapter 2 in more detail.

Second, the characteristics of the haptic information need to be determined. How large must the forces be? When forces are too large, they are likely to cause fatigue and nuisance; if they are too small, they will not be perceived. The haptic signals do not have to be only forces, pedal stiffness or damping could perhaps be used as well. The optimal haptic characteristics are determined by a variety of factors, including perception limits, transfered information, comfort, fatigue and – perhaps most importantly – the neuromuscular dynamics of the driver's foot interacting with the gas pedal. Finally, for a real-life prototype, choices for the actuator needed to be made, and new sensor technology needed to be developed, which was done by Nissan Research Center and an American university. Other universities could assume that the inaccuracies and time delays of the developed sensor system were negligible, which is therefore also assumed in the rest of this thesis.

#### **Prototype Evaluation Challenges**

The designed DSS prototype should be evaluated experimentally, to quantify the actual effect on driver behaviour. One of the main challenges is to determine correct metrics for car-following performance and control effort, and to understand how these metrics interact and what factors influence them. Another challenge is to devise an experimental design that allows data analysis, while still provoking realistic driving behaviour. These challenges were addressed and culminated in a driving simulator evaluation for the final DSS prototype, which is presented in the last chapters of this thesis.

However, a more thorough evaluation is necessary that addresses known human factor issues like behavorial adaptation, driver distraction, response to system failure, driver acceptance and opinion of the system. This was done by other project partners.

#### **Fundamental Analysis Challenges**

As stated earlier, possible problems of a sub-optimal haptic DSS design could include nuisance, fatigue, or undesirable reflexive response to the haptic feedback. Therefor it is vital to understand its effect on the driver's neuromuscular dynamics (perception and motion control). To this end a thorough analysis of neuromuscular properties was done at DUT, most of which is described in this thesis. The analysis consisted of theory, experiments and modeling, and addressed areas of perception, muscle use and adaptation during the haptic feedback.

In order to understand the biomechanical topics in this thesis a brief introduction to human motion control will be given. More detailed information is widely available in literature (e.g. Kandel et al., 2000).

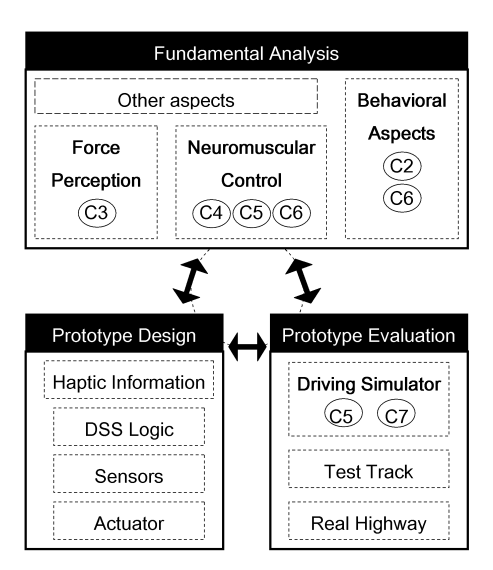


**Figure 1.2:** Schematic overview of the three main research areas of the project: fundamental theory, prototype design and prototype evaluation. New knowledge obtained in one of the areas will impact the other areas, shown by the arrows. C2-C7 denote the chapters contained in this thesis, showing in which research area they contributed to the project.

#### 1.4 A brief introduction to Human Motion Control

You cut up a thing that's alive and beautiful to find out how it's alive and why it's beautiful, and before you know it, it's neither of those things...

Clive Barker (writer, painter)

Humans are able to physically interact with their surroundings and move around in them in an efficient way. The human motion control system is highly complex and adaptable, but its essentials can be likened to those of a robot: a linkage (skeleton), actuators (muscles), a sensor system (proprioceptors) and a controller (the central nervous system (CNS)) which is connected to the actuators and sensors by wires (nerves).

## 1.4.1 The Central Nervous System (Controller)

The CNS consists of the brain and the spinal cord. It receives and integrates the feed-back from the proprioceptive sensors with feedback from other sensors (e.g., vision) and feed-forward control (planned movements). The CNS can send a neural command to the muscles to contract or relax. Neural commands travel along afferent<sup>8</sup> and effer-

<sup>&</sup>lt;sup>8</sup>Afferent: traveling towards the CNS

ent<sup>9</sup> nerves via electrochemical processes. The traveled distance is one of the factors that influence the transport time delays.

#### 1.4.2 Muscles (Actuators)

Muscles generate force, which is exerted on the skeleton through the tendon that connects them to it. A muscle consists of several thousand motor units: each of which constituting a set of parallel muscle fibres commanded by a single  $\alpha$ -motoneuron. The neuron is a gathering point of neural commands from the brain and other parts of the CNS, and is located in the spinal cord. A command from an  $\alpha$ -motoneuron causes many muscle fibers to generate muscle force, which results in measurable electrical activity. Electromyography (EMG) is based on this phenomenon. The dynamics of muscle activation have been widely studied and are usually described by a first or second order process.

An important property of muscles is that the generated force does not only depend on the activation level, but also on muscle length and stretch velocity. The so-called force-length and force-velocity relations can be simplified to stiffness and viscosity during linearized conditions (i.e., relatively small changes around an operating point).

A higher level of muscle activation increases the muscle stiffness and viscosity. This phenomenon explains why muscle co-contraction is an effective way to stabilize a joint: although there is no change in the resulting torque around the joint, the increased activation of the muscles have caused them to become more stiff and viscous, thereby increasing the joint's instantaneous resistance to perturbations.

## 1.4.3 Proprioceptors (Sensors)

When your eyes are closed, you are still aware of the movements and spatial orientation of your body. This ability arises from sensory organs within the body, called proprioceptors. They include the vestibular system, joint sensors, skin receptors, muscle spindles and Golgi tendon organs.

The vestibular system is located in the middle ear and gives information about the orientation and acceleration of the head. Its response can be neglected when accelerations are small, which is the case during the relatively smooth car-following studied in this project.

Joint (or capsule) sensors sense the position of joints, and skin receptors (or tactile sensors) are sensitive to touch, pressure, vibrations, temperature and pain. Both types of sensors send the information to higher levels of the CNS.

Muscle spindles and Golgi Tendon Organs (GTOs) provide information about forces and positions of the muscles. The information is sent to higher levels of the CNS, but also straight back to the  $\alpha$ -motoneuron, forming a fast feedback loop. These feedback loops are called spinal reflexes. Compared to feedback from other sensors, spinal reflexes allow for substantially faster contributions to motion control. Compared to muscle co-contraction, reflexive feedback is an energy-efficient way to respond to perturbations,

<sup>&</sup>lt;sup>9</sup>Efferent: originating from the CNS

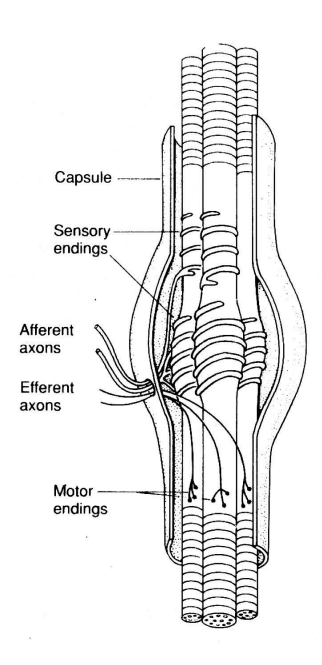


Figure 1.3: Physiology of a muscle spindle, see text for details (adapted from Kandel et al., 2000).

although the inherent neural transport delays limit the frequency-bandwidth of effective response.

Since muscle spindles and GTOs are the most important proprioceptors for the current thesis, they are discussed in more detail in the following paragraphs.

**Muscle spindles** Muscle spindles are small sensory receptors within the muscle, positioned parallel to the muscle fibres. When the muscle stretches, the muscle spindle stretches as well and fires, sending information back to the CNS and the  $\alpha$ -motoneuron through two types of afferent neurons (the so-called Ia and II endings). Ia endings are most sensitive to muscle stretch velocity and II endings to muscle stretch. The sensitivity of the afferents can be adapted independently by the CNS through efferent  $\gamma$ -motoneurons.

Essentially, the muscle spindle reflex acts as a position and velocity feedback loop, of which the feedback gains can be adapted. The muscle spindle reflex has been widely studied, and is generally thought to increase the joint's dynamic resistance against forces. Recent studies showed that the gain of the reflex loop can also shift sign (De Vlugt, 2004; Schouten, 2004), meaning that the muscle spindle gains then do not excite the  $\alpha$ -motoneuron, but inhibit it, resulting in decreased resistance (less stiff).

**Golgi tendon organs** GTOs are located where the muscle is attached to the tendon, and have one single afferent neuron (lb). The afferent ending diverges into many end-

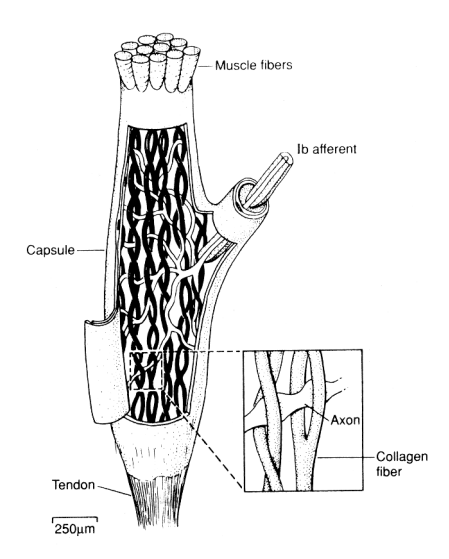


**Figure 1.4:** Physiology of a Golgi tendon organ, see text for details. (Adapted from Kandel et al., 2000)

ings (see Figure 1.4), that are squeezed when the GTO is stretched, causing them to send a signal to the CNS. The stretch of a GTO depends linearly on the force in the tendon (and the muscle). Unlike muscle spindles, there are no efferents that directly influence the sensitivity, but other processes of adaptation have been shown, which will not be explained here for reasons of brevity.

Essentially, the GTO reflex acts as a force feedback loop, and may contribute substantially to human motion control. Surprisingly, much less literature is available about the functionality and adaptability of GTO reflexes, and in many movement studies they are neglected. Usually GTOs are assumed to have an inhibitory effect on muscle activation, making the force feedback reflex a mechanism to reduce the dynamic resistance against forces. Theoretical studies have argued that the gains of the GTO reflex can be adapted and even shift sign (Prochaska et al., 1997a), meaning that the GTO gains then do not inhibit but excite the  $\alpha$ -motoneuron, resulting in increased resistance (more stiff).

During interaction with the haptic DSS, the force feedback functionality of the GTO reflex is expected to play an important role.

#### 1.4.4 Measuring neuromuscular dynamics

The neuromuscular mechanisms described in the previous section all act together during motion control, showing a combined behaviour that has elastic, viscous and inertial properties. Many experimental studies (Abbink et al., 2004a; De Vlugt, 2004; Schouten, 2004), have shown that these properties can be adapted through changes in muscle co-contraction and reflexive activity. A relatively common method of describing neuro-

muscular dynamics is by estimating the admittance, which is used throughout this thesis. Admittance is the causal, dynamic relationship between a force (input) and position (output), and can be viewed as a measure of the displacement that a force causes. It can be estimated by frequency response functions (FRFs) in response to a force perturbation, and roughly resembles a second-order system. At low frequencies the elastic properties dominate the behaviour, at high frequencies the inertia causes admittances always decreases.

#### 1.4.5 Implications for haptic feedback

How does all this affect the design of a haptic feedback system? The literature indicates that human response to forces is not constant, but dynamic and subject to adaptation as a result of many factors. In other words, drivers can choose (consciously or subconsciously) to either resist forces from the DSS or give way to them, which will have a great impact on the functioning of the system and on car-following behaviour in general. When drivers resist the forces, they will use their reflexes together with high levels of muscle co-contraction, which will show as a small admittance. Obviously this situation is not wanted: it is a sign that drivers do not understand or trust the haptic feedback, and will be accompanied by fatigue and nuisance. Ideally, drivers should adopt the highest admittance possible, which means that a feedback force results in a large pedal displacement, and that drivers immediately follow the suggestions of the DSS. It is hypothesized that optimal haptic feedback will cause drivers to minimize muscle co-contractions (which would increase stiffness and cause fatigue) but instead make maximal use of their spinal reflexes (which will help to give way to the forces faster than by a conscious reaction).

#### 1.5 Goal of the thesis

The goal of this thesis is to perform an analysis of the impact of continuous haptic gas pedal feedback on driver behaviour during car-following, both at the level of car-following behaviour and at the level of neuromuscular motion control behaviour.

In order to understand the motion control behaviour of the foot during gas pedal manipulations, research must be done on force perception, muscle use, the dynamic response to forces, and how reflexes, muscle co-contraction and planned movements act together to realize that response.

The analysis is aimed to provide theoretical, experimental and modeling knowledge of driver behaviour when using a haptic DSS prototype. This knowledge should help in the actual design of that prototype, but should also be valid to assist in possible further improvements of the design.

## 1.6 Research Approach

To accomplish the goal, this thesis follows a research approach based on DUT's expertise in cybernetics<sup>10</sup> and neuromuscular modeling and experimenting.

Why use a cybernetic approach? Car following constitutes a closed-loop system: the separation states influence the driver's control actions, which in turn influence the separation states. This complicates the finding of causal relationships. Although valuable information can be gained by simply examining the separation states, understanding is missed about changes in the subsystems (such as the driver). For example, driving with the DSS might entail decreased variations in the relative distance. But what is the cause of this beneficial result: are drivers merely more concentrated now, or are their responses earlier, or are their control actions more precise? Some of this information may be gained through subjective measurements (questionnaires), but drivers may very not be conscious at all of the dynamic characteristics of their control strategies. Car-following control behaviour is an operational and skilled-based task (Rasmussen, 1983): drivers communicate with the gas pedal through signals (instead of rules or symbols), which can be hard to report subjectively, but which *can* be measured.

Cybernetic techniques use relevant measured signals, and estimate the dynamics of subsystems using closed-loop identification. For example, by relating driver inputs (e.g. relative velocity) to driver outputs (e.g. gas pedal depression) the driver control behaviour is quantified, which can be subsequently examined for changes with respect to gains, time delay and noise. The resulting mathematical models can be used not only to describe driver behaviour, but also to predict it and relate it to particular settings of the system being designed (in this case the DSS). As a result, the developed analysis can be used to optimize the DSS to a desired critertion (e.g., minimal control effort, maximal performance, maximal admittance). This optimi

**Cybernetic analysis cycle: theory, experiments, models** The cybernetic analysis is described that consists of theoretical, experimental and modeling research. Knowledge gained in each of these areas impacts the other areas, resulting in a cycle.

The theoretical knowledge is used to formulate hypotheses, make decisions about how to perform and analyze experiments, and what are the most relevant properties needed to model behaviour. Conceptual frameworks and computational models, must provide insight into the dynamics of the interacting systems (driver, DSS, car and lead vehicle). Experiments must be done to test the hypotheses and gather data to validate computational models. For that purpose a simplified driving simulator was developed and linked to a high-fidelity force-controlled actuator. The experimental results will allow for new insights and improvements in the theories and models, closing the analysis cycle, which can reiterated until satisfied.

<sup>&</sup>lt;sup>10</sup>Cybernetics describe human control behaviour with techniques derived from control theory: in terms of gains, time delays and noise.

**Design Cycle: Analysis, Design, Evaluation** After a thorough analysis of the problem, synthesis is the next step: how to use the gained knowledge to improve the actual design of the haptic DSS? The full design cycle between analysis, design and evaluation (see Figure 1.2) can be reiterated to further improved the design. In the project several versions of the DSS were tested and evaluated (Mulder et al., 2005a), ultimately resulting in the final prototype design. This prototype was used in the driving simulator studies described in this thesis.

Note that the purpose of this thesis was not to design the optimal DSS, but to develop the analysis techniques needed to do so and show they can be used to understand the resulting changes in driver behaviour.

#### 1.7 Thesis Outline

The body of this thesis can be divided into two parts. The first part (Chapters 2-4) describes fundamental theoretical and experimental studies which helped in the design of the final prototype, and also in the understanding of resulting driver behaviour with that prototype. The second part (Chapters 5-7) contains experimental and modeling studies done to evaluate of the designed prototype of the DSS, but also to understand the changes that the DSS provokes in driver behaviour on a fundamental level. See also Figure 1.2 for a graphical representation of where each chapter contributed in the overall prototype design cycle.

Except for **Chapter 1** (Introduction) and **Chapter 8** (Discussion), each chapter contains a paper that is either submitted or published, and they have been preserved in their original format. Although this allows the different chapters to be read separately, it also results in some similar elements (mainly in the introductions of some chapters).

**Chapter 2** contains a theoretical analysis of the car-following task, and advantages and disadvantages of existing car-following assistance systems (binary warning systems and ACC). It shows the motivation for an alternative ADAS design, that uses continuous haptic feedback on the gas pedal. Expected benefits and limitations are discussed.

**Chapter 3** addresses the question of what drivers can sense. It contains the results of a force perception experiment of the foot on a gas pedal. Force perception limits were determined as a function of frequency content of the applied forces, and footwear worn by the drivers.

**Chapter 4** describes how drivers use their leg muscles to realize pedal forces. It contains an experimental analysis where lower leg muscle activity was measured using EMG techniques, during several constant forces and pedal positions that could be expected during normal and haptically supported car following.

How does a designed haptic DSS influence driver behaviour? **Chapter 5** answers this question by presenting the results of a car-following experiment, where the impact of a haptic DSS on driver behaviour was measured and quantified using closed-loop system identification techniques. The driver's response to two perturbations was measured: a visual perturbation (lead vehicle speed profile) and a torque perturbation. They were

simultaneously applied in the experiment, but were separated in the frequency domain. Because of this, the admittance of the ankle-foot complex could be estimated during actual car-following behaviour. Simultaneously, the total driver's response to lead vehicle perturbations is estimated with a frequency response function. For further comparison, the admittance was estimated during so-called 'classical tasks': maintaining a fixed pedal position, maintaining a constant force, and being relaxed.

**Chapter 6** aims to model the observed changes in driver behaviour due to haptic feedback. It proposes a detailed linear driver model describing the separate contributions of visual and spinal control actions to car following. Model parameters describe, amongst others, GTO and muscle spindle feedback, muscle visco-elasticity, and a visual controller. The parameters were quantified using the experimental data described in Chapter 5. The parameterized model was validated with time-domain and frequency-domain metrics.

**Chapter 7** investigates driver behaviour outside of the operating point studied in the previous two chapters. It contains an experimental investigation of the possible negative effects of the DSS when a lead vehicle brakes hard and feedback forces mount rapidly. A sudden large feedback force might result in a stretch reflex, causing the pedal to be depressed. To investigate whether this occurs, the driver's response (pedal force and position, EMG activity) to DSS forces that arise from a hard-braking lead vehicle was measured, and analyzed with respect to possible negative effects.

Finally, **Chapter 8** discusses the main conclusions, points out the limitations of the research approach and discusses recommendations and implications for future research.

# The Motivation for a Continuous Haptic Driver Support System

David A. Abbink, Erwin R. Boer, Mark Mulder submitted to Human Factors in Ergonomics

Insisting on perfect safety is for people who don't have the balls to live in the real world.

– Mary Shafer

The last years, increased effort has been dedicated to the design of systems that assist the driver in car following. The need for assistance systems arises from the fallibility of the visual feedback loop, for example due to inattention. Existing driver assistance systems either automate the car-following task or support drivers with binary warning systems to redirect their attention when necessary.

The goal of this paper is to discuss the benefits and limitations of these systems, and to show the possibilities of an alternative design approach. To attain the goal, a theoretic analysis is presented, that views car following as a closed-loop control task that requires sufficient feedback about the separation (relative distance, relative velocity) to a lead vehicle. A task analysis helps to identify the areas where the current systems assist the driver well, and where they do not.

The new design approach aims to keep the human in the loop, by supplementing the semi-continuous visual feedback loop with an additional continuous feedback loop, namely haptic feedback applied directly at the gas pedal. Expected benefits compared to existing systems include: better situation awareness (even during periods of visual inattention) and faster responses (the haptic feedback is available directly at the gas pedal, allowing the use of fast reflexes). Several design issues are presented, such as the prevention of nuisance and fatigue, deciding which separation states the feedback is based upon, and challenges in determining the correct characteristics of the haptic signals.

It is concluded that haptic feedback on the gas pedal is a promising way of supporting drivers, although experimental human-in-the-loop studies remain necessary to study the resulting driver response.

#### 2.1 Introduction

A great deal of literature is available on automation and alerting systems (Sheridan, 1992), and both have been applied in many areas such as aviation (McRuer et al., 1971; Bill and Woods, 1994), power plant management, and medical care (Meyer and Bitan, 2002).

In the last decade, automation and support systems have also been introduced on the automotive market (Carsten and Nilsson, 2001; Hoedemaeker, 1999). They are generally called Advanced Driver Assistance Systems (ADAS), and include parking support, lateral warning systems, cruise control and adaptive cruise control (ACC). The scope of this paper is on longitudinal control, and the ADAS that aim to support the driver therein. While literature (e.g., Carsten and Nilsson, 2001; Hoedemaeker, 1999) has recognized the beneficial effects of ADAS, it has also pointed out many issues ranging from unwanted behavioral adaptation to nuisance.

**Longitudinal Control Tasks** In order to understand where and how drivers can be better assisted, it is useful to analyze the tasks needed for longitudinal control. It has been argued (Boer and Hoedemaeker, 1998) that car following takes place at the tactical and operational level (from the strategical-tactical-operational task hierarchy, Michon, 1985). Tactical tasks describe interaction with traffic, which requires some cognition (situation assessment and short-term planning). Operational tasks describe the direct vehicle control (through gas pedal and steering wheel), and involve little cognition. This task-hierarchy has been related (Hale et al., 1990) to the knowledge-rule-skill taxonomy (Rasmussen, 1983): for experienced drivers tactical tasks are rule-based, and operational tasks skill-based.

With experience, drivers develop mental models (Boer and Hoedemaeker, 1998) of the task, allowing predictions about what will occur, and what control actions are likely to be needed soon. In other words, the more experienced drivers are, the less cognition is used: control actions will be more skill-based and have a decreased response time. Another way to distinguish driving tasks, is according to their criticality, which could be related to the time left to avoid an unwanted situation. Car following is a situation of medium criticality: it can quickly escalate into a high-critical situation, especially at close following distances.

**Goal of the Study** The purpose of the present article is to analyze the benefits and limitations of current car-following ADAS with respect to the levels of cognition and criticality; and to show the opportunities and potential for an alternative design approach.

#### 2.2 Car following

Car following at its simplest can be described as following a lead vehicle at a certain distance. Lead vehicle changes in speed need to be matched in order to avoid a rearend collision, and the driver needs visual feedback to close the loop and perform well.

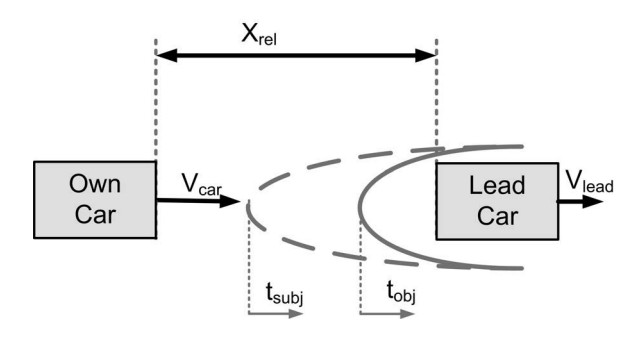


Figure 2.1: Simplified representation of a car (with speed vcar) following a lead vehicle (with speed  $v_{lead}$ ) that is slowing down.  $x_{rel}$  is the relative distance between the two vehicles.  $t_{obj}$  represents the objectively calculated last time at which the driver must brake to avoid a crash, given a certain reduction in  $v_{lead}$ . In reality, drivers will feel more comfortable reacting earlier, at a subjective  $t_{subj}$ .

Drivers display intermittent control actions to keep the separation large enough (in case the front car suddenly decelerates) but not too large (to avoid other cars cutting in).

This is illustrated in Figure 2.1, which depicts a vehicle following a lead vehicle at a certain distance  $(x_{rel})$ . The following distance will only change as a result of changes in relative velocity  $(v_{rel})$  between the two cars. By using the gas pedal and brake (operational task), the velocity of the lead vehicle can be matched: if  $v_{rel}$  is zero, no crash can occur. Because it requires a lot of control effort to match the velocity of the lead vehicle perfectly, drivers follow at a certain distance they feel comfortable with at that time. In a sense,  $x_{rel}$  acts as a buffer to absorb (unexpected) variations in lead vehicle velocity, which can be considered a tactical choice.

Car-following literature often employs an optimal-control framework and uses position and velocity metrics to describe the interaction between the lead vehicle and following vehicle (Brackstone and McDonald, 1999). However, it has been argued that drivers do not aim to optimize, but to satisfice (Boer, 2000). In other words, when a situation is acceptable, drivers will usually not spend control effort to further optimize it. Furthermore, much literature has shown that human behaviour can better be captured by so-called perceptual variables (Boer, 2000). Distance-related behaviour can be better described by the time headway  $(THW^1)$ , and velocity-related behaviour by the inverse time-tocontact  $(iTTC^2)$ .

Driver assessment studies have shown that these metrics interact (Boer, 2000; de Winter et al., accepted). For example, variations in iTTC are automatically smaller at a larger THW: the changes in lead vehicle velocity have a smaller effect at a larger separation. The previously mentioned interaction between control effort (gas pedal and brake actions) and performance (e.g., iTTC or THW) is another example of interacting metrics. The interaction complicates driver assessment, and the design of adequate support

 $<sup>{}^{1}</sup>THW = rac{x_{rel}}{v_{car}}$ , with  $x_{rel}$  the relative position, and  $v_{car}$  the own vehicle velocity  ${}^{2}iTTC = rac{v_{rel}}{x_{rel}}$ , with  $v_{rel}$  the relative velocity between the lead vehicle and own vehicle

and automation systems.

No matter what metrics one uses to describe car following, if drivers do not adequately monitor the visual cues about changes in the separation, accidents may occur. Driver inattention is the main cause (Knipling et al., 1993) of rear-end collisions: fatigue, distraction and the need for multi-tasking induce drivers to momentarily interrupt the visual feedback loop, resulting in inadequate response if a critical situation occurs.

Two other properties of car-following complicate the design of support and automation systems, perhaps even more so than for applications in aviation or process industry.

Low-critical tactical tasks During most car-following conditions, drivers need to spend little effort on the operational tasks to remain safe. Gibson recognized as early as in 1938 (Gibson and Crooks, 1938) that – rather than driving on the limits of safety – drivers maintain a larger separation with the lead vehicle. As mentioned earlier, drivers realize that they need a safety margin to absorb unexpected hazards. But what is deemed acceptable may differ from driver to driver, (and also within drivers) depending on driver needs (safety, comfort, punctuality, kick, multi-tasking) and abilities (skill, experience) (Boer and Hoedemaeker, 1998). The relatively loose traffic regulations (compared to aviation regulations) allow for these differences in tactical driving behavior.

Aggressive drivers will follow at a close separation (tail-gating) and cautious drivers will follow at a large one. Such different driving styles are echoed in many other driving characteristics (Hoedemaeker, 1999; West et al., 1992; Fancher and Ervin, 1998; Van Winsum and Heino, 1996) such as: tendency to speed, choice of THW (tailgating or not), conforming to the traffic flow, and the need for driving-related multitasking (steering, scanning for road signs) or relaxation-related multitasking (changing music/radio station, conversing, looking at scenery).

Note that following at a relatively large separation allows the driver the comfort of only using the gas pedal to maintain a safe distance (reduced control effort for a similar performance). Too large separation might result in other cars cutting in, which increases the criticality.

**High-critical operational task** The criticality of a car-following situation may escalate within a second, offering the driver little time for tactical considerations (assess the situation, weigh the possibilities for action, and choose the adequate response).

Figure 2.1 shows a driving situation where a decelerating lead vehicle is being followed. Suppose the deceleration of the vehicle is large enough to potentially cause a crash, then one could calculate the very last moment to react (e.g. brake) in order to prevent the crash, represented by the objective time threshold  $t_{obj}$ . The subjective time of reaction  $t_{subj}$  is usually earlier, because drivers realize their estimate of  $t_{obj}$  may be wrong: the relevant variables for the estimation are either i) difficult to estimate accurately due to perception limits, or ii) based on a fuzzy model (own response time, road condition, own vehicle responsiveness, expectations on lead vehicles future behavior). Aggressive drivers who are confident in their abilities will adopt a small safety margin (with  $t_{subj}$  being relatively close to  $t_{obj}$ ), while more cautious drivers prefer to react at a large  $t_{subj}$ . At

increasing criticality, the differences in driving behaviour will be more related to the skill of the drivers, and less to personal choices.

## 2.3 Existing Driver Assistance Systems

Several longitudinal driver assistance systems have been developed, that aim to aid drivers in their car-following tasks. Essentially such systems avoid the hazardous consequences of driver inattention, which can be viewed as discontinuities in the visual feedback loop (see Figure 2.2A). If the separation states (e.g. relative position and velocity) change dangerously at a time when visual feedback is momentarily absent, no corrective action will be taken. Essentially, longitudinal ADAS aim to close the loop in the car-following task, thereby mitigating the hazards, reducing driver work load and/or improving safety.

In ADAS design, two juxtaposed design philosophies can be recognized: i) the driver is supported, yet retains the control authority<sup>3</sup> in the direct control loop (support); or ii) the authority of task execution is shifted to an autonomous system, and the driver now monitors the automated control loop (automation).

Note that the boundary between automation and support is not a strict or clear one: there are several levels of shared authority (Sheridan, 1992) between unsupported, supported and automated control, although the existing frameworks lack descriptive power when applied to continuous closed-loop control tasks.

#### 2.3.1 ADAS that automate longitudinal tasks

Automation systems for longitudinal control have been gradually becoming available on the market. The most well-known example is the adaptive cruise control (ACC): essentially a cruise control that automatically adapts speed to keep a safe distance to a lead vehicle. The ACC takes over control authority at the operational level: the driver is not part of the direct control loop, and has assumed the role of supervisory controller. His tasks are now to provide a set point to the ACC, monitor its performance and if necessary, overrule and resume control (see the block diagram in Figure 2.2C). The ACC works only within certain boundaries: for example, when the lead vehicle deceleration is too large, the system warns the driver with an auditory signal to resume control.

**Issues with Automation** Literature has widely described (e.g., Riley, 1994; Woods, 1994; Endsley and Kiris, 1994; Bill and Woods, 1994) the general issues exist with automation. One of the issues is lack of situational awareness: operators may not realize when the controller malfunctions or reaches its boundaries of authority. Handing back control to the operator in such a instances may be a complicated by inattention of the operator or even reduced skills after a period of not training them. Moreover, an automated system is only as smart as it is designed to be, and the human ability to respond well to unpredictable situations is often considered invaluable in critical or less predictable

<sup>&</sup>lt;sup>3</sup>Control authority is defined here as being in command of the control actions of a certain task

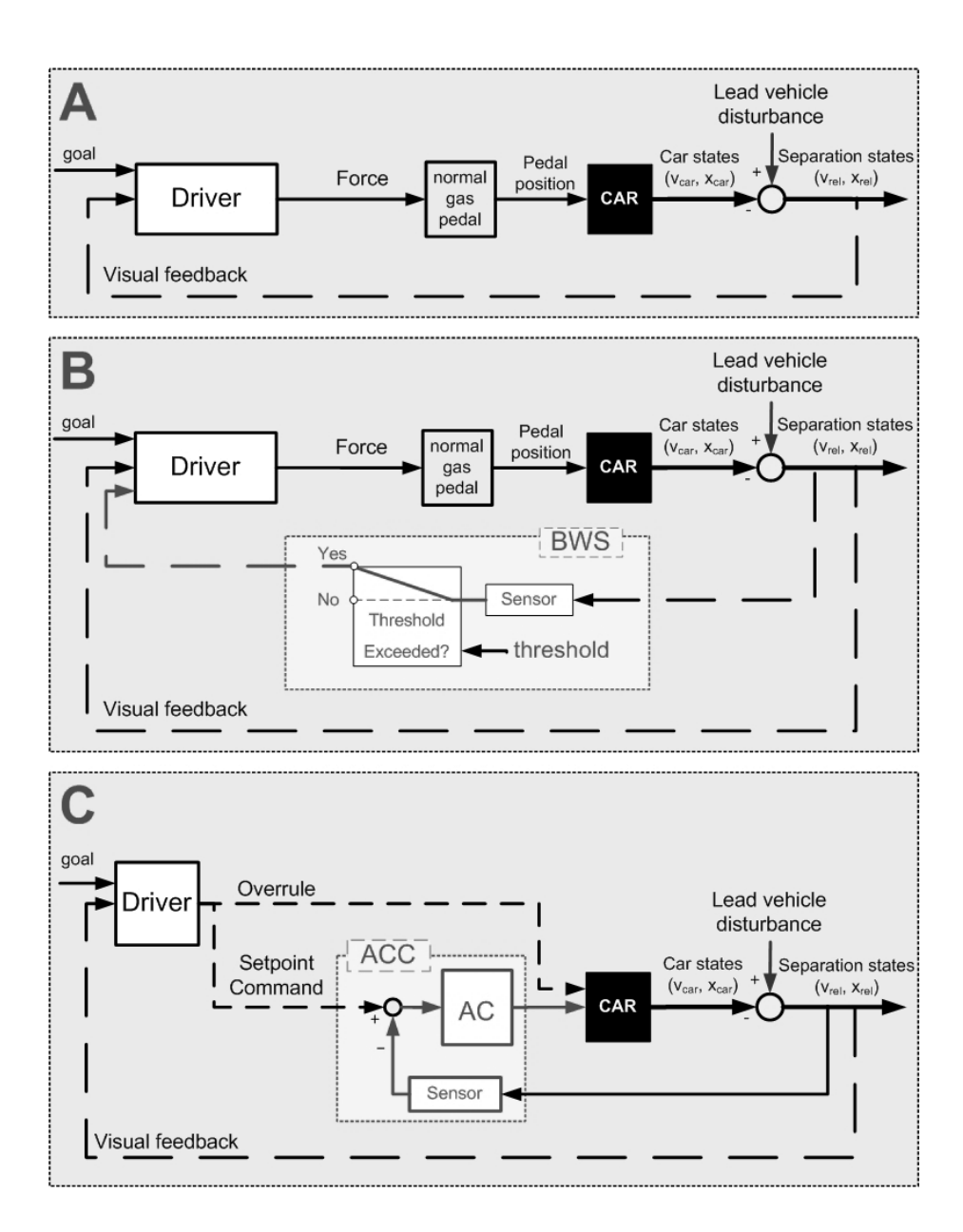


**Figure 2.2:** Block diagrams of three car-following situations: unsupported (A), supported by a binary warning system (B) and automated with ACC (C). The visual feedback is shown with a dashed line, denoting the intermittent nature of the information flow. In situation A en B the driver acts as a direct controller, in situation C the direct controller is automatic (AC) and the driver acts a supervisor.

systems.

These general issues associated with supervising an automated system have also been reported during car-following with the ACC (Hoedemaeker, 1999; Fancher and Ervin, 1998; Carsten and Nilsson, 2001): undesirable behavioral adaptation such as loss of situational awareness (complacency, reduced vigilance) or risk homeostasis (reducing the safety benefits by driving faster or doing more lane-changes).

#### 2.3.2 ADAS that support longitudinal tasks

ADAS that provide drivers with longitudinal support have also been developed, in the form of collision warning systems. Such systems are based on binary warning systems (BWS), and consist of a sensor that measures a signal and compares it to a previously set threshold. If it is exceeded, a signal (usually auditory) will be sent to the driver. The block diagram for a BWS is given in Figure 2.2B.

BWS aid in the perception phase (Meyer and Bitan, 2002) by relieving the driver of the need to continuously monitor system variables. After the warning the driver is responsible for assessing the situation and taking the necessary control actions.

One example found in literature (Lee et al., 2002) describes an auditory BWS for imminent crashes, which had a substantial beneficial effect on collision avoidance. An early auditory warning signal (re)directed the driver's attention, and resulted in an 80% decrease in rear-end collisions during 30 minute drives in a simulator.

**General Issues with Support** The general limitations of BWS have been widely recognized in literature. The most important issue with BWS is the detrimental effect of false alarms (the cry-wolf phenomenon: Breznitz, 1983; Bliss et al., 1995; Pritchett, 2001). Unexpected warnings can destroy the mental model: the driver thought he was doing fine, but the BWS says otherwise. This is helpful when the feedback is correct: it will prompt the correct action and refine the mental model for future occasions. On the other hand when the feedback was incorrect it will harm the trust in the system, and therefore its usefulness.

Moreover, setting the correct threshold level to trigger the BWS can be complicated. If too many warning signals (beeps, flashes or buzzes) go off, they will cause nuisance and information overload. To avoid this usually only critical warnings are communicated. Moreover, one threshold may feel right for some, but too late or too early for others. This may be an additional source of nuisance, and complicate ADAS design.

The previously mentioned BWS (Lee et al., 2002) was studied only for a short period of driving, and despite the encouraging results, the authors rightfully warn about possible long-term effects of nuisance and false alarms undermining the found safety benefits.

#### Implications for ADAS design

Table 2.1 summarizes under what conditions the existing ADAS offer assistance for the drivers during longitudinal tasks. It shows that the BWS only offer support in a highly critical situation – by redirecting attention after a critical boundary has been passed. They do not help in communicating where drivers are with respect to that boundary, and

**Table 2.1:** A task-hierarchy, summarizing the longitudinal tasks that currents ADAS can aid the driver in. ACC is the Advanced Cruise Control, and BWS are binary warning systems (see text for detail). The symbols that are used to describe the nature of the assistance are A for automation and BW for support through a binary warning

Task	Criticality	ACC	BWS
Tactical	low	Α	-
assistance	medium	Α	-
(traffic interaction)	high	BW	BW
Operational	low	Α	-
assistance	medium	Α	-
(vehicle control)	high	-	-

whether they approaching it or getting away from it. The need for rate information can be met in BWS by setting not one but several thresholds levels, and providing more urgent warning signals at higher levels of criticality. However, there is a limit to how many levels can be implemented due to nuisance and driver overload.

Additionally, no support is given at the operational level, the level of actual control. The ACC automates the control tasks (with the exception of critical situations), which means a partial automation in the tactical tasks as well (such as time headway choice). If the situation becomes too critical, the ACC gives a binary warning to take over control again, but will not support the right control action.

Instead of automating the control actions, they could be supported (through haptic, audio or visual means). Such skill-based support would have a higher level of authority (Sheridan, 1992), guiding the driver in the right control action, although the final control authority remains with the driver (otherwise the support turns into automation). Concluding, two areas of support remain unaddressed by current ADAS:

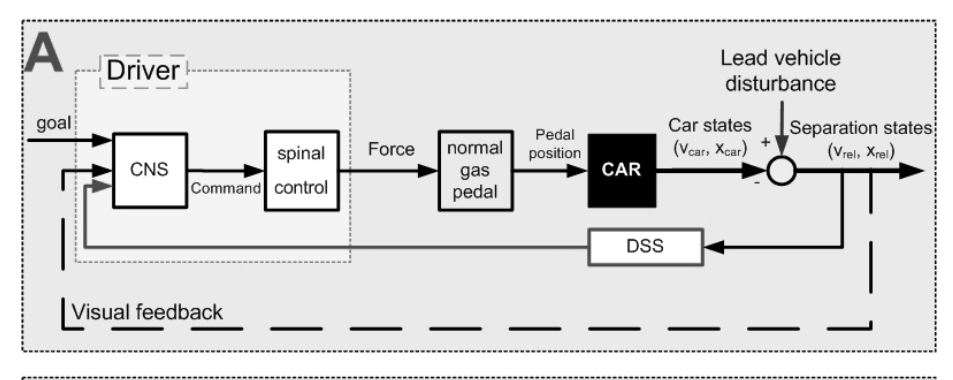
- 1. communication of criticality at the tactical level
- 2. support of control actions at the operational level

For slow system dynamics, low operator workloads and large time-horizons for corrective actions, the need to support these two areas may be small: the operator has enough time to assess the situation and resolve it himself. However, during car-following where impending hazards require a fast response the driver is expected to benefit from such support.

# 2.4 Alternative design approach for support systems

An alternative approach to ADAS is to design a system that provides the driver with an additional continuous feedback loop. If designed well, this would keep the driver in the loop and support him during in the tactical tasks (assessing the traffic situation).

In Figure 2.3A the general block diagram of a continuous driver support system (DSS) is shown. It can be seen that the proposed alternative offers an additional contin-



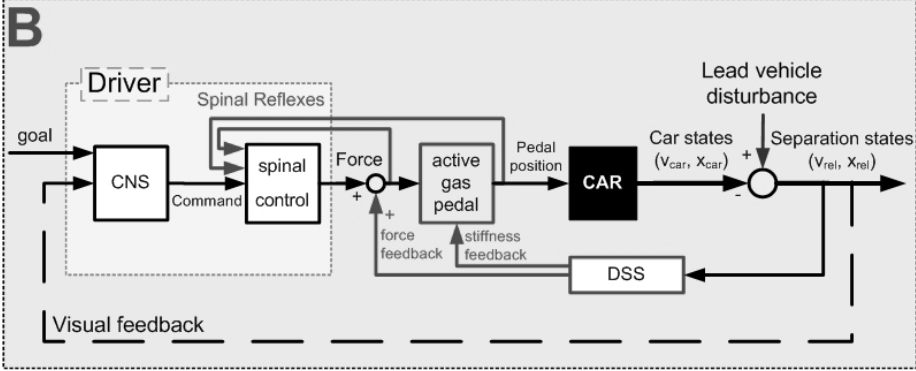


**Figure 2.3:** Block diagrams of proposed additional continuous feedback loops. The visual feedback is shown with a dashed line, denoting the intermittent nature of the information flow, whereas the continuous feedback loops are shown with solid lines. The top diagram (A) shows a general driver support system (DSS), which may provide continuous feedback to the driver about the separation state. The feedback may be composed of haptic, visual or audio cues, which have to be interpreted by the CNS. The bottom diagram (B) shows a system which provides continuous haptic feedback at the gas pedal, which enables responses on a spinal level.

uous feedback loop, supplementing the intermittent visual feedback loop. A good system would continuously communicate hazard, and assist in the development of a correct mental model of the task. The extra loops eliminates the possibility of 'looking away', but should not cause nuisance or increase the mental workload.

That is also where the main design problem lies: how to present continuous information in a clear and unobtrusive way? There are three possible sensory modalities through which to offer the continuous feedback: the visual channel, the auditory channel, and the haptic channel.

### 2.4.1 Available Sensory Channels

The auditory channel is often used in BWS. It is well known that binary audio signals are often considered a nuisance (Pritchett, 2001), and they may interfere with other auditory tasks or preferences (talking, listening to the radio). How much more irritating will a *continuous* audio signal be, where hazard level is matched to volume, pitch or frequency? Alternatively, the visual channel could be used. It is the main natural channel for informational feedback, whether enhanced by technology or not. It is possible to relay much information (central and peripheral) and to perceive two things at one time (making it easy to compare signal to a goal). Enhanced displays could be designed to form an enhanced continuous feedback loop. However, during car-following the visual channel is already engaged and -more dangerously- still subject to neglect: despite enhancements, when the operator looks the other way the visual feedback loop is broken. Ambient lighting could be used as a continuous peripheral indication of the hazard that the driver is in. Yet it may still be unclear from what direction the hazard is coming, and may cause nuisance as well.

The haptic channel is likely to be the least intrusive in providing continuous signals, provided the forces are not too large or high-frequent.

### 2.4.2 Continuous Haptic Feedback on Gas Pedal

The haptic channel offers the additional design option of providing the feedback directly on the gas pedal, coupling feedback to control. Continuous gas pedal feedback can be used to suggest the right control action, providing support at the operational level.

Figure 2.3B shows the block diagram of a haptic DSS, which translates the system state (relative position and velocity) continuously to a force on the gas pedal. The driver can choose to give way or resist these informational forces, and so still remains responsible for the gas pedal position and therefore the control input to the car.

The proposed system might be compared to a flight director. Flight directors have been developed to support pilots in flying along a certain flight path (McRuer et al., 1971). The flight director integrates information about the current aircraft states and the aircraft states required to follow the path, and continuously translates them to two sets of cross hairs on a visual display: if they are matched the pilot is following the correct path. The system simplifies the complex task of correctly flying the aircraft to a much more simple visual compensatory task.

The proposed haptic driver support system operates in a similar way. It integrates information about the current system states (e.g., relative distance and velocity to the lead vehicle) and desired system state (e.g., relative velocity is zero) and translates the difference continuously to a haptic display. Note that the pedal position has the same function as during normal driving (to control acceleration), but the feedback forces assist the driver in manipulating the gas pedal correctly. Essentially, if the driver keeps the force constant he will be doing the right actions toward the desired system state. It is therefore expected that drivers will adopt a force-task strategy, and will adapt their neuromuscular system accordingly (Abbink et al., 2004a). Normally drivers control the gas pedal position (position task).

In a way, the continuous haptic feedback facilitates the tactical (rule-based) task, changing it to an operational task (skill-based).

### 2.4.3 Expected Benefits

Designing a support system with the design approach of continuous haptic feedback may partly or entirely resolve the discussed issues with BWS and automation. The driver can remain in the loop, but also be supported in the assessment phase as well as the control phase. Several additional benefits are expected with the continuous haptic feedback system, compared to BWS.

Less need for cognition: faster response The support is skill-based, and the correct response to a force that pushes the gas pedal back is evident: to release the gas pedal. Therefore, an active contribution of the driver to gas pedal release is expected to be much more quick: the driver is already at the control channel he needs to use to mitigate the hazard with. Spinal reflexes are expected to contribute to the control action, which have much shorter time-delays than responses to visual stimuli (50 ms and 200-500 ms respectively). Moreover, the feedback force already has a passive contribution in the right direction.

In a sense the system aids a control response that immediately reduces criticality even passively (i.e. before driver actively controls), but never without driver consent. The importance of cognition for good control is reduced, which ensures a quick response: less thinking, more correct action.

In contrast, BWS demand cognitive attention before the corrective action is taken. This takes time, and momentarily draws attention away from other tasks the driver was engaged in (which may or may not be good). It is well known that the effect is especially large when different warning signals go off simultaneously (Pritchett, 2001), complicating the implementation of other driver assistance systems. Continuous haptic feedback is expected to more easily allow other continuous haptic feedback systems (for example on the steering wheel).

Better internal model: better driver acceptance For BWS, the designed warning thresholds are set so that warnings do not occur too often (in order to avoid nuisance). This may prevent drivers from developing a good representation of the safety boundaries. Additionally, when a warning signal occurs that the driver is not expecting, his internal model is ruined: everything appeared to be safe, but apparently it is not. After the signal the situation needs to be reassessed: if the warning is correct, the driver will be surprised and react slower; if it was a false alarm, the driver will lose trust in the system, with all resulting consequences. There is little chance of improving performance the next to time to prevent a new warning signal, because there is no rate information on the criticality.

The continuous haptic DSS will communicate system boundaries continuously, although in a subtle way, helping the driver to refine his internal model without much cognitive effort. The DSS will stimulate subtle, continuous control actions that mitigate hazards even

28 CHAPTER 2

before they reach the criticality where a BWS would trigger. Also, the lack of predefined thresholds will prevent mismatches between the mental model of the driver and that of the system designer.

Continuous communication of system functionality It is known from literature that if an operator depends on a system when it fails in a hazardous situation, he will generally be late in noticing the failure and taking corrective actions (the issue of over-reliance (Pritchett, 2001)). The proposed DSS continuously communicates forces, and therefore informs the driver that the system is working. Moreover, he will be continuously trained in the correct way to respond to its cues (compared to the less often needed response to events that trigger BWS).

### 2.5 Discussion

In the previous pages the limitations of existing driver assistance systems have been illustrated, and the hypothetical benefits of haptic continuous feedback during car following have been put forward in this paper. However, two main design challenges need to be overcome before a continuous haptic feedback can provide the benefits discussed above. First: how to use measured signals to describe a hazard level, and second: what haptic signals to use to communicate that hazard level?

# 2.5.1 Properties of the Haptic Feedback

### Magnitude

The magnitude of the feedback is very important: if it is too small it may not be noticed, and if it is too large it may result in fatigue or nuisance, or in an extreme case unwanted 'automation' (where the forces are so large that the driver cannot overrule them).

Haptic perception limits need to be determined to get a grasp of what forces can still be perceived consciously. Different types of footwear may lead to different levels of force perception and therefore system effectiveness.

However, drivers will also respond subconsciously to haptic feedback, due to passive and reflexive properties of the interaction of the foot with the gas pedal. How large this response is depends on the neuromuscular dynamics: they can be stiff when drivers are set to resist forces or they can be compliant, when drivers will give way to the forces. Neuromuscular studies at Delft University of Technology (De Vlugt, 2004; Schouten, 2004; van Paassen, 1994) have led to experimental techniques and detailed models, which have describe how reflexes and muscle activation influence the endpoint biomechanical dynamics of a limb. These can be estimated with the admittance, a measure for dynamic compliance; or how much way drivers give to a feedback force. The best effect of continuous haptic feedback will be found for a large admittance: drivers will not benefit from feedback forces if they resist them.

Also, it should be verified that sudden forces resulting from an unexpectedly braking lead vehicle do not result in a kick-back reflex on the gas pedal.

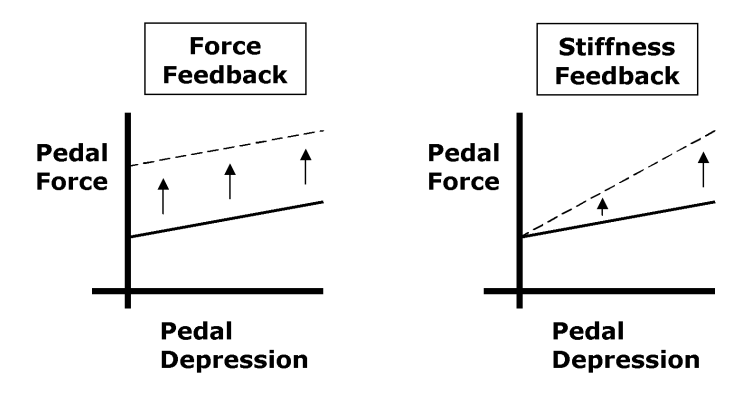


**Figure 2.4:** Gas pedal characteristics during force feedback (left) and stiffness feedback (right). The solid lines are the standard gas pedal characteristics (a pre-loaded spring). The changes in pedal characteristics by haptic feedback are denoted by the arrows: the dotted line corresponds to a situation with a higher level of hazard.

#### Force versus Stiffness Feedback

The hazard level can be related to an added force on the gas pedal (force feedback, see Figure 2.4), but also to an added stiffness. This is expected to offer additional benefits. First of all, besides the change in force that drivers will feel when they keep the pedal constant, they may also perceive a change in stiffness when they move the pedal, allowing probing of the environment. Moreover, drivers have a strong haptic cue that immediately communicates that they should *not* accelerate in a dangerous situation.

### Translating criticality to haptics

The second design challenge lies in how to translate system state variables (e.g. relative position and velocity) to haptic information. The translation should not be too sensitive to slight changes (nuisance) nor too insensitive (lack of information). The visual information and the haptic information should complement each other and not contradict each other. Given the fact that drivers always need to respond to changes in relative velocity (or iTTC) in order to avoid escalation of criticality, such information should be incorporated in the feedback algorithm. In that way, keeping a force constant will mean keeping the relative velocity zero, which is the desired state for safe following. A reduced role should be made available for the choice of THW: drivers have their own preferred separation which they accept or find comfortable.

The correct choice of variables, and how they are weighed will be one of the main challenges in the design of a continuous haptic DSS.

### 2.5.2 Future Applications

Theoretically, in any continuous control situation where the task is time-critical, continuous haptic feedback on the control channels is expected to allow for greater user acceptance and faster responses. Expected areas of application include the automotive industry (lateral steering) and the aviation industry (guiding planes and helicopters through restricted airspace). More benefit is expected where regulations are relatively loose, and allow users to search for their own preferred strategies.

If the design challenges are met successfully, the continuous haptic feedback system is expected to be a promising alternative for the existing assistance systems. However, human behavior is hard to predict accurately. Behavioral adaptation has been shown in many aviation studies (Pritchett, 2001), driving studies on ACC (see Hoedemaeker, 1999 for review) and BWS in general (Meyer and Bitan, 2002).

Empirical studies remain a necessity to investigate how humans will use assistance systems (Carsten and Nilsson, 2001) and what roles the designed support system will eventually assume (Pritchett, 2001).

### 2.6 Conclusions

- It is helpful to view the impact of advanced driver assistance systems (ADAS) on car-following behavior from a closed-loop perspective: drivers need to have informative feedback of the separation states they are controlling. The visual feedback loop, is interrupted in case of inattention, thereby causing possible hazards, and motivating the need for ADAS.
- ADAS can be divided into support systems and automation systems. Longitudinal
  support systems use binary warning signals to restore the visual feedback loop
  when necessary (tactical support in high-critical situations).
   Automation systems create an automatic continuous control loop that performs
  operational and tactical tasks, except in critical situations where the driver is
  warned to resume control.
- There are opportunities for better ADAS due to two reasons. First, literature has
  recognized several issues associated with automation (e.g., over-reliance, loss of
  attention and skills) and binary warning systems (e.g., false alarms, nuisance).
  Second, two areas of support remain unaddressed by current ADAS: communication of criticality level for tactical tasks; and support of control actions at the
  operational level.
- A new design for car-following support is proposed, which provides continuous haptic feedback directly on the gas pedal. If designed well, this system can result in several benefits:
  - 1. The driver remains in the direct control loop, avoiding issues with automation.
  - 2. Better situation awareness: the criticality of the traffic interaction is continuously communicated (instead of only the high-critical situations).

- Simplification of tactical task to operational task: the gas pedal forces suggest the right control action, drivers do not need to think about what to do, they just need to give way. This will most likely result in much faster responses, and reduced control effort.
- 4. The haptic feedback loop can (temporarily) replace the visual feedback loop, reducing the impact of temporary visual inattention.
- Although continuous haptic feedback on the gas pedal seems promising, experimental studies of the proposed system are necessary to validate the hypothesized benefits, and investigate potential drawbacks such as unwanted behavioral adaptation.

# **Force Perception Measurements at the Foot**

David A. Abbink, Frans C.T. van der Helm Published in: *Proceedings of the IEEE International Conference* on Systems, Man and Cybernetics, Den Haag, the Netherlands, October 2004

If the doors of perception were cleansed everything would appear to man as it is: infinite.

- William Blake

The goal of this study is to determine the effect of amplitude and frequency of force sinusoids on force perception of the foot, in order to design an effective haptic feedback system for gas pedals. Eight subjects were asked to push a gas pedal to a constant position against a background force of 25 N. Force perception was determined for three frequencies and three types of footwear by requiring subjects to respond with 'yes' or 'no' after each force sinusoid. Psychometric functions were calculated from the data, relating the ratio of yes answers (averaged over all subjects) to the amplitude of the force sinusoid. Although large standard deviations were found for low ratio's, a statistically significant Just Noticeable Difference (JND) could be determined for the upper boundary of perception. Increasing the frequency of the stimulus decreased the JND. Footwear was shown to have a substantial impact on the JND at all frequencies, the largest effect occurring at the lowest frequency.

### 3.1 Introduction

A new driver support system is under development by Delft University of Technology (DUT), in cooperation with Nissan Research Center. The goal is to investigate the possible benefits of providing haptic feedback on the gas pedal during car following. Lead vehicles will be detected by sensors, and the spatio-temporal separation will be translated to a corresponding force on the gas pedal. An electric actuator supplies this feedback in the form of a force, or a virtually increased stiffness of the gas pedal.

At DUT the research focuses on how drivers will react to imposed forces during non-critical driving conditions, i.e. when pedal deviations (and forces due to haptic feedback) are relatively small and low-frequent. The purpose of the support system is to increase controllability, while negative side effects like fatigue should be avoided. During continuous force feedback it is important to know what forces drivers can perceive. When forces are below the perception threshold, the foot will be moved according to the endpoint foot admittance. In this case the driver is unaware of the feedback that the system offers. When forces are perceived, drivers are aware of the system's force feedback and now have the choice to consciously respond to it.

Unfortunately no literature on force perception of the foot was found. However, much research has been done in the field of determining force perception and Just Noticeable Differences (JND's) on the upper extremity. A large difficulty with determining force perception is that people do not respond to identical stimuli consistently, only when forces are above the limits of perception, or well below. The transition area, ranging from stimuli that are always detected to stimuli that are never detected, is not sharp. This is usually attributed to noise in the neurosensor system. In literature, force perception for the upper extremity has been shown to be influenced by background force and force amplitude (Jones, 1989; Pang et al., 1991; Tan et al., 1992) and frequency content of the force signal (Tan et al., 1994). Since direct measurements to the perception sensors is not possible, and humans are involved to think about (and express) whether they felt something or not, the measurements will most likely also be influenced by factors such as attention, motivation, personality, fatigue and therefore the measurement method. The goal of this study is to investigate force perception for the foot, aiming to identify the perception boundaries for different parameters, and the transition area in between. The hypothesis is that the dependencies on amplitude and frequency that were shown for the upper extremities will also be found for the foot. However, the main contribution of this study will be to provide quantitative perception data. Footwear is an expected

### 3.2 Method

# 3.2.1 Subjects

Eight subjects (4 male, 4 female) between the age of 18 and 24 participated in the experiment. All subjects were right-handed and had no medical record of neurological disorder or injuries to the lower extremities. The subjects gave informed consent to the

influence, therefore the experiment will be done for different types of footwear.



Figure 3.1: Subject depressing the gas pedal in the operating point, while wearing a bowling shoe

experimental procedure.

### 3.2.2 Apparatus

The experimental setup that was used consists of a high-performance force-controlled manipulator, designed to closely resemble a gas pedal as encountered in an average car. The subject's foot rests on the floor and on the pedal (see Figure 3.1), which moves around a rotation point at a moment arm of 18 cm with a total motion range of 20 degrees. A force load cell is mounted on a rod with a moment arm to the rotation point of 7.6 cm. The manipulator is silent when applying forces, and no audio cues accompany the imposed forces.

# 3.2.3 Signals

The measurement method used for the experiment is generally called the 'method of constant stimuli' meaning that the same stimulus was applied several times, each time asking the subject if they noticed the stimulus or not. The experimental conditions that all subject were tested for are shown in Table 3.1.

A force amplitude was tested as a raised cosine function starting at zero, rising to its maximal value (corresponding to the amplitude), and then falling back to zero, all in a period of 1, 2 or 3.3 seconds, depending on the frequency. Each sinusoid was preceded by a random onset time between 1.5 and 4 seconds, and ended with a short haptic buzz, applied at a random time (between 0.5s and 3s) after the sinusoid reached zero. A single series consisted of all force amplitudes ranging from 1 to 14 N for a given frequency. Three trials with a zero force were mixed in between, to test for the reporting of stimuli that cannot be sensed (false alarms). A single series roughly lasted between 80-140 seconds, depending on the frequency of the force signals. There were six repetitions for each frequency, each repetition having a unique randomized order of pre-

Freq	Force Amplitude [N]	Footwear				
0.3	0, 0, 0, 1, 2, 3, 4, 5,	Sock				
	6, 7, 8, 9, 10, 12, 14					
0.5	0, 0, 0, 1, 2, 3, 4, 5,	Bowling Shoe				
	6, 7, 8, 9, 10, 12, 14					
1.0	0, 0, 0, 1, 2, 3, 4, 5,	Sneaker				
	6, 7, 8, 9, 10, 12, 14					

Table 3.1: Experimental conditions.

senting the sinusoids of different amplitudes. In total the subjects received for each type of footwear a session of 18 series, lasting about 45 minutes. The first 18 series were done for the sock, after which the subjects could take a break, put on the bowling shoe and repeat the experiment. The bowling shoes had a hard, inflexible, smooth leather sole, like businessmen's shoes. Subsequently, part of the experiment subjects received a second break, after which the 18 series were repeated for the sneaker. The sneakers had relatively flexible, rubber soles. Identical shoes, available in different sizes, were used for all subjects, to reduce intra-subject variability. The total experiment duration was around 160 minutes, including explanation, training, and breaks.

### 3.2.4 Task Instruction

Subjects were seated and asked to place their foot on the gas pedal, and depress it to the operating point of 25% pedal depression, which corresponded to 25 Newton on the ball of the foot. Before each series the subjects were shown their actual position and the position of the operating point on a screen in front of them. After this calibration the screen was turned off so the subject had no visual feedback to give cues about forces or displacements.

Subjects were told that each time a haptic buzz occurred a force might have been applied to their foot. They were asked to respond with 'yes' if they perceived the additional force, and 'no' if they did not. Subjects were told that sometimes no force was applied, so they could not always respond with yes.

A training period was executed to familiarize subjects with the tests and to reduce learning effects.

# 3.2.5 Analysis

The experiment leader recorded all 'yes' and 'no' answers after each buzz by clicking on the right or left mouse button, respectively. Its output was automatically recorded with the force and position data of the trial. Additionally, for checking purposes, an assistant manually entered the answers in pre-prepared Excel sheets.

The fraction of 'yes' answers for each condition was calculated. The results were averaged over all subjects, and statistically analyzed. The percentage was the dependent variable, and the type of footwear, force frequency and amplitude were the independent

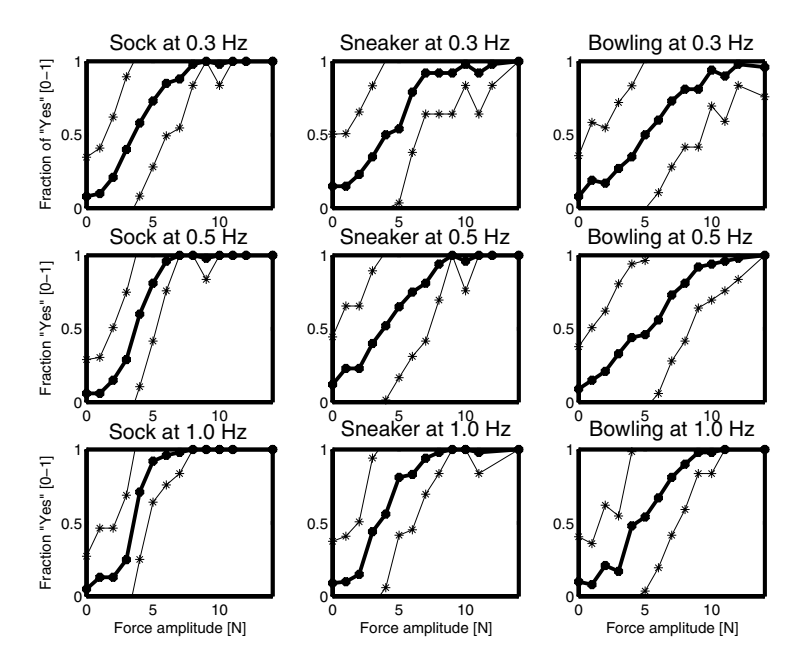


**Figure 3.2:** Psychometric functions averaged over all 8 subjects (thick line) with standard deviations (thin line). The columns show the different footwear types: socks (left), sneaker (middle) and bowling shoe (right). The rows show the different frequencies: 0.3 Hz (top), 0.5 Hz (middle) and 1.0 Hz (bottom)

variables.

# 3.3 Results

The experiment leader could check online if drift in pedal position was apparent, and in that case subjects were notified of the fact and asked to relax. This usually occurred during the training phase.

Psychometric functions were calculated from the data, and analyzed with respect to standard deviation. Figure 3.2 shows nine psychometric functions, one for each combination of footwear and frequency. The fraction of 'yes' answers is plotted against the amplitude of the force sinusoid. Note that for a single subject, the fraction ranges from 0 (0 out of 6 repetitions are reported to be noticed) to 1 (6 out of 6), with a resolution of  $\frac{1}{6}$ . The fraction shown is the average over all eight test subjects. The standard deviation is shown in red.

It is apparent that there was a large variability between test subjects, which was worst for the bowling shoe. For all experimental conditions studied the standard deviation blows up at the middle force amplitudes, and is smallest at the high force amplitudes. However,

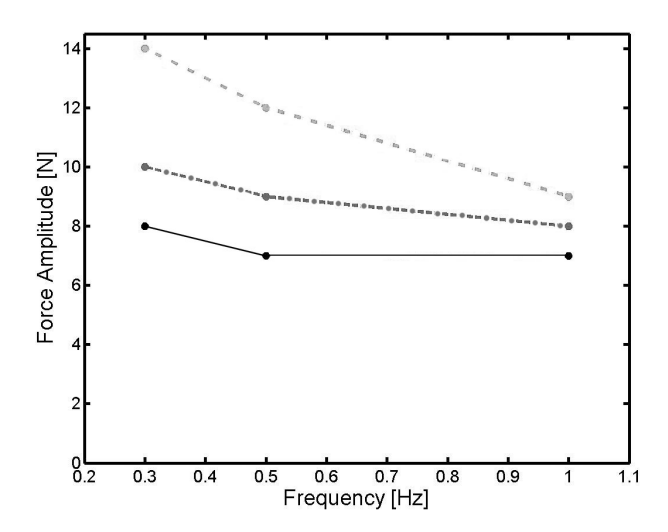


**Figure 3.3:**  $JND_{98\%}$  (averaged over 6 subjects) plotted against the 3 frequencies of the force sinusoids. The top (dashed) line shows the results while wearing the bowling shoe, the middle (dash-dotted) line for the sneaker, and the bottom (solid) line for socks.

the standard deviation is too large at lower fractions of 'yes' answers to say anything conclusive about general behaviour. Statistical significant information can therefore – in this experiment – only be derived for the upper boundary.

# 3.3.1 Effect of Force Amplitude

All subjects sometimes reported feeling a zero force (called false alarm). For most subjects this constituted a small percentage of all given zero forces (2-6%), but two of the subjects showed considerably more (13% and 21%). Apparently more eager to respond with 'yes' than others, they were removed from further analysis about the upper boundary.

The fraction of 'yes' responses increases with increasing force amplitudes, going to 1 for the largest amplitudes. The upper boundary of perception is defined as the largest force that was perceived by the averaged subject more than 98% of the time, and with a standard deviation smaller than 0.15. This measure was called the Just Noticeable Difference at 98%, or  $JND_{98\%}$ . For the lowest frequency the  $JND_{98\%}$  values are 8, 10 and 14 N for perception with the sock, sneaker and bowling shoe, respectively. The background force was constant at 25 N, resulting in Weber ratios of 32%, 46% and 52%.

### 3.3.2 Effect of Frequency

Figure 3.3 shows the results of upper perception boundary  $JND_{98\%}$  plotted against the frequencies, for all footwear. The general trend of increasing frequency can be seen: smaller force stimuli can be perceived when presented at a higher frequency. The upper perception boundary decreases while the lower boundary does not change much. The effect is seen for all footwear, but most clearly for the bowling shoe.

Also, the variability between subjects decreases with increasing frequency.

#### 3.3.3 Effect of Footwear

As can be seen in Figure 3.3 the  $JND_{98\%}$  was lowest while wearing socks, increased with sneakers, and increased even further with the bowling shoe.

### 3.4 Discussion

With this experiment the perception limit could be determined as a general indication for driver perception. The value can be used as an indication for how large a force must be when it is necessary to communicate a signal that every driver must feel. Further experiments need to be done with more test subjects, and to investigate the effect of background force. The present data are useful information regarding car driving, since 25 N is an acceptable force for longer lasting tasks.

# 3.4.1 Inter-Subject Variability

Another area which needs further investigation is the transition area from 0-100% detection, which is now characterized by much inter-subject variability. The large standard deviations in the transition could possibly be reduced by presenting a greater number of repetitions of the trials. A higher resolution of the number of repetitions and force amplitudes would reduce the impact of a subject responding differently to a single stimulus compared to another subject. However, subjects are still likely to show different behaviour. Some subjects are conservative in answering if they felt a force ("if I'm not sure I won't say anything"), while others might show less restrain ("I am in doubt, surely there must have been something"). The measurement method applied here does not rule that effect out.

Another option of measuring force perception characteristics would be to use the 'two alternative forced choice' method, where a reference and comparison stimulus are presented after each other. Subjects then have to indicate if the comparison stimulus was larger or smaller than (or in some cases equal to) the reference stimulus. Personal strategies get averaged out this way, thereby probably reducing the variability between subjects as well. However the experiment takes twice as long.

Also, it has to be noted that although for scientific purposes a reduced variability due to different measurement method is good, the current method more closely resembles the real situation in which drivers would find themselves when using a force feedback system on the gaspedal, with all inter-subject variability associated with that.

### 3.4.2 Effect of frequency and footwear

The results suggest that the influence of footwear on force perception diminishes for higher frequencies, the three graphs in Figure 3 seem to converge. Apparently low-frequent changes can be best perceived without the influence of additional footwear.

### 3.5 Conclusions

Under the conditions studied, force perception is shown to be dependent on amplitude and frequency of the force signal, for all three types of footwear.

- With increasing amplitude, forces are reported to be felt more often
- With increasing frequency, forces are reported to be felt at a lower amplitude

A statistically significant measure for the Just Noticeable Difference in force was defined at 98% detection: the  $JND_{98\%}$ . It decreased with increasing frequency for all types of footwear, and was lowest for trials done with the sock, slightly higher for the sneaker, and highest for the bowling shoe. The  $JND_{98\%}$  was 14 N for the worst condition (low frequency stimuli while wearing the bowling shoe) and 7 N for the best condition (high frequency stimuli while wearing the sock).

All subjects sometimes reported feeling a zero force. For most subjects this was a low percentage of all of the applied zero forces (2-6%).

# **EMG Measurements of Lower Leg Muscles** during Isometric Gas Pedal Manipulation

David A. Abbink, Frans C.T. van der Helm Submitted to: *Journal of Electromyography and Kinesthesiology* 

You come to nature with all your theories, and she knocks them all flat. – Renoir

The goal of this paper is to gain a better understanding of muscle use during driving, by analyzing electromyographic activity of relevant muscles while pushing down on a gas pedal over a range of forces and pedal positions. Lower leg muscles responsible for dorsiflexion and plantar flexion were measured with surface electrodes. It was hypothesized that 1) a minimum of activity for all relevant muscles will be found when the pedal force is equal to the weight of the foot, and 2) that the dorsiflexor will show increased activity when this background force is lower, and 3) that plantar flexors will be active when the background force is higher and 4) that co-contraction will not occur.

The first three hypotheses were proved experimentally, but co-contraction was found when the foot needed to be pulled up. Standard gas pedals mainly operate in the area of co-contraction, so a minor adjustment to the pedal could lead to more relaxed gas pedal use.

42 CHAPTER 4

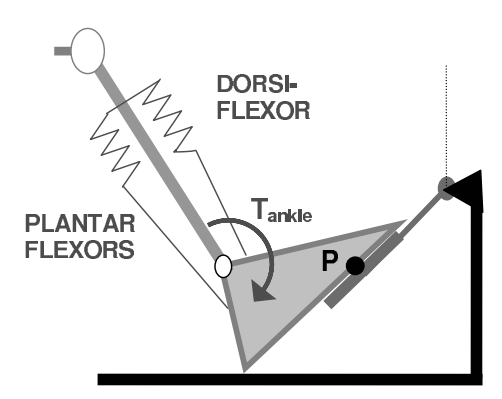


**Figure 4.1:** Schematic representation of the foot interacting with the gas pedal. Muscles are shown as springs, with the dorsiflexor and plantar flexors generating a net torque  $T_{ankle}$ , which is translated in this study to a contact force at point P.

### 4.1 Introduction

Recent developments of driver support systems have shown promising applications for using continuous force feedback on the gas pedal to inform drivers of longitudinal hazards, for example during car-following (Mulder et al., 2004a, 2005b). The effect of the additional forces on the control effort of the driver is mostly investigated through subjective measurements: a detailed examination of muscle activity during gas pedal manipulation is lacking.

Drivers control the longitudinal motion of their vehicle by manipulating the gas pedal with their foot. In general, gas pedal movements are effected by moving the foot upwards and downwards, while the heel is resting on the floor of the car-chassis. This kind of foot motion is caused mainly by the contractions of four lower leg muscles. Three muscles in the calf cause the foot to be pushed down (plantar flexion): the gastrocnemius lateralis (GL), the gastrocnemius medialis (GM) and the soleus (SO). One muscle at the shin causes the foot to be pulled up (dorsiflexion): the tibialis anterior (TA). Figure 4.1 shows a schematic representation of the foot while manipulating the gas pedal. The combined activity of these four muscles determines the net torque around the ankle joint, and the amount of physical work a driver is delivering. By contracting both plantar-and dorsiflexors at the same time (co-contraction) the stiffness of the ankle joint can be increased to resist unwanted perturbations.

Much research has been done on quantifying muscle activity of lower leg muscles with electromyography (EMG). The studies employ EMG in combination with mechanical variables (force and position) to investigate for example the dynamics of ankle compliance (Agarwal et al., 1977b), the reflexive and intrinsic contributions to ankle stiffness (Mirbagheri et al., 2000; Toft et al., 1991), and muscle activity during maximal voluntary contractions for different ankle and knee positions (Arampatzis et al., 2006). However, all these studies investigate the ankle, whereas experiments about the ankle-foot com-

plex during gas pedal manipulation are more rare (e.g. Wang et al. (1996)) and do not include EMG. The present study aims to address that lack.

The goal of this paper is to provide an experimental analysis of relevant muscle activity at ankle positions and forces that can be encountered during driving. The method will be useful not only for establishing a range of comfortable additional feedback forces, but also for establishing optimal characteristics of a normal gas pedal. The EMG of two of the main actors in generating dorsal- and plantar flexion (GL and TA) will be measured during isometric conditions for different force levels and work point positions. Based on simple mechanics and the assumption of metabolic energy minimization, it is hypothesized that for every position there is a minimum of muscle activity in both dorsiflexor and plantar flexors, occurring when the gas pedal force balances the weight of the foot in that position. Since in that situation no muscle activity is necessary, none is expected. Furthermore, it is hypothesized that when more force needs to be generated only the plantar flexors will show increased activity, and only the dorsiflexor when less force is needed. In other words, co-contraction is not expected since it is not functional for simply pushing a pedal: the resulting increase in ankle stiffness does not serve a goal that warrants the expense of extra metabolic energy. The EMG measurements obtained in this experiment are an objective measure of control effort in these conditions.

### 4.2 Methods

### 4.2.1 Subjects

Ten subjects (6 male, 4 female) between 20-24 years old participated in the experiment<sup>1</sup>. All were healthy, and had no medical record or complaints with respect to neuromuscular impairments. The subjects were not familiar with the purpose of the study, were not paid for their efforts and gave informed consent to the experimental procedure.

# 4.2.2 Experimental Setup

The used experimental setup resembles a standard gas pedal, with a high fidelity force controlled actuator capable of imposing forces and positions on the gas pedal. The pedal depression could vary over a range that resembled that of a standard gas pedal. Subjects were seated on an adjustable car seat, asked to remove their footwear and place their right foot on the gas pedal, in a way that felt comfortable for them as if expecting a long drive (see Figure 4.2). A screen in front of the subject showed the actual force exerted on the pedal, as well as the target force.

# 4.2.3 Measured Signals

The torque around the rotation point of the manipulator was measured at 250 Hz. In order to provide a more intuitive representation the torque is translated to  $F_c$ , the force

<sup>&</sup>lt;sup>1</sup>The measurements were conducted by N. den Haak and P. Overes, both students at Delft Technical University.

44 CHAPTER 4



**Figure 4.2:** Side view of a subject pushing against the gas pedal at a pedal position of 5 degrees. The EMG electrodes on the gastrocnemius lateralis and tibialis anterior can be seen.

Table 4.1: Positions and force levels used in the experiment

	Isor	Force Levels [N]		
Pedal		Ankle	Pedal	
0% 0 [deg] dorsiflexion		dorsiflexion, $\pm$ 5 [deg]	Relax, 22, 40, 55	
25% 5 [deg]		neutral, $\pm$ 0 [deg]	Relax, 22, 40, 55	
50%	10 [deg]	plantar flexion, $\pm$ 5 [deg]	Relax, 22, 40, 55	
75%	15 [deg]	plantar flexion, $\pm$ 10 [deg]	Relax, 22, 40, 55	

at the contact point of the foot with the pedal. A positive  $F_c$  denotes a force that pushes the pedal downwards. Pedal rotations were also measured at 250 Hz.

Muscle activity was measured by disc-shaped (⊘30 mm) differential (34 mm interspacing) electrodes (Ag/AgCl), placed and oriented (standarized according to SENIAM Recommendations (1999)) over the lateral head of the gastrocnemius (GL) and over the tibialis anterior (TA). In order to check if − for these experimental conditions − GL activity is representative for other plantar flexors, the EMG activity of the soleus (SO) and gastrocnemius medialis (GM) was also measured for four of the subjects. Skin conduction was improved by using hydrogel, local shaving of the skin, abrasion with sandpaper and cleaning with alcohol. The EMG signals were pre-amplified, high-pass filtered (analogue, 3rd order Butterworth, cut-off frequency at 20 Hz, 18 dB/oct) to prevent any motion artifacts, rectified and low-pass filtered (analogue, 3rd order Butterworth, cut-off frequency at 100 Hz, 18 dB/oct) to prevent aliasing. The signals were measured at 250 Hz (DSpace AD converter, 16-bit resolution) and digitally stored for offline analysis.

### 4.2.4 Experiment description

Table 4.1 lists the operating-point positions and force tasks during the actual experiment. Subjects received the task instruction to push against the fixated pedal with a constant pedal force. The required force was shown together with the actually exerted force on a computer screen in front of the subject. Subjects were asked to push with the ball of their foot – not with their toes – and not to change the position of their heel on the floor once the experiment had started. For each of the positions, four force tasks were required, yielding 16 separate trials. Each trial lasted 20 seconds, and was presented twice for averaging purposes. The trials were presented in a random order to the subject. Except the largest force, all forces are in the range of forces encountered with a standard gas pedal. The larger force was chosen to represent a situation when a large amount of force feedback would be added to the gas pedal characteristics (for example when driving dangerously close to a lead vehicle).

At the start of the experiment, a calibration was done in each position in order to relate  $EMG_{exp}$  (the activity measured during the actual experiment) to  $EMG_{max}$  (activity during maximal voluntary contractions). To determine the  $EMG_{max}$  of the plantar flexor(s), subjects were asked to alternatively push maximally for approximately 3 seconds and then relax for a similar time. This was first trained briefly, and then done during an interval of 20 seconds, yielding three realizations that were averaged to provide  $EMG_{max}$  and the accompanying force  $F_{c_{max}}$ . The same was done for a maximal pulling task in order to determine the  $EMG_{max}$  for the TA, in which case the foot was strapped to the pedal to make pulling possible.

# 4.2.5 Analysis

All measured signals were assumed to be time-invariant, and time-averaged to provide single values, which were averaged over the two repetitions. The measured endpoint force  $F_c$  is represented as consisting of two parts:

$$F_c = F_{mus} + F_{pas} \tag{4.1}$$

where  $F_{mus}$  is the active contribution (due to muscle forces exerting a torque around the ankle), and  $F_{pas}$  is the passive contribution (due to the weight of the foot and possibly passive stiffness in extreme ankle positions).  $F_{pas}$  is determined in each position during the relax task and subsequently subtracted from  $F_c$  to calculate  $F_{mus}$ . The maximal force  $F_{c-max}$  was also compensated for  $F_{pas}$ , yielding the maximal muscle force  $F_{max}$ . In order to better compare EMG activity at different pedal positions (within and between subjects) a relative measure was calculated with

$$EMG_{rel} = \frac{EMG_{exp}}{EMG_{max}} \tag{4.2}$$

yielding the normalized  $EMG_{rel}$  for each muscle and for each pedal position.

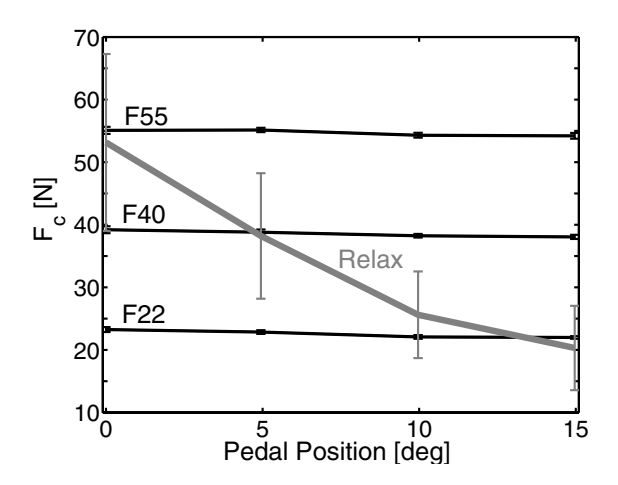


**Figure 4.3:** Generated forces for the four force tasks, F52, F40, F22, and Relax (thick line) averaged over eight subjects, at each of the four pedal positions. The error bars denote the standard deviation between the subjects.

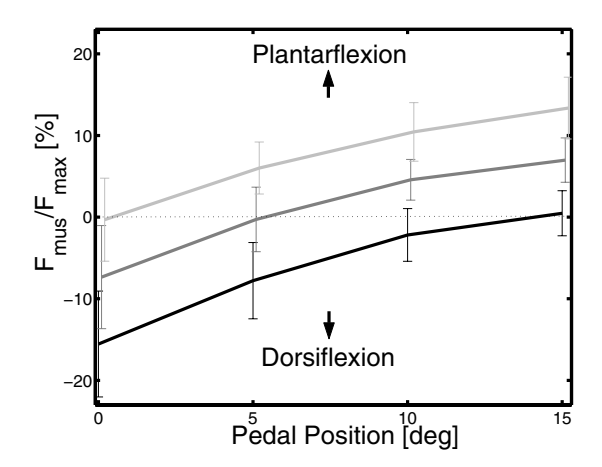
### 4.3 Results

Two of the female subjects showed a considerably lower  $F_{max}$  than the other subjects. More effort was required by these two subjects to realize the force tasks ( $F_{mus}/F_{max}$  ranged between -30% and +30% instead of -15% and +15%). The resulting higher levels of  $EMG_{rel}$  even caused some fatigue in the two subjects, all of which complicated the comparisons with the other subjects. Therefore all following results are shown for the remaining eight subjects.

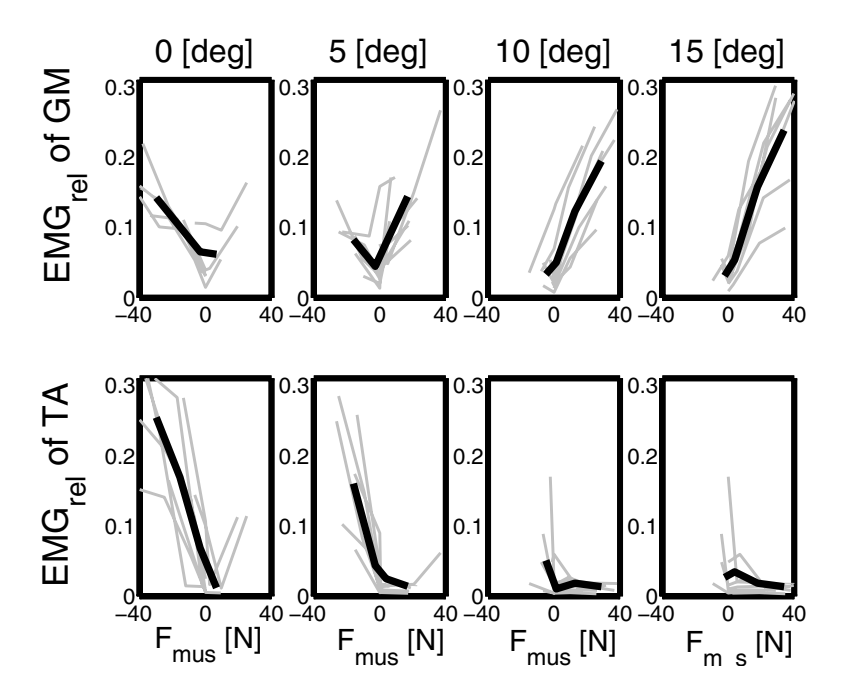
Figure 4.3 shows  $F_c$  at each pedal position, averaged over all subjects. The thick line shows the averaged force measured during the relax task, when  $F_c$  equals  $F_{pas}$ . There is a considerable amount of variation in  $F_{pas}$ , due to varying subject characteristics (e.g. segmental mass, foot size). However, it can be clearly seen that  $F_{pas}$  decreases with increasing plantar flexion. Therefore – to take an example – at 15 degrees pedal position subjects have to actively push much harder to realize a force task of 52 N than at 0 degrees, where  $F_{pas}$  already constitutes a large part of the required force  $F_c$ .

Figure 4.4 shows how much muscle force  $F_{mus}$  subjects needed to generate in order to maintain the required force  $F_c$ , at each pedal position. Note that a positive force would lead to plantar flexion, if the pedal position would not have been fixed.

Figure 4.5 shows  $EMG_{rel}$  of GL (top) and TA (bottom), for each value of  $F_{mus}$ . At 0 degrees almost all subjects needed to exert a pulling force ( $F_{mus}$ <0), compensating  $F_{pas}$  in order to reach the required force  $F_c$  (see also Figure 4.4). A larger force task meant they had to pull less, resulting in less  $EMG_{rel}$ . TA activity is seen to increase for a higher pulling force. But – unexpectedly – also GL activity increases, which indicates co-contraction.



**Figure 4.4:** The relative magnitude of muscle force ( $F_{mus}$ ) scaled by  $F_{max}$ ) exerted during the three force tasks (top line F52, bottom line: F22), shown for each pedal position. The thick lines denote the mean over all eight subjects, the error bars show the standard deviation.



**Figure 4.5:** The thick line shows  $F_{mus}$  against  $EMG_{rel}$ , both averaged over all eight subjects, while the thin lines show the results for each subject. Each line connects the results of four measurements. The top four graphs show the results for the gastrocnemius lateralis (GL), the bottom four for the tibialis anterior (TA). A pushing force (plantar flexing) is defined as positive.

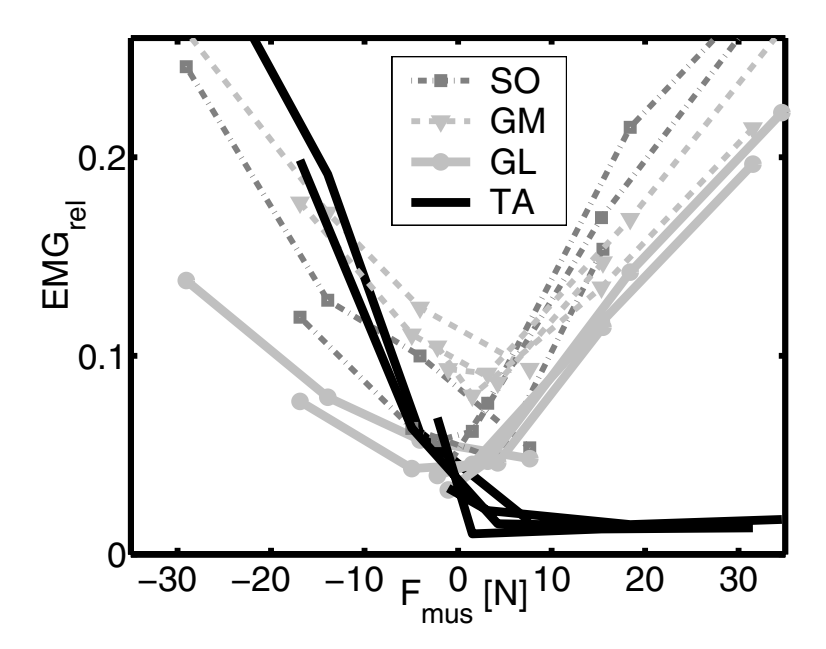


**Figure 4.6:**  $EMG_{rel}$  plotted against  $F_{mus}$ . The results for each pedal position are shown in the same graph. The results of GL and TA activity is shown, averaged over all eight subjects. The dotted lines denote the  $EMG_{rel}$  of soleus (SO) and gastrocnemius medialis (GM), averaged over four subjects.

At a position of 5 degrees subjects needed to exert a pulling force for the lower levels of force tasks, and a pushing force for the higher levels of force tasks. A minimum of  $EMG_{rel}$  was found for both muscles when  $F_{mus}$  was zero (meaning the  $F_c$  being identical to  $F_{pas}$ ). For the other two positions, the average subject had to actively push to reach each force task. A pushing force was realized by GL activation. The TA activity is negligible, meaning that co-contraction did not occur while exerting plantar flexion forces.

The four averaged lines that were shown separately for every position in Figure 4.5 are shown in the same graph in Figure 4.6. The dip at  $EMG_{rel}$ =0 is clearly visible, as well as the fact that for positive values of  $F_{mus}$  (pushing) only GL is active, and for negative values of  $F_{mus}$  (pulling) both TA and GL are active. The results of the four subjects of whom also the activity of the soleus (SO) and gastrocnemius medialis (GM) were measured are also shown in Figure 4.6. The GL and TA activity of the subgroup closely resembles that of the total group. In the subgroup the two other plantar flexors show the same trends as the GL: substantial activity for positive  $F_{mus}$ , but also for negative  $F_{mus}$ . The findings indicate that for the studied conditions GL activity is representative for other plantar flexor activity, and that pulling the foot up results in substantial activity of all lower leg muscles.

### 4.4 Discussion

As hypothesized, when a pushing  $F_{mus}$  was required, plantar flexor  $EMG_{rel}$  was found which increased for higher force levels. Dorsiflexor  $EMG_{rel}$  was found when a pulling  $F_{mus}$  was required, and also increased for higher force levels. However, the co-contraction of all muscles for negative  $F_{mus}$  was not expected. Muscle co-contraction stabilizes the ankle joint at the cost of a high expenditure of metabolic energy. Since the pedal positions were fixed by the manipulator during each trial, stability was already guaranteed by the environment. Mechanically not necessary, and energetically not optimal, the co-contraction seems to be a useless expenditure of energy: to maintain the same endpoint force the TA has to generate even more activity to overcome the opposing force caused by the activation of the plantar flexors. Similar results (co-contraction at sub-maximal contraction levels during isometric experiments) were not found in literature. Although other studies (Mademli et al., 2004) report co-contraction at maximal voluntary contractions, they assume that during sub-maximal dorsiflexion antagonistic activity is negligible, which this study contradicts. A study that examined dynamic ankle behavior (Mirbagheri et al., 2000) reports an increase in overall ankle joint stiffness at dorsiflexion, as well as an increased gastrocnemius EMG response to the dynamic force perturbations. This agrees with the increased GL activity found in the present study for dorsiflexion.

What could be the cause of the co-contraction occurring at negative but not at positive levels of  $F_{mus}$ ? If it would only have occurred at pedal position of zero degrees, it could perhaps have been attributed to the ankle joint being in a (relatively) extreme position of dorsiflexion. But subjects also show co-contraction at a pedal position of 5 degrees, indicating it occurs due to a negative  $F_{mus}$ , not solely due to dorsiflexion. The task of compensating for the weight (negative  $F_{mus}$ ) might be different then pushing the foot further down (positive  $F_{mus}$ ). Perhaps an explanation must be sought in the functionality of balance control while standing. When the dorsiflexor is active the foot is lifted off the ground and there is an increased need for stability to prevent toppling. Decreased stability does not occur when the foot is pushed down on the ground. The observed co-contraction is consistent with this explanation, and suggests there could be a cross-coupling between plantar flexor activity and dorsiflexor activity that is always present, even when stability is guaranteed as in the current experiment.

# 4.4.1 Implications for gas pedal use and design

A most common complaint after long driving is cramp or fatigue in the shin muscle (TA). It is therefore no wonder that cruise control systems are popular and generally reported to increase comfort substantially. The fact that drivers report fatigue in the dorsiflexor and not in the plantar flexors is in itself a sign that generally drivers need to pull their foot up against its own weight.

Figure 4.7 shows the characteristic of an average gas pedal, which behaves like a pretensioned spring. In the same graph the averaged  $F_{pas}$  is plotted, which could be seen earlier in Figure 4.3. For ease of interpretation in a driving situation, the pedal position is now shown as a percentage of maximal depression (see Table 4.1). Note that

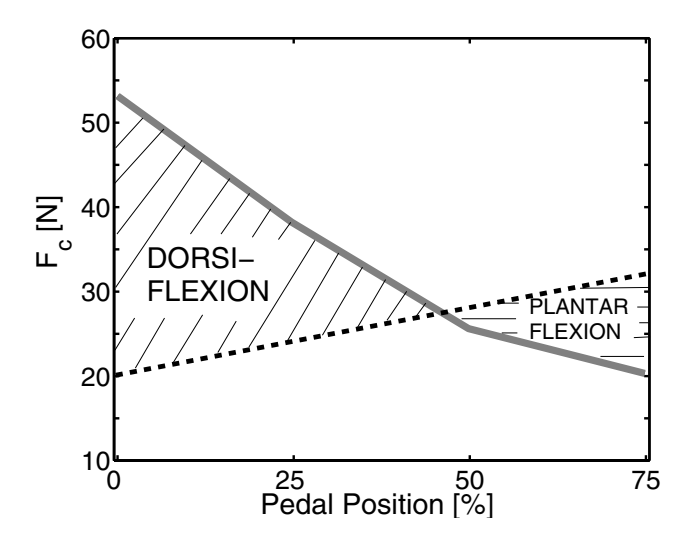


**Figure 4.7:** The averaged  $F_{pas}$  (solid) plotted against a standard gas pedal characteristic (dashed). Pedal positions are shown in percentage of total pedal depression.

in the diagonally shaded area at the left a dorsiflexing force needs to be exerted to keep the pedal in that position. In most cars, a pedal depression level of 15%-30% is needed to maintain highway speeds, which for the average driver lies in an area of dorsiflexion. In this study co-contraction was found during dorsiflexion. That means even more dorsiflexor activity is needed in order to compensate for the opposing torque of the contracted plantar flexors. The co-contraction causes unnecessary expenditure of metabolic energy, at long last causing fatigue.

In future studies,  $F_{pas}$  should be measured for a large population of drivers. The gas pedal characteristics could be optimized for certain driving conditions. Ideally a gas pedal would result in minimal muscle activity for any driving situation, meaning that both shaded areas in Figure 4.7 should be minimized. However, the dorsiflexion area should be emphasized, since it entails co-contraction and since the dorsiflexor is much weaker than the plantar flexors, fatigueing earlier. A constraint in optimizing the characteristic is that the gas pedal should always come back to 0% pedal depression when released, so the characteristic should be monotonously ascending. By shifting the intersection point between  $F_{pas}$  and the stiffness characteristic, one can change the point of minimal EMG activity. Since most time is spent on highways – and not accelerating – it would make sense to shift this point of low  $EMG_{rel}$  towards lower pedal depressions, which could be accomplished simply by increasing the background force by 10-15 N.

### 4.5 Conclusions

The total pedal contact force  $F_c$  was separated into an active part ( $F_{mus}$ , caused by muscle contractions) and a passive part ( $F_{pas}$ , the force that the foot exerts when muscles are relaxed). For the experimental conditions studied, the following conclusions can be drawn:

- $F_{pas}$  is not constant over the gas pedal positions, but substantially increases with dorsiflexion.
- The tibialis anterior (TA) is only active when pulling the foot up (i.e.  $F_c < F_{pas}$ ). EMG activity is absent when  $F_c > F_{pas}$ .
- Plantar flexors like the gastrocnemius lateralis are active when pushing the foot down, but also when pulling the foot up.
- Common gas pedals are tuned so that the average driver needs to pull his/her
  foot up at the pedal positions where most time is spent driving. The resulting cocontraction unnecessarily fatigues lower leg muscles, which could be prevented
  by a larger force (± 10 [N]).

# Measuring the Effects of Haptic Feedback on Neuromuscular Control and Car-Following Behaviour.

David A. Abbink, Mark Mulder, Frans C.T. van der Helm, Max Mulder, Erwin R. Boer Submitted to: *Biological Cybernetics* 

The cause is hidden. The effect is visible to all. - Ovidius

In previous research a driver support system (DSS) was developed that uses continuous haptic feedback on the gas pedal to inform drivers of the separation to the lead vehicle. The influence of biomechanical properties on the effectiveness of the DSS is largely unknown. The goal of this paper is to experimentally determine the effect of the DSS on motion control of the ankle-foot complex, as well as on car-following behaviour in general.

An experiment was conducted in a simplified driving simulator, where subjects (n=10) were required to follow a lead vehicle – with and without the aid of the DSS – at a constant time headway of 1 second. During the experiment the lead vehicle speed was varied using an unpredictable sinusoid perturbation. In order to estimate the dynamic response of the ankle-foot complex (i.e., the admittance), small stochastic torque perturbations were applied to the pedal. Both perturbations were separated in the frequency domain to allow the simultaneous estimation of frequency response functions of the car-following control behaviour, and of the admittance. For comparison to previous experiments, the admittance was also estimated during three classical tasks (maintain pedal position, relax, maintain pedal force).

The main hypothesis of the experiment was that the DSS would provoke drivers to adopt a force task, resulting in a larger admittance compared to other tasks; and that drivers would need less control effort to realize the same car-following performance. Time and frequency domain analyses supported these hypotheses. Additionally, the haptic feedback elicited less EMG activity, and could replace the visual feedback temporarily. Overall, the DSS was concluded to have a beneficial effect on car-following.

54 CHAPTER 5

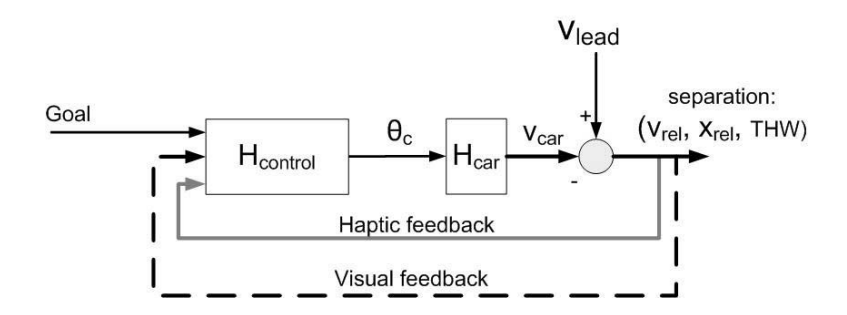


Figure 5.1: Simplified conceptual model of a closed-loop car-following situation, where the visual feedback is supplemented by haptic feedback.  $H_{control}$  captures the total response to changes in separation states, constituted by the interaction between driver and the haptic gas pedal, with the pedal displacements ( $\theta_c$ ) as output. The driver aims to reduce the impact of lead vehicle speed perturbations ( $v_{lead}$ ), in order to minimize the changes in the separation (e.g., relative velocity  $v_{rel}$ ).

### 5.1 Introduction

Car following is a task that most drivers can accomplish successfully when they pay attention and use available visual cues of the separation to the lead vehicle. However, the driver is not only involved in car following, but also in other necessary driving tasks such as steering or route-planning. Additionally, drivers may engage in non-driving related activities, such as conversation with other passengers, using cellphones, or looking at the scenery. The majority of the rear-end collisions (Knipling et al., 1993) occur when the driver is distracted or inattentive.

Consequentially, more and more research is dedicated to the design of advanced driver assistance systems (ADAS) that relieve (visual) workload and provide alternatives for maintaining a safe speed, a safe separation or for communicating hazardous situations to the driver. Issues with current ADAS are widely described in literature (for an overview, see Hoedemaeker, 1999).

A promising approach to improve driving comfort and safety during car following on highways is to support drivers with haptic feedback. By translating the separation to the lead vehicle continuously to easily interpretable haptic information (e.g., pedal forces or stiffness), the driver now has access to an additional information channel (see Fig 5.1). In other words, if a lead vehicle slows down, the separation decreases, which the DSS translates continuously to an increasing force and stiffness on the gas pedal. The additional pedal force already suggests the proper control action: to release the gas pedal. In any case, the driver is always in control and can at any time choose to either overrule

the haptic information and either keep the *pedal position* constant (by pushing harder to counteract the feedback forces), or to follow the haptic information and keep the *pedal force* constant (by giving way to the gas pedal).

Ideally, the haptic driver support system (DSS) allows the driver to remain in the loop,

is comfortable and results in benefits for the driver with respect to comfort and safety. In previous research several DSS prototypes were developed and tested in a driving simulator environment. A number of experimental studies (Mulder et al., 2004a, Mulder et al., 2004b, Mulder et al., 2005b) showed beneficial results while driving with a haptic DSS compared to unassisted driving, the general conclusion being that drivers need less effort to generate the same performance. Car-following performance was defined by variations of time headway (THW) and inverse time-to-contact (iTTC). The reduced effort was shown by a decrease in pedal control actions  $\theta_c$ . Additionally, a cross-over analysis (Mulder et al., 2005a,b) yielded a reduced total time-delay when responding to lead vehicle perturbations.

Although the beneficial results are promising, it still remains unclear how drivers actually realize such benefits. This is crucial in understanding the impact of the DSS and may be used to improve future designs.

It has been hypothesized previously (Abbink et al., 2004a; Mulder et al., 2004a) that good haptic feedback induces drivers to change the task of their foot on the gas pedal from a 'maintain position' task to a 'maintain force' task. A second hypothesis was that spinal reflexes will be used to accomplish the force task, thereby reducing response time considerably, and also reducing the visual load (which was supported by Mulder et al., 2004a).

Such hypotheses cannot be tested with the current techniques without a more in-depth analysis of the motion control of the lower limb. There is a substantial amount of literature available on limb dynamics, which are described by the admittance (the causal dynamic relationship between force (input) and position (output)). Techniques to estimate the admittance with Frequency Response Functions (FRFs) have been successfully applied to upper extremity movements (Van der Helm et al., 2002), as well as the ankle joint (Agarwal et al, 1977b; Mirbagheri et al., 2000; Toft et al., 1991). All mentioned studies show that limbs approximately behave like mass-spring-damper systems and show the human capability to change the visco-elastic properties of a limb by muscle (co-)contraction and by reflexive feedback. Recently, these techniques have been applied to the ankle-foot complex in a driving posture (Abbink et al., 2004a), where subjects showed a substantial increase in admittance during a 'relax' task (RT), compared to a 'maintain position' task (PT). Muscle activity was measured using electromyography (EMG) techniques, and was very high during the PT (due to maximal co-contraction), and negligible for the RT (due to the muscle relaxation). It is hypothesized that a 'maintain force' task will increase the admittance even further, at low levels of muscle activity. However, the question remains if motion behaviour measured during classical tasks (e.g. maintain position or force) is comparable to that measured while driving (with or without a DSS). Unfortunately, available literature offers no techniques to measure the admittance while engaged in another control task. Hence, a new experimental study is proposed.

The goal of the study is to quantify the impact of continuous haptic DSS on driver control strategies during car-following, both at the level of car-following behaviour and at the level of neuromuscular motion control behaviour. The goal is realized by:

1. estimating the total response  $H_{control}$  to lead vehicle perturbation, while driving

**Table 5.1:** Hypotheses concerning the comparison of car-following performance  $(CF_P)$  and control effort  $(CF_{CE})$ , the frequency response function  $H_{control}$ , the admittance and the EMG for each different task. The three car-following tasks are: driving with visual feedback only (V), driving with visual and haptic feedback (VH), and driving with haptic feedback only (H). The three classical tasks are: maintain position (PT), maintain force (FT) and relax (FT).

	$CF_P$	$CF_{CE}$	$H_{control}$	Admittance	EMG
V	baseline	baseline	baseline	medium	baseline
VH	similar	less	lower	large	lower than V
Н	worse	similar	low	large	low
PT	-	-	-	small high	high
RT	-	-	-	medium	zero
FT	-	-	-	large	low

with and without DSS; and by relate this FRF to car-following performance and workload metrics (e.g. THW, iTTC) and other simulator studies.

estimating the admittance of the ankle-foot complex while car-following with and without DSS; and by relating the admittances to admittances estimated while performing three classical tasks (relax, maintain force and maintain position).

An additional task will be used to test the limits of the haptic feedback loop: requiring drivers to follow a lead vehicle with only haptic feedback. It is expected that car-following will still be possible, although at a lower performance level. The main hypotheses concerning the effect of task perception on the magnitude of the admittance and of the EMG activity are summarized in table 5.1.

### 5.2 Methods

# 5.2.1 Subjects

Ten subjects (of which 5 male) between the age of 20 and 23 participated in the experiment. All subjects had their drivers license for several years and had no medical record of neurological disorders or injuries to the lower extremities. The subjects were not familiar with the purpose of the study, were paid for their efforts and gave informed consent to the experimental procedure.

# 5.2.2 Apparatus

The experimental setup consists of a driver seat, a computer screen for visualization and a gas pedal. A high fidelity force controlled actuator was capable of imposing forces on the gas pedal, as well as simulating a range of stiffnesses and dampings. The pedal characteristics were set to resemble those of a common gas pedal: the pedal force progressed linearly from 20 N at 0% pedal depression, to 36 N at maximum pedal

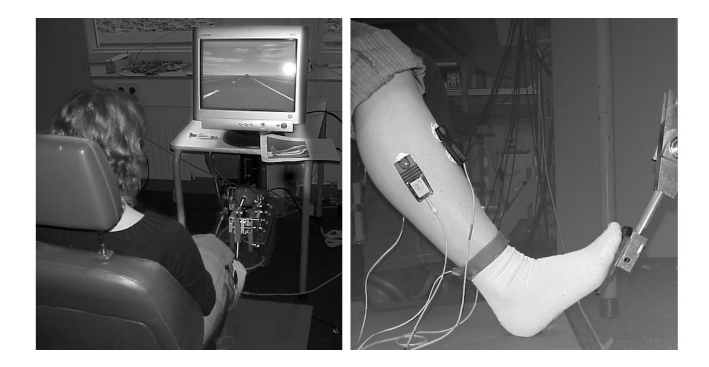


**Figure 5.2:** At the left an overview is shown of a subject driving in the simulator. On the right a side view is shown of a subject pushing against the gas pedal at the operating point of 25% pedal depression (=5 degrees).

depression (with 0-100% pedal depression being 0-20 degrees pedal rotation). Subjects were asked to remove their footwear and place their right foot on the gas pedal, and sit in a way that felt comfortable for them as if expecting a long drive (see Figure 5.2). The screen in front of the subject showed task-related information: force during a force task, position during a position task, and a road with a lead vehicle during the driving tasks. Subjects were seated at a  $\pm 1.5$  meter distance to a 17" screen, resulting in smaller visual angles compared to the driving simulator used in Mulder et al., 2005b.

# 5.2.3 Experiment Protocol

The experiment consisted of two main parts: 1) admittance measurements during three classical tasks 2) car following during three conditions, with and without torque perturbation admittance measurements.

EMG measurements were performed at the start and end of the experiment, to calibrate the EMG measurements during the main experiment.

#### Electromyography

EMG activity was used to measure muscle activity for the relevant lower leg muscles. Disc-shaped (⊘30 mm) differential (34 mm inter-spacing) electrodes (Ag/AgCl), were placed and oriented (standardized according to SENIAM Recommendations, 1999) over the three plantar flexors: soleus (SO), gastrocnemius lateralis (GL) and medialis (GM); and over the dorsiflexing tibialis anterior (TA). Skin conduction was improved by using hydrogel, local shaving of the skin, abrasion with sandpaper and cleaning with alcohol. The EMG signals were pre-amplified, high-pass filtered (analogue, 3rd order Butterworth, cut-off frequency at 20 Hz, 18 dB/oct) to prevent any motion artifacts, rectified and low-pass filtered (analogue, 3rd order Butterworth, cut-off frequency at 100 Hz, 18 dB/oct) to prevent aliasing. The signals were measured at 250 Hz (DSpace AD converter, 16-bit resolution) and digitally stored for off-line analysis.

**Table 5.2:** Structure of the main experiment, consisting of classical tasks (PT, RT, FT) and carfollowing tasks (V, VH, H). See text section (5.2.3 for more information.  $F_{sample}$  is the sample frequency and  $t_{anl}$  the time duration of all analyzed signals.

	Task	Repetitions	Perturbation	F <sub>sample</sub>	$t_{anl}$
	PT,RT,FT	2	$T_{dist}$	250 [Hz]	65.536 [s]
	V, VH, H	4	$T_{dist}$ , $v_{lead}$	200 [Hz]	81.92 [s]
Ì	$V^*, VH^*, H^*$	4	v <sub>lead</sub>	200 [Hz]	81.92 [s]

**EMG Calibration before and after the main experiment** An isometric calibration experiment was done to calculate the maximum voluntary contractions (MVC), as well as to relate EMG activity to a selection of forces that could reasonably be expected to be encountered while driving. The gas pedal position was fixed ( $\theta_c$  = 5 degrees = 25% pedal depression) and subjects were asked to alternately push maximally (plantar flexion) for approximately 3 seconds and then relax for a similar time, during an interval of 20 seconds. The same was done for a maximal pulling task (dorsal flexion), where the foot was strapped to the pedal to allow pulling. Subsequently, subjects were asked to generate a series of randomized constant forces on the gaspedal for 40 seconds. The force levels were 5, 10, 20, 30, 40 or 50 [N], each shown as a red target line on the screen. The actual pedal force was shown as a white line, so subjects could monitor their performance. An extra trial was mixed in where the subject had to totally relax all muscles. The entire sequence was repeated at the end of the main experiment, to check for fatigue, which was negligible. The calibrations before and after the main experiment were averaged.

#### **Classical tasks**

**Task Instruction** Subjects were asked to perform three randomized classical tasks: minimize pedal deviations (PT), stay totally relaxed (RT), and minimize deviations in the pedal force (FT). The subjects could see their performance (reference position or force against the actual value) on the screen in front of them, but during the relax task the screen was turned off to prevent any distraction. Each task was repeated twice for averaging purposes, and was preceded by training.

**Torque Perturbation** While performing the task, a continuous stochastic torque perturbation  $T_{dist}$  was applied to the pedal. The perturbation is a multisine, generated offline in the frequency domain. The phase was randomized to yield an unpredictable signal, and the cresting technique (Pintelon and Schoukens, 2001; De Vlugt et al., 2003a) was used to prevent large peaks in the time domain.  $T_{dist}$  contains full power from 0.02 up to 0.5 Hz, and a 5% fraction of that power at several logarithmically spaced frequency points up to 25 Hz (see Figure 5.3). Within the full power section, only every third band of two frequency points contains power, in order to improve the signal-to-noise ratio and to allow 'space in the frequencies', where only the visual perturbation signal will contain power (see section 5.2.3).

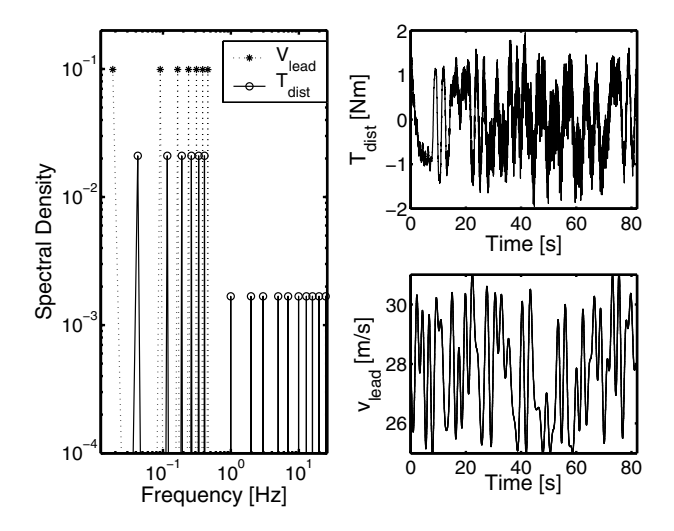


**Figure 5.3:** The generated perturbation signals  $T_{dist}$  and  $v_{lead}$  in frequency domain (left) and time domain (right).

An inverse fast Fourier transformation (IFFT) yielded a repeatable time-domain signal, which was cut to last 70 seconds. During the experiment,  $T_{dist}$  was scaled so that the standard deviation of the resulting pedal displacements was approximately 0.5 degrees (to ensure linearity).

**Measured Signals during Classical Tasks** The following signals were measured at 250 Hz: the contact torque  $T_c(t)$  [Nm], the torque perturbation  $T_{dist}(t)$  [Nm], the pedal depression  $\theta_c(t)$  [rad] and the four EMG signals, EMG(t) [V].

### **Driving tasks**

The main part of the experiment consisted of a simplified driving simulation. The computer screen showed a realistic representation of a straight road and a lead vehicle. The driving simulator did not have a brake pedal or a steering wheel.

**Task Instruction** The subjects were instructed to 'maintain a constant THW of 1 second to the lead vehicle, as well as possible'. The exact separation (THW=1) was shown at the start of each trial as a red square. After subjects had reached a constant operating point ( $v_{car} \approx 28 \, [\text{m/s}]$ ;  $\theta_c \approx 25\%$  pedal depression) the red calibration square disappeared and after a random amount of seconds the lead vehicle speed was perturbed, and small torque perturbations were added to the gaspedal. After 94 seconds the perturbations stopped, and the calibration square was shown again for 10 seconds.

This signified the end of the repetition, and allowed subjects to correct for possible drift in THW. A full trial consisted of four such repetitions, lasting about 8 minutes in total. Trials were done for three driving conditions: normal driving with visual feedback (V), driving with the haptic feedback system and visual feedback (VH) and driving with only haptic feedback (H), during which the screen was turned off).

Each driving condition was trained for some time, and pseudo-randomized: the H condition was always preceded by the VH condition to make sure the drivers had a good feeling of how the haptic feedback related to visual information. The torque perturbations could be felt, but were small enough not to interfere with the car-following task. To check for this, each condition was also repeated without the torque perturbations  $(V^*, VH^*, H^*)$ .

**Lead Vehicle Velocity Perturbation** The lead vehicle velocity perturbation  $v_{lead}(t)$  was designed in the same way as  $T_{dist}(t)$ : a phase-randomized, crested multisine containing power between 0.02-0.5 Hz. A different time realization of  $v_{lead}$  was made for each driving condition (V, VH, H) in order to prevent driver anticipation after several repetitions.

Frequency Separation of the Perturbations A frequency separation method was employed in order to be able to separate the response to both  $T_{dist}(t)$  and  $v_{lead}(t)$ . The two perturbations were designed in the frequency domain to contain power at different frequency points in the area of full power (between 0.02-0.5 Hz). The set of frequency points were divided into repetitive segments of three bands, each containing two frequency points. The first band of two frequency points  $f_v$  only contained power for the visual perturbation, the following band  $f_t$  only for the torque perturbations, and the third band  $f_r$  did not contain any power (see Figure 5.3), after which the following contained power for  $f_v$ , and so on.

Beyond 0.5 Hz, the visual perturbation did not contain any power, but the torque perturbations were similar to those used for the classical tasks and contained reduced power up to 25 Hz. The reduced power enabled the identification of the admittance at higher frequencies, while at the same time the control behaviour of the driver is assumed to be solely adapted to the frequencies of full power. This assumption was verified during pilot studies.

**Measured Signals during Car Following** During the car following experiment, all signals were measured at 200 Hz. In addition to the measured signals during the classical tasks, car following data was measured as well: the lead vehicle perturbation  $v_{lead}(t)$  [m/s], the own vehicle speed  $v_{car}(t)$  [m/s], and the relative separation  $x_{rel}(t)$  [m].

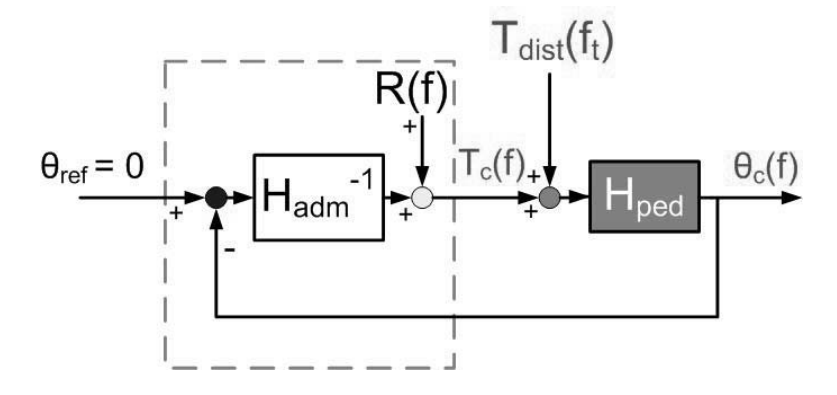


**Figure 5.4:** Measurement scheme during a classical position task. The pedal dynamics and the human ankle-foot dynamics  $H_{adm}^{-1}$  form a closed-loop system.  $H_{adm}^{-1}$  is modeled as a quasi-linear system, meaning that all non-linearities are captured in the remnant R.

#### 5.2.4 Data Analysis

#### **Signals**

The first seconds of each measured signal were discarded to reduce onset effects, leaving exactly 16834 samples (convenient for fast Fourier transforms) for identification. For all trials, the EMG(t) measured for each muscle was scaled by its respective  $EMG_{max}$  (the EMG measured during MVC).

$$EMG_{rel}(t) = \frac{EMG(t)}{EMG_{max}}$$
(5.1)

The signals measured during car following were used to calculate two important metrics that are often used in literature as driving metrics, the THW and the inverse time-to-contact iTTC:

$$THW(t) = \frac{x_{rel}(t)}{v_{car}(t)}$$
 (5.2)

$$iTTC(t) = \frac{v_{rel}(t)}{x_{rel}(t)}$$
 (5.3)

with  $v_{rel}(t)$  defined as:

$$v_{rel}(t) = v_{lead}(t) - v_{car}(t)$$

$$(5.4)$$

#### **Frequency Domain Analysis**

Frequency domain analysis was done for each condition on the time-average over all repetitions.

Classical Tasks Due to the interaction between manipulator and foot, closed-loop identification is needed to estimate the admittance. An external signal is needed from outside the closed loop, for which the external perturbation  $T_{dist}(s)$  is used. Figure 5.4 shows a frequency domain measurement scheme for a classical position task. The figure can be restructured for a force task scheme too, but the identification procedure remains the same. The relationship between the torque  $T_c$  (input) and the pedal rotations  $\theta_c$  (output), i.e. the admittance, is for each task estimated at the frequencies  $f_t$ , according to:

$$\hat{H}_{adm} = \hat{H}_{T_c\theta}(f_t) = \frac{\hat{S}_{T_{dist}\theta}(f_t)}{\hat{S}_{T_{dist}T_c}(f_t)}$$
(5.5)

The term  $\hat{S}_{T_{dist}\theta}$  is the estimate for the cross-spectral density of disturbance  $T_{dist}(t)$  and  $\theta_c(t)$ , whereas  $\hat{S}_{T_{dist}T_c}$  is the cross-spectral density of disturbance  $T_{dist}(t)$  and  $T_c(t)$ . All spectral densities were averaged over two adjacent frequencies to reduce the variance.

The coherence function is used to determine the approximation involved by using linear models, and is estimated according to:

$$\hat{\Gamma}_{T_{dist}\theta}^{2}(f_{t}) = \frac{|\hat{S}_{T_{dist}\theta}(f_{t})|^{2}}{\hat{S}_{T_{tirt}T_{tirt}}(f_{t})\hat{S}_{\theta\theta}(f_{t})}$$
(5.6)

The coherence is an indication of the amount of linearity of the system in response to the external perturbation. For a linear system, the coherence function equals one when there is no noise (linearization or measurement noise), and zero in the worst case.

**Car-Following Tasks** The measurement scheme is slightly more complex while car-following (see Figure 5.5). Now the pedal deviations are the input of the longitudinal car dynamics  $H_{car}$ . The relative velocity is perturbed by  $v_{lead}(f_v)$  and the resulting separation is fed back to the driver either through visual (V) or haptic feedback (H), or a combination of both (VH).

At the center of the scheme, the admittance measurement scheme from Figure 5.4 can still be recognized. The admittance can be estimated at the frequencies  $f_t$ , using the same procedures used for the classical tasks (see Eq. 5.5).

Several other FRFs can now also be estimated:  $H_{control}$  (the total dynamic response to

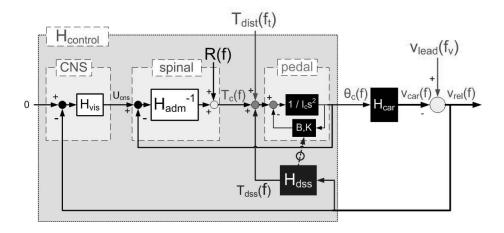


**Figure 5.5:** Measurement scheme of a driver in a car following task.  $H_{control}$  is the total driving FRF and consists of a visual part  $H_{vis}$ , a spinal control part represented by the admittance  $H_{adm}^{-1}$ , and the pedal with a certain inertia  $I_c$ , damping B and stiffness K. The output of  $H_{control}$  is a pedal position  $\theta_c$  which is the input for the car kinematics  $H_{car}$ . The velocity of the car is perturbed by  $v_{lead}(f_v)$ , which results in changes in  $v_{rel}$  that the driver tries to control back to zero. When the DSS system is switched on, it will provide informational torques  $T_{dss}$  to the driver, as well as changes in the pedal stiffness K.  $T_{dist}(f_t)$  is applied to the pedal in order to estimate  $H_{adm}$ .

 $v_{rel}$ ) and the longitudinal car kinematics  $H_{car}^{1}$  (with input  $\theta_c$  and output  $v_{car}$ ).  $H_{control}$  was estimated at the frequencies  $f_v$  where  $v_{lead}$  had power, according to:

$$\hat{H}_{control}(f_v) = \frac{\hat{S}_{v_{lead}\theta}(f_v)}{\hat{S}_{v_{lead}v_{rel}}(f_v)},\tag{5.7}$$

with the coherence:

$$\hat{\Gamma}_{v_{lead}v_{rel}}^{2}(f_{v}) = \frac{|\hat{S}_{v_{lead}v_{rel}}(f_{v})|^{2}}{\hat{S}_{v_{lead}v_{lead}}(f_{v})\hat{S}_{v_{rel}v_{rel}}(f_{v})}$$
(5.8)

#### **Time Domain Analysis**

For ease of interpretation, the torques are converted to forces at the contact point of the foot with the pedal (moment arm of 0.188 [m]) and the pedal rotations are shown in degrees. The following car-following performance metrics were used (see Mulder et al., 2005b): the standard deviations of THW(t) and the standard deviation of iTTC(t). The standard deviation of  $\theta_c(t)$  is used as an objective metric of control effort.

 $<sup>^{1}</sup>$ The car dynamics  $H_{car}$  were estimated with high coherences, resembling a first order system and matching very well the FRF of the car model used in the simulation (see also Mulder et al., 2005a). It is not discussed further in this paper.

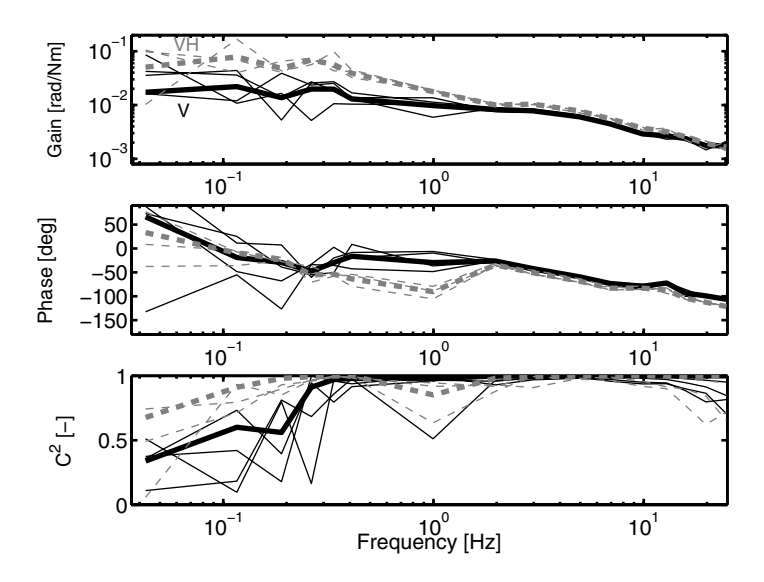


**Figure 5.6:** Admittance of a typical subject, estimated during two driving tasks: driving with only visual feedback (V, solid), and with visual and haptic feedback (VH, dashed). The top plot shows the magnitude of the admittance, the middle plot the phase lag, and the bottom plot the coherence squared. The thin lines show each of the four repetitions, the thick line is the average.

The means of the time-averaged  $EMG_{rel}$  for each muscle are used as a measure of (co-)contraction, which is used as an objective measure of control effort during both the car-following and classical tasks.

#### 5.3 Results

As hypothesized – although still a remarkable result – the haptic DSS allowed successful car following without any visual feedback (condition H). Apparently the haptic feedback loop was informative enough that it could replace the visual feedback temporarily (in this case, 92 seconds). It required concentration though, and subjects often reported they preferred to also have the visual feedback available.

For all trials and subjects, three crashes occurred during a H repetition, all when  $T_{dist}$  was present, which could mask the information of the DSS: no crashes occurred during  $H^*$  or any of the other tasks). Additionally, eight instances of extreme drift occurred: defined as when the THW reached values of over 2.5 seconds.

Crashes and extreme drift all occurred after more than half of the time had passed, and the trials containing them were removed from further analysis (leaving three repetitions per condition instead of four).

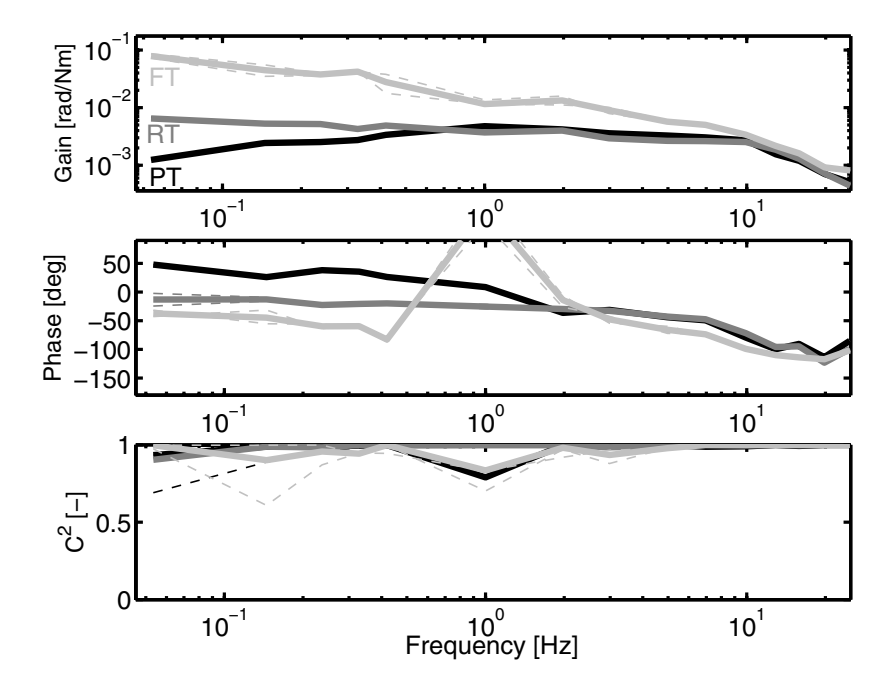


**Figure 5.7:** Admittance of a typical subject, estimated during each of the three tasks: maintain force (FT), relax (RT) and maintain position (PT). The top graph shows the magnitude of the admittance, the middle graph the phase lag, and the bottom graph the squared coherence. The thin dashed lines show each of the two repetitions, the thick line shows the results for the time-average over the two repetitions.

#### 5.3.1 FRFs of the Admittance

All subjects showed the ability to adapt their admittance, except for two subjects. They did not show an increase in admittance during FT compared to RT, nor during VH compared to V. Most likely these subjects required more training than the rest, and they were removed from further analysis.

**Coherence** For all subjects, the admittance could be estimated with high coherences  $(\hat{\Gamma}^2_{T_{dist}\theta} \geq 0.8)$ , for both classical tasks and car-followings tasks. The coherence deteriorated for some subjects at the lowest frequencies (and then most during condition V). The generally high coherences indicate that linear techniques may be used.

**Car Following** The admittance of a typical subject is shown in Figure 5.6 for two of the driving conditions, V and VH. Some intra-subject variability in the admittance is present, yet it can be clearly seen that below 1-2 Hz the admittance is larger during

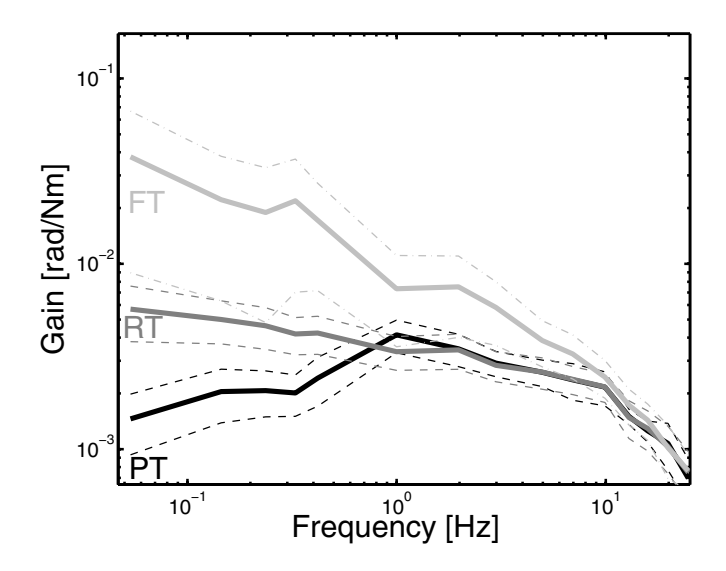


**Figure 5.8:** The magnitude of the admittance averaged over all subjects, estimated during each of the three classical tasks: maintain force (FT), relax (RT) and maintain position (PT). The thick line is the average, the thin lines show the standard deviation over all subjects.

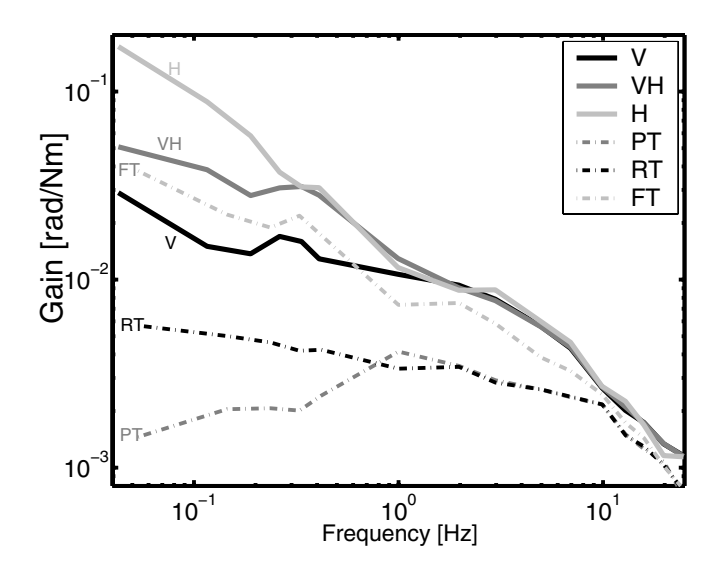


**Figure 5.9:** The magnitude of the admittance averaged over all subjects, estimated during every classical task (FT, RT, PT; dash-dotted lines) and every driving task (V, VH, H; solid lines).

VH compared to V. In general the admittances estimated during driving were more noisy (lower coherence, more variability) than during the classical tasks, which was to be expected.

**Classical Tasks** Figure 5.7 shows the admittance during classical tasks for another typical subject. The ability to adapt the admittance to best accomplish a task is clearly shown: the largest admittance is found during FT, the smallest admittance during PT and the admittance during RT lies in between. The intra-subject variability was substantially smaller during classical tasks, compared to car-following tasks.

The inter-subject variability during classical tasks is shown in Figure 5.8 where the admittances were averaged over all eight subjects, and the standard deviation is shown by the thin dotted lines.

**Comparison** In Figure 5.9) the admittances of car-following task are shown together with the admittances during classical tasks. The admittances were averaged over all eight subjects. It can be seen that the admittance during normal driving (V) lies between RT and FT, while with haptic feedback (both VH and H) the admittance increases even beyond FT.

#### **5.3.2** FRFs of $H_{control}$

 $H_{control}$  (the total response to  $v_{rel}$ ) could be estimated with relatively high coherences ( $\hat{\Gamma}^2_{v_{lead}v_{rel}} \geq 0.8$ ) during V and VH, although the coherences decreased somewhat at the higher frequencies (above 0.2 Hz), especially during V. During H the coherences were generally lower ( $\hat{\Gamma}^2_{v_{lead}v_{rel}} \geq 0.6$ ).

Figure 5.10 shows  $H_{control}$  for a typical subject. When comparing  $H_{control}$  during VH to that during V, a shift is notable: a smaller amplitude at lower frequencies, and a larger amplitude at higher frequencies. This means that at lower frequencies the drivers reacted with less pedal displacements  $\theta_c$  to the same changes in  $v_{rel}(t)$ .

The figure also shows that the driving trials with  $T_{dist}$  ((V,VH; solid lines) are similar to the driving trials without ( $V^*,VH^*$ ; striped lines), except for driving during with haptic feedback only. In that case, the coherence and  $H_{control}$  were smaller when  $T_{dist}$  was present(H), compared to when it was absent ( $H^*$ ).

#### 5.3.3 Time Domain Analysis

**Car-Following Tasks** The effect of the DSS on car-following performance and workload metrics were the same as found in (Mulder et al., 2005b): a decreased workload (lower standard deviation of  $\theta_c$ ) was sufficient to realize the same performance (similar standard deviation of THW and iTTC).

The only time domain analysis will be shown for the EMG results. Figure 5.11 shows how  $EMG_{rel}$  is smaller during haptic feedback for every subject. As can be seen, the results did not vary when torque perturbations were applied or not.

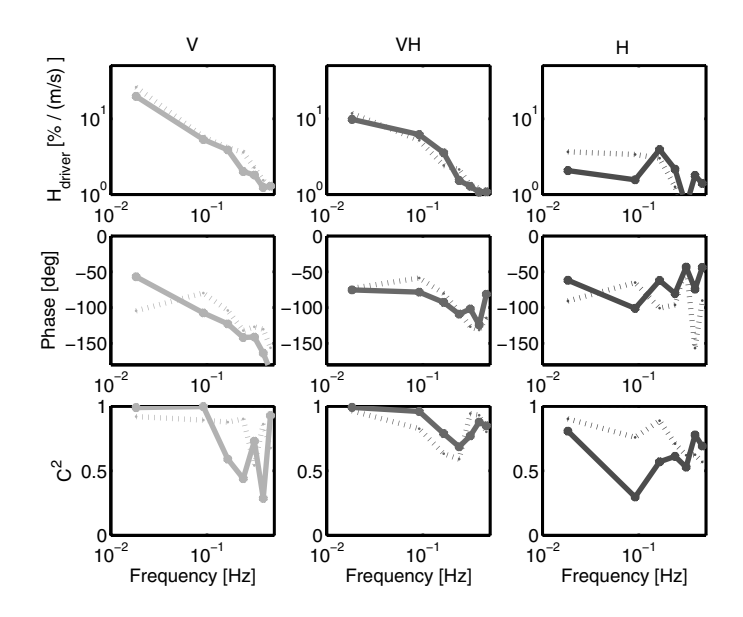


**Figure 5.10:** The gain, phase and coherence of  $H_{control}$  of typical subject. The solid lines denote conditions V, VH, and H (from left to right). The striped lines denote the same DSS conditions, but then without the torque perturbations.

**Classical Tasks** Figure 5.12 shows the  $EMG_{rel}$  results for the classical tasks: during PT there is a lot of co-contraction, during the RT there is very little muscle activation, and during the FT there is some muscle activation.

#### 5.4 Discussion

The time-domain and frequency domain results indicate that the control strategies of the subjects changed considerably when they received the additional haptic feedback from the DSS. The objectives of the study – to simultaneously estimate FRFs of the response to lead vehicle speed perturbations and to gas pedal torque perturbations – were realized by separating the perturbations in the frequency domain, and then applying them at the same time.

Coherences were generally high coherences, justifying the linear identification tools under these conditions. Additionally, the torque perturbations that were needed to estimate the motion control behaviour of the ankle-foot complex (i.e. the admittance) did not substantially influence the overall car-following control behaviour.

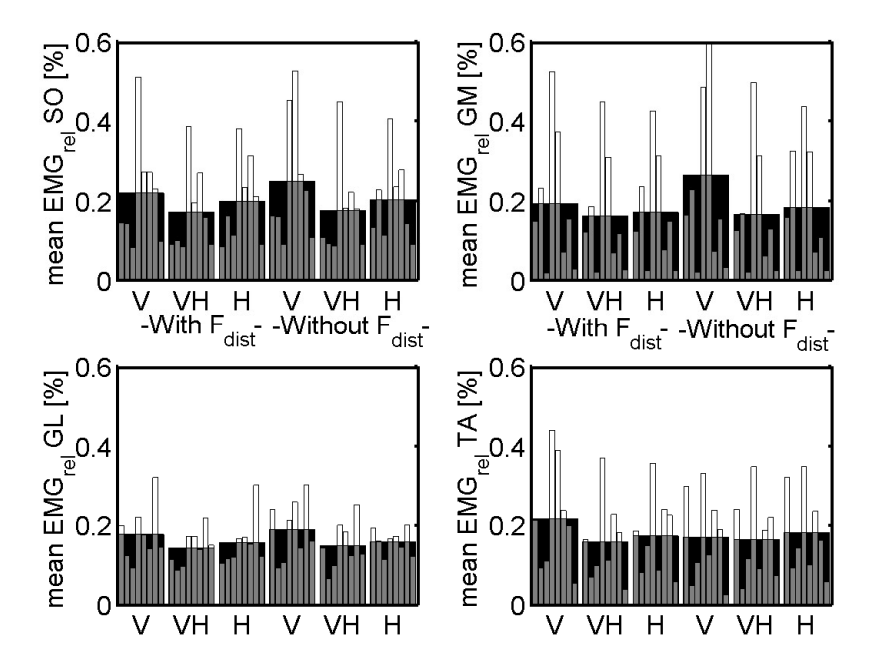


**Figure 5.11:**  $EMG_{rel}$  of each muscle during all the driving tasks, averaged over all subjects. Small transparent bars show individual results.

#### 5.4.1 Effect of DSS on Car Following

The general effect of the DSS on car-following – reduced control effort (described by the standard deviation of pedal depressions) to realize the same performance (described by the standard deviation of THW or iTTC) – relates well to other studies with a haptic DSS (Mulder et al., 2004a,b). Especially relevant is the similarity to an experiment done in the same period, using the same subjects and the same experimental conditions, but in a more realistic driving simulator Mulder et al., 2005b. Both time-domain metrics and  $H_{control}$  match the results of that experiment, indicating that the simplified driving simulator used in the current study was good enough to capture relevant car-following behaviour for the given experimental conditions.

The fact that car-following with only haptic feedback (H) was possible for a prolonged period, indicated that the haptic feedback can temporarily replace the visual feedback loop in case of visual inattention. However, drivers indicated they preferred to also have visual feedback, suggesting it is not likely that the DSS will evoke more driver visual inattention. This needs to be investigated in future experiments.

70 CHAPTER 5

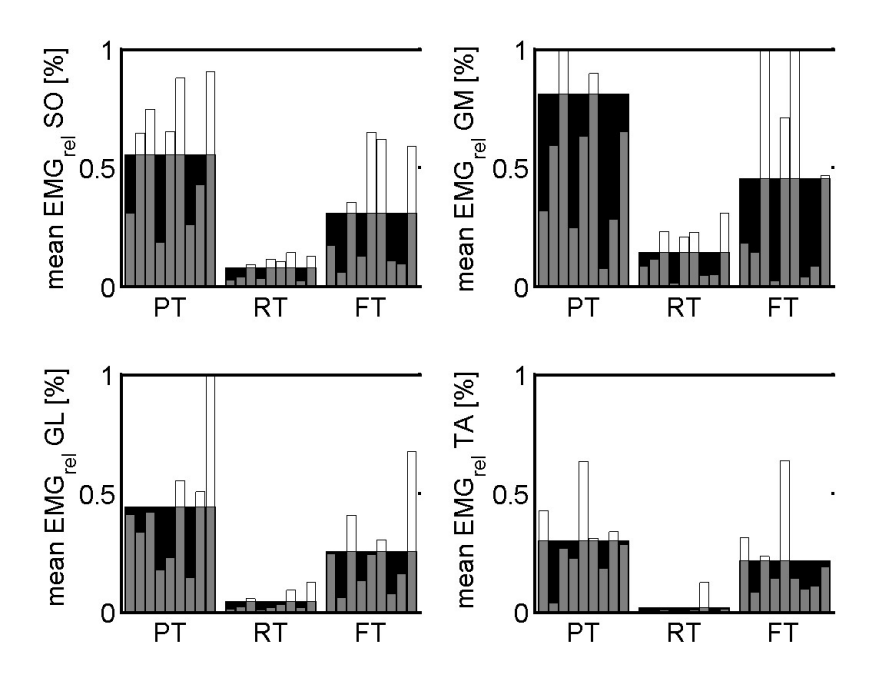


**Figure 5.12:**  $EMG_{rel}$  of each muscle during all the classical tasks, averaged over all subjects. Small transparent bars show individual results.

**FRF of**  $H_{control}$  For all subjects, the FRF of  $H_{control}$  showed that the DSS evoked a shift in the frequency characteristics of the response when compared to unassisted driving. The amplitude of the pedal rotations was larger at higher frequencies (above 0.1-0.2 Hz), and smaller at lower frequencies. This corresponds to the observed decrease in standard deviation of  $\theta_{c}$ : a relative increase in amplitudes at low frequencies will cause a larger standard deviation than a relative increase of amplitudes at higher frequencies (that are already lower due to the 1st order characteristics of  $H_{control}$ ).

#### 5.4.2 Effect of DSS on Admittance

The admittance was used to describe the spinal contribution to the overall response  $H_{control}$ . At frequencies above 10 Hz, the admittance of all tasks (car-following and classical) converged; inertial properties dominated the behaviour there. At lower frequencies subjects displayed a substantial adaptation range of the admittance (the smallest during the maximal PT, the largest during driving with haptic feedback.

The DSS provoked drivers to adopt a force task strategy, and to increase their admit-

tance. Above 1 Hz the admittances measured during RT and FT are roughly comparable in magnitude to studies that estimate ankle joint dynamics during similar tasks with higher bandwidth perturbations (e.g. Agarwal et al, 1977b; Toft et al., 1991). The admittances estimated during PT and RT are closely comparable to a previous study done on the ankle-foot complex manipulating a gas pedal (Abbink et al., 2004a).

The adaptability of the admittance is the result of – amongst others – muscle-co contraction and reflexive activity (by muscle spindles and Golgi tendon organs). The extent to which these mechanisms contribute to the admittance is an interesting question, that has implications for the design. The contributions have been quantified for the upper extremity during classical position task in previous studies (Van der Helm et al., 2002), which made use of a parameterized neuromusculoskeletal model. Due to the low frequencies, contributions of slower feedback systems (like visual feedback and tactile feedback) cannot immediately be excluded.

Driving with DSS increased the admittance even beyond the force task. However, the observed differences between classical tasks and car-following tasks could partly be the effect of amplitude non-linearity, a well-known biomechanical property (Cathers et al., 1999) that states that increased amplitudes of deviation result in increased admittance. The amplitudes during the three classical tasks were comparable ( $STD\theta \approx 0.7[deg]$ ), but substantially smaller compared to those during the three car-following tasks as well ( $STD\theta \approx 3[deg]$ ). This difference makes that direct comparisons must be taken with caution, until it has been investigated how large the amplitude effect is for these experimental conditions.

**Implications** Results for admittance at frequencies well below 1 Hz - such as estimated in the current experiment - have not been reported previously. The admittances are usually estimated only above 1 Hz, which may be well suited to determine the mass-spring-damper characteristics of a limb, but cannot be extended to fully explain motion control during low-frequency control tasks such as car-following. The current method is a first step toward such understanding and is expected to also be applicable to other continuous control tasks (e.g. steering a car).

**Future Research** Two main research questions remain. First of all it was hypothesized that driving with DSS would result in increased reflexive activity. To fully answer this more research is necessary, although two supporting results can be given. The first is that the difference in admittance between V and VH is substantial, and cannot be explained by the slight decrease in muscle co-contraction alone. The second was found by a cross-over model parameterization study, performed on the same subjects (Mulder et al., 2005a,b): the results showed a decrease in total time delay. Such a fast response time could be the result of increased use of fast reflexive control.

The second research question is the relative contributions of visual control actions and spinal control actions to car-following behaviour. It is hypothesized that the visual gains contained in  $H_{vis}$  will be smaller while using the DSS: since  $H_{control}$  is constituted by  $H_{vis}$ , and the admittance the DSS provokes an increased admittance, while the total  $H_{control}$  is similar or even smaller.

To address such research questions and hypotheses a driver model is needed. It needs to be detailed enough to describe changes in neuromuscular control at the level of reflexive and muscle-contractions; and should also be able to describe the interaction between spinal and visual contributions to car-following control behaviour. In an upcoming research study such a model is proposed and parameterized.

#### 5.5 Conclusions

For the experimental conditions studied, the following conclusions are drawn:

- The DSS provides drivers with an additional haptic feedback loop for car-following, that can even replace the visual feedback loop temporarily.
- When visual feedback is supplemented with haptic feedback, beneficial changes
  in car-following behaviour were found: less control effort is needed to realize the
  same car following performance. This was shown by a decrease in the standard
  deviation of pedal positions (accompanied by decrease in all lower leg muscle
  activity) for the same performance metrics such as the standard deviation of time
  headway and time-to-contact.
- A successful technique was proposed to simultaneously estimate the frequency response functions (FRFs) in response to torque perturbation (the admittance) and lead vehicle perturbations (H<sub>control</sub>). Both FRFs could be estimated with high coherences while following a lead vehicle with and without the aid of a haptic driver support system (DSS). The torque perturbations needed to estimate the admittance did not influence the car-following behaviour substantially.
- The DSS caused a shift in pedal control actions from large-amplitude and low-frequent toward smaller-amplitude and higher frequent: the FRF of  $H_{control}$  (with input relative velocity and output pedal position) had a smaller gain at low frequencies and a slightly increased gain at higher frequencies. This frequency-domain result corresponds to the found decrease in pedal displacements.
- The DSS causes drivers to adopt a force task strategy. The admittance with DSS
  was substantially larger compared to unassisted driving. The ability to adapt the
  admittance was also shown for so-called 'classical tasks': the largest admittance
  is measured during a force task, followed by a relax task, followed by the position
  task.

# Modeling the Effects of Haptic Feedback on Neuromuscular Control and Car-Following Behaviour.

David A. Abbink, Frans C. T. van der Helm, Mark Mulder, Max Mulder, Erwin R. Boer Submitted to: *Biological Cybernetics* 

Everything should be made as simple as possible, but not one bit simpler.

– Albert Einstein

In previous research a haptic driver support system was evaluated, that enabled drivers to realize the same car-following performance with a reduced control effort. Drivers were shown to adopt a force-task strategy: giving way to the feedback torques.

The goal of this paper is to understand how drivers realized the observed control behaviour, both at the level of car-following and of neuromuscular motion control. To attain the goal, a computational linear driver model was developed that contained a neuromusculo-skeletal (NMS) part in addition to a visual control part. The NMS part was modeled by several physiological parameters such as: intrinsic visco-elasticity due to muscle co-contraction; force feedback by the Golgi tendon organ reflex; position and velocity feedback by the muscle spindle reflex; neural time delays; inertia. The visual controller was modeled as a simple PD controller with time-delays. Model parameters were quantified using car-following data previously obtained in a driving simulator, where subjects (n=8) were asked to maintain a constant time headway to a lead vehicle, with and without the haptic DSS. The parameter fit procedure was repeatable and yielded a driver model that predicts car-following metrics, pedal positions and forces accurately (both in time and frequency domain).

The NMS parameters showed that drivers gave way to the haptic feedback torques through increased Golgi tendon organ activity and decreased muscle co-contraction. The visual gains were found to decrease for all subjects. It is concluded that the DSS allows some part of the necessary control actions to be done on a spinal level, thereby reducing the visual workload of the drivers.

74 CHAPTER 6

#### 6.1 Introduction

A promising approach to improve driving comfort and safety on highways is to provide drivers with a support system that aids them in tasks such as car following. In previous research a haptic driver support system (DSS) was developed and tested in a driving simulator environment (Mulder et al., 2004a,b, 2005b; de Winter et al., 2006). The DSS provided drivers with haptic feedback, which was realized by measuring the separation to the lead vehicle, and translating that information continuously to additional torques on the gas pedal.

The influence of the DSS was shown to be beneficial. By looking only at car-following performance metrics, the results were marginally positive (e.g. slightly smaller standard deviation of time headway (THW<sup>1</sup>) and inverse time-to-contact (iTTC<sup>2</sup>). However, the driver's control inputs were also measured (gas pedal torque and deviations), and their standard deviation was shown to decrease with the DSS. Apparently, drivers needed less control effort to reach a similar (or even slightly better) performance.

Although the beneficial results are promising, it remains unclear how drivers actually realize such benefits. Did the DSS cause increased visual attention or motivation, or improved perception of the separation states? Or did part of the control actions already take place on a spinal level, through fast reflexive response to the pedal torques?

General car-following models When trying to deduce driver control strategies, a driver model is indispensable. Numerous car-following models have been proposed (for a review, see Brackstone and McDonald, 1999), although only several recent models have been validated. Car-following is generally modeled as a closed-loop control task, where the driver uses perceived signals (e.g. relative velocity and position) to control the separation between his car and the lead vehicle. However, driver control actions are usually not measured (Fang et al., 2001, Ranjitkar et al., 2005). Most car-following models are therefore not very detailed, and examine the relationship between the velocities or accelerations of the vehicles, without addressing driver control actions. Figure 6.1 shows a more detailed measurement scheme of a driver in a car-following task. The most detailed models in literature (Bengtsson et al., 2001, Mulder et al., 2005b) capture the dynamics of  $H_{control}$ . It has relative velocity  $v_{rel}$  (plus  $x_{rel}$ ) as input, and gas pedal position  $\theta_c$  as output, which in turn is the input for the car kinematics  $H_{car}$ . Differences between the velocity of the car  $v_{car}$  and the lead vehicle  $v_{lead}$ , result in  $v_{rel}$ , which the driver is assumed to control back to zero. The relative position  $x_{rel}$ , obtained by integrating  $v_{rel}$ , will be controlled to an acceptable value.

A detailed car-following model Although such modeling may be suitable for many applications, it lacks the detail to address the present case, where additional torques from the DSS influence the driver's control of the pedal position. Therefore, a more detailed driver model was proposed by (Abbink et al., submitted), where  $H_{control}$  is decom-

 $<sup>{}^{1}</sup>THW = rac{x_{rel}}{v_{car}}$ , with  $x_{rel}$  the relative position, and  $v_{car}$  the own vehicle velocity  ${}^{2}iTTC = rac{v_{rel}}{x_{rel}}$ , with  $v_{rel}$  the relative velocity between the lead vehicle and own vehicle

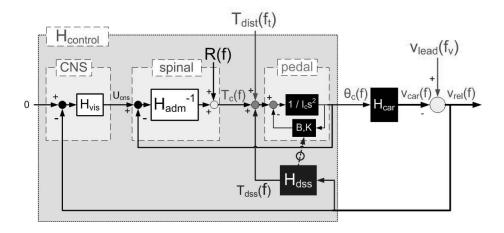


**Figure 6.1:** Closed-loop frequency-domain measurement scheme of a driver in a car-following task, as used in Abbink et al., submitted.  $H_{control}$  was identified using the lead vehicle perturbation  $v_{lead}$  at frequencies  $f_v$ , and was modeled as containing four subsystems. The pedal dynamics and driver support system  $(H_{dss})$  are known, while  $H_{adm}$  was estimated using a pedal torque disturbance  $T_{dist}$  at frequencies  $f_v$ . More information is given in the text.

posed into four sub-systems. The first is the visual controller  $H_{vis}$ . It gives a supra-spinal command input to the second part: a spinal neuro-musculo-skeletal (NMS) model, described as an admittance  $^3H_{adm}$ . The output of the NMS model is the gas pedal torque  $T_c$ . The gas pedal position is determined by the sum of all torques acting upon it, and by the pedal dynamics, which are described by its inertia  $I_c$ , stiffness K (and damping B). The fourth sub-system describes the haptic driver support system  $H_{dss}$ . When the DSS is switched on, it will provide torques  $T_{dss}$  to the gas pedal, as well as changes in the pedal stiffness K. A full description of the designed DSS can be found in Mulder et al., 2005b.

Several sub-systems can be identified by measuring the response to perturbations: with  $v_{lead}$  the frequency response function (FRF) of  $H_{control}$  can be estimated, and with  $T_{dist}$  the FRF of  $H_{adm}$ . This was done in a driving simulator study (Abbink et al., submitted) in which eight subjects were asked to perform a car-following task with and without the haptic DSS. Besides confirming previous research that the DSS enabled similar car-following performance with reduced control effort, one of the most important results was that the DSS entailed a substantial increase in the admittance  $H_{adm}$ . In other words, drivers became more slack and gave way to the DSS torques. It was hypothesized that most of this increase was due to reflexive activity, which would also explain the decrease in overall response time found in previous haptic DSS research (Mulder et al., 2005a,b). A second hypothesis was that  $H_{vis}$  could be smaller, since some of the control actions

 $<sup>^3</sup>$ The admittance is a common way to describe NMS dynamics, and constitutes the causal dynamic relationship between  $T_c$  and  $\theta_c$ 

**Table 6.1:** Properties of the data obtained in the experimental study (Abbink et al., submitted).  $F_{sample}$  is the sample frequency,  $t_{anl}$  the time duration of all analyzed signals,  $(f_{low})$  denotes the lowest frequency contained in a signal,  $f_{hi}$  the highest. Other abbreviations and data properties are discussed in the text of paragraph 6.2.1

	Task	Perturbation	Repetitions	F <sub>sample</sub>	$t_{anl}$
Ì	V, VH, H	$T_{dist}, v_{lead}$	4	200 [Hz]	81.92 [s]
•	$V^*, VH^*, H^*$	v <sub>lead</sub>	4	200 [Hz]	81.92 [s]
ĺ	PT,RT,FT	$T_{dist}$	2	250 [Hz]	65.536 [s]

Frequencies	Perturbation	$f_{low}$	$f_{hi}$
$f_v$	$v_{lead}$	0.02 [Hz]	0.5 [Hz]
$f_t$	$T_{dist}$ (full)	0.04 [Hz]	0.5 [Hz]
	$T_{dist}$ (red.)	1 [Hz]	25 [Hz]
$f_r$	none	remaining frequencie	

were already done on a spinal level.

Parameterizing the detailed car-following model The goal of the present study is to investigate these two hypotheses, and to understand how drivers realized the observed control behaviour, both at the level of car-following and of neuromuscular motion control. In order to attain this goal, a driver model is designed that parameterizes  $H_{vis}$  and  $H_{adm}$ and – subsequently – the parameters are quantified using experimental data.  $H_{vis}$  will be described as a simple PD controller.  $H_{adm}$  will be described by physiological parameters such as limb inertia, intrinsic visco-elasticity due to muscle co-contraction, force feedback by Golgi tendon organs (GTO's) and muscle stretch and stretch velocity feedback from muscle spindles, muscle activation dynamics and neural time delays. Ample research exists in which NMS properties are described with such parameters, both for the upper extremity (De Vlugt, 2004; De Vlugt and Van der Helm, 2006; Schouten, 2004; Van der Helm et al., 2002) and for the lower extremity (Kirsch and Kearney, 1997; Mirbagheri et al., 2000; Paul et al., 2005; Toft et al., 1991); but never for the anklefoot complex in interaction with a gas pedal. Furthermore, the NMS response is usually studied during classical tasks (e.g. 'maintain position', 'relax', 'maintain force'), not while simultaneously engaged in a daily-life task like car following. In that case, the response is not only the result of NMS dynamics ( $H_{adm}$ ), but also of supra-spinal processes ( $H_{vis}$ ). The separation of the two is complicated, and this study proposes a novel method to do SO.

#### 6.2 Method

A driver model was designed and parameterized on driving simulator data. A full description of the method to obtain that data can be found in Abbink et al., submitted. For convenience it is also summarized in the next paragraph (also see Table 6.1).

The parameters were quantified in two stages. In the first stage, the NMS parameters were obtained by a frequency-domain fit of a NMS model to  $\hat{H}_{adm}$ . In the second stage, the estimated NMS parameters were entered into a SIMULINK model that also described other sub-models (the car dynamics, pedal dynamics, DSS), and then the visual parameters were obtained by a time domain fit.

#### 6.2.1 Summary of Used Data

Eight healthy and experienced drivers participated in an experiment (Abbink et al., submitted) consisting of three main parts. The most important part was a car-following experiment where subjects were asked to maintain a constant THW of 1 second. Their control behaviour was determined in response to two unpredictable multi-sines perturbations  $T_{dist}$  and  $v_{lead}$ , which were separated in the frequency domain. The lead vehicle speed  $v_{lead}$  contained power only at frequencies  $f_v$  (bandwidth 0.02-0.5 Hz). At these frequencies  $H_{control}$  could be estimated. While car following, small torque perturbations ( $T_{dist}$ ) were applied to the gas pedal at separate frequencies  $f_t$  (full power bandwidth 0.04-0.5 Hz, reduced power bandwidth from 1-25 Hz). At these frequencies the torque perturbations were used to estimate  $H_{adm}$ . Any remaining frequency points not contained in  $f_t$  and  $f_v$  are called  $f_r$ , which is the frequency set of the remnant R that describes responses not linearly related to either perturbation.

Car-following behaviour was measured at 200 Hz under three conditions: with only visual feedback (V); with visual and haptic feedback (VH); and without visual feedback, using only the haptic feedback from the DSS (H). The two other main parts of the experiment were done to obtain baseline conditions. One consisted of a repetition of the same car-following conditions but without the small torque perturbations. By comparing the two it was ensured that  $T_{dist}$  did not influence the car following. The other comparison part consisted of classical admittance measurements. They were measured at 250 Hz during three classical tasks: minimize pedal rotations (position task, PT), minimize pedal torque deviations (force task, FT) and relax (relax task, RT).

While performing each trial the following signals were measured: the contact torque  $T_c(t)$  [Nm], the torque perturbation  $T_{dist}(t)$  [Nm], the pedal depression  $\theta_c(t)$  [rad] and EMG signals of four relevant lower leg muscles. During car following the following signals were measured as well: the lead vehicle perturbation  $v_{lead}(t)$  [m/s], the own vehicle speed  $v_{car}(t)$  [m/s], and the relative separation  $x_{rel}(t)$  [m]. The first seconds of all signals were discarded in order to reduce potential onset effects and to yield signals containing exactly 16384 ( $2^{14}$ ) samples, which is convenient for fast Fourier transform (FFT) analysis. Note that signals measured during car-following and classical tasks have slightly different time and frequency domain characteristics, due to the two different sample frequencies (see Table 6.1).

#### 6.2.2 Admittance Parameterization

The admittance parameterization was done in four steps (see Figure 6.2). In the first step, a Box Jenkins model was fitted on resampled time-domain signals, averaged over all repetitions. In the second step, a frequency-domain parameterized NMS model

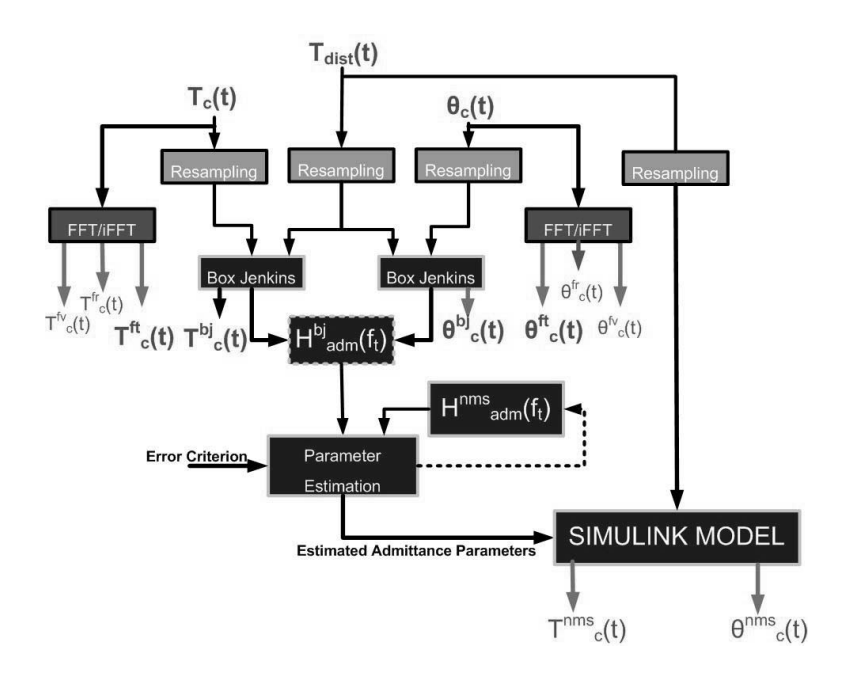


**Figure 6.2:** Overview of all steps to obtain the NMS parameters and signals for validation of the fit. Box Jenkins models were fitted to the resampled time-domain data, and used to determine the frequency response function  $\hat{H}^{bj}_{adm}(f_t)$ . The parameters of the NMS model  $H^{nms}_{adm}(f_t)$  were determined iteratively, by minimizing an error criterion. Model validation was done in time-domain, by entering the estimated parameters in a computational model (in SIMULINK) and comparing torque and position in the time domain.

 $H_{adm}^{nms}(f_t)$  was developed. In the third step, it was fitted to the frequency domain output of the Box Jenkins model  $\hat{H}_{adm}^{bj}(f_t)$ , by minimizing an error criterion. The output of this step was a set of NMS parameters. Finally, the validity of the parameter fitting procedure was determined by checking several frequency and time-domain properties of the fits. The following paragraphs describe the steps in more detail.

**Box Jenkins Fitting** A Box Jenkins model is a variation on the better known autoregressive models ARX and ARMAX. Autoregressive models produce signals with reduced noise-components (in this case  $T_c^{bj}(t)$  and  $\theta_c^{bj}(t)$ ). Fitting the parameters of a NMS model to FRFs of these signals – instead of to the raw data – has been previously shown to lead to better parameter fits (De Vlugt and Van der Helm, 2006).

The general structure of a Box Jenkins model describes the output y(t) as a result of linear input u(t) and remnant noise e(t), according to:

$$y(t) = \frac{B(q)}{F(q)}u(t - n_k) + \frac{C(q)}{D(q)}e(t)$$
(6.1)

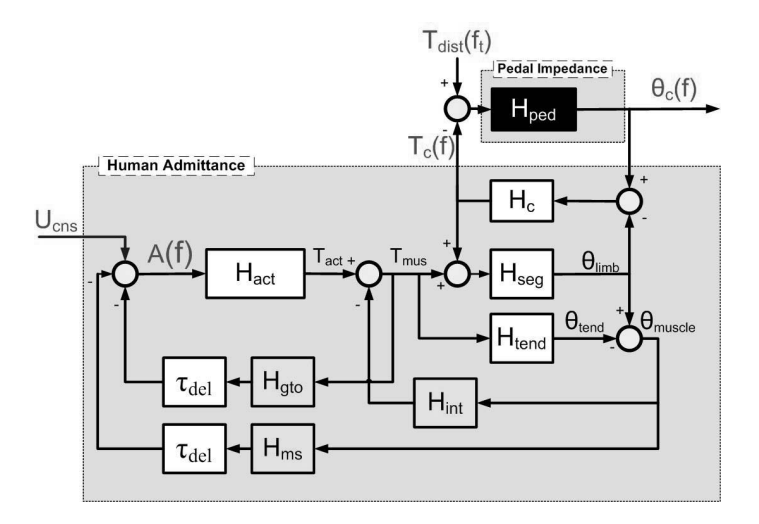


**Figure 6.3:** Linear frequency domain block scheme of the NMS model  $H_{adm}$ .

where  $n_k$  is a time delay (zero in this case), and B, F, C and D are polynomials of shift operator q, that each may have a different order and different coefficients. The coefficients of the polynomials are estimated by minimizing e(t).

Box Jenkins was used because it can better capture e(t) than other autoregressive models. When estimating signals in response to  $T_{dist}$ , all other inputs are considered to be noise e(t), including  $v_{lead}$  which is a considerable 'source of noise'. Because  $v_{lead}$  enters the system at a different point, e(t) cannot be assumed to be white noise or even to have the same color (filtering) as u(t). Therefore, the flexible structure of Box Jenkins (with noise-shaping filter  $\frac{C(q)}{D(q)}$ ) leads to better results than ARX or ARMAX<sup>4</sup> structures. The fitting was done on resampled data (factor 4) so that frequencies beyond the bandwidth of the perturbation were not weighed too heavily in the fit. The Box Jenkins procedure used  $T_{dist}$  as the input to yield two frequency domain models,  $\hat{H}_{\theta,T_{dist}}$  and  $\hat{H}_{t_c,T_{dist}}$ , both evaluated at frequency  $f_t$ . The two transfer functions were used to simulate  $T_c^{bj}(t)$  and  $\theta_c^{bj}(t)$ . Also the admittance of the Box Jenkins models was estimated by:

$$\hat{H}_{adm}^{bj} = \frac{\hat{H}_{\theta, T_{dist}}}{\hat{H}_{T_c, T_{dist}}} \tag{6.2}$$

The order of the model (11th order for all polynomials) was chosen iteratively, by checking both the frequency domain fit and the time domain fit (VAFs) for the best characteristics.

<sup>&</sup>lt;sup>4</sup>Note that for the classical tasks  $v_{lead}$  was not present, and an ARMAX structure was best (in that case e(t) was assumed to have the same filtering as u(t) (meaning D(q)=F(q)).

**Parameterized Linear NMS Model**  $H_{adm}$  was parameterized by a linear NMS model, which describes the dynamics of the ankle-foot complex interacting with the gas pedal. A block diagram is shown in Figure 6.3.

The inputs of the NMS model are  $T_{dist}(f_t)$  and  $\theta_{ref}(f)$ , a supra spinal signal representing the reference pedal position (assumed to be zero at frequencies  $f_t$ ). The measurable model outputs are  $T_c(f)$  and  $\theta_c(f)$ . All signals and parameters are defined at the pedal rotation point, with torques acting around it.

The model structure is an extension of NMS models previously proposed in our research group (Van der Helm et al., 2002, De Vlugt, 2004, De Vlugt and Van der Helm, 2006, Schouten, 2004). It contains the following components, described at endpoint: intrinsic muscle stiffness and damping; second order muscle activation dynamics; muscle stretch and stretch velocity feedback from muscle spindles; force feedback from GTOs, tendon stiffness and contact visco-elasticity. The model is represented in the frequency domain where s ( $=j2\pi f$ ) denotes the laplace operator.

The motion of the inertia  $I_{seg}$  is the result of the sum of  $T_c(s)$  and  $T_{mus}(s)$ , the torque exerted by all the muscles. The motion is given by:

$$\theta_{limb}(s) = H_{seg}(s) \left[ T_c(s) + T_{mus}(s) \right], \tag{6.3}$$

where

$$H_{seg}(s) = \frac{1}{I_{seg}s^2}$$

with  $I_{seg}$  the endpoint inertia of the limb. It contains everything moving *after* the force sensor, so not only the ankle-foot complex, but also the part of the gas pedal linkage after the force sensor (which was previously estimated;  $I_{linkage} = 23.3 \ gm^2$ ).

 $T_{mus}$  consists of an intrinsic and a reflexive component, according to:

$$T_{mus}(s) = -H_{int}(s)\theta_{mus}(s) + H_{act}(s)A(s)$$
(6.4)

The intrinsic component describes the increase in muscle stiffness and damping due to (co-)contraction, according to:

$$H_{int}(s) = k_{int} + b_{int}s$$

with  $k_{int}$  and  $b_{int}$  representing the muscle stiffness and damping of already activated muscles, respectively.

The reflexive component is defined by muscle spindle dynamics, GTO dynamics and muscle activation dynamics. Muscle activation describes the process of active muscle force build-up following a neural activation signal A(s). It is approximated by a second-order model (Bobet and Norman, 1990; De Vlugt, 2004; Olney and Winter, 1985; Schouten, 2004):

$$H_{act}(s) = \frac{1}{(\frac{1}{\omega_0^2})s^2 + \frac{2\beta}{\omega_0}s + 1}$$

with eigen-frequency  $f_0$  (= $\frac{\omega_0}{2\pi}$ ) and relative damping  $\beta$ , which was assumed to be 0.7 (critically damped). The activation signal A(s) is the result of muscle spindle and GTO feedback, according to:

$$A(s) = -H_{ms}(s)\theta_{muscle}(s) - H_{gto}(s)T_{mus}(s) + U_{cns}(s), \tag{6.5}$$

with muscle spindle dynamics:

$$H_{ms}(s) = (k_{pos} + k_{vel}s) e^{-s \tau_{del}}$$

and GTO dynamics:

$$H_{gto}(s) = k_f e^{-s \tau_{del}}$$
,

and  $U_{cns}(s)$  the supra-spinal command (assumed zero at  $f_t$ ).

Reflexive feedback is characterized by an inherent time delay, modeled as a fixed  $\tau_{del}$  of 40 ms. This value is often reported in literature for mono-synaptic reflexes in the lower extremities (e.g. Kirsch and Kearney, 1997; Toft et al., 1991; Mirbagheri et al., 2000). The results of the parameter fit procedure was robust to changes in  $\tau_{del}$  over  $\pm 10$  ms. Muscle spindle parameters  $k_{pos}$  and  $k_{vel}$  represent the gains of the mono synaptic stretch and stretch velocity feedback. Their sign is allowed to be either positive or negative (excitory or inhibitory).  $k_f$  is the gain of the GTO feedback, often thought to have an inhibitory effect. However, it has been shown previously (Prochaska et al., 1997a) that during locomotion the GTO can have an excitory effect. The sign of the GTO gain is therefore allowed to be either positive (defined as inhibitory) or negative (excitory).

Tendons act as a serial elastic element to the muscles, resulting in a difference between  $\theta_{limb}$  and  $\theta_{muscle}$ . The stiffness of the tendon is described by  $k_{tend}$ ; and  $H_{tend}$  by:

$$H_{tend}(s) = \frac{1}{-k_{tend}} \tag{6.6}$$

Pedal rotations do not only cause joint rotations, but also small displacements of the skin or soft tissue. This effect is described by contact dynamics, according to:

$$T_c(s) = H_c(s) \left[\theta_c(s) - \theta_{limb}(s)\right]$$
(6.7)

with:

$$H_c(s) = k_{con} + b_{con}s$$

Contact elasticity and viscosity are represented by  $k_{con}$  and  $b_{con}$  respectively. The complete parameterized NMS model then follows from (6.3)-(6.7):

$$H_{adm}^{nms} = \frac{\theta_c}{T_c} = \frac{1}{H_c} + \frac{1}{H_{seg}^{-1} + [H_{act}H_{ms} + H_{int}]H_{filt}}$$
(6.8)

with:

$$H_{filt} = \frac{1}{1 - \left[\frac{k_{tend}}{k_{tend}H_{int}}\right]\left[H_{gto} + \frac{H_{ms}}{k_{tend}}\right]H_{act}}$$

**Parameter fit procedure**  $H_{adm}^{nms}$  was described by twelve NMS parameters (see equation 6.8): three that were assumed to be constant over all subjects and all conditions; three that were estimated for each subject, but were assumed not to vary over the conditions and therefore fixed; and six that were allowed to vary over all conditions.

Two of the three constant parameters have already been mentioned in paragraph 6.2.2 ( $\tau_{del}$ =0.04 [s] and  $\beta$ =0.7). The third, the muscle stretch feedback gain  $k_{pos}$ , was assumed to be zero. This parameter showed an extremely large standard error of the mean, meaning it could not be estimated reliably. The parameter had a negligible contribution to the error criterion and could assume any value. The values of the other parameters did not change much with the absence or presence of  $k_{pos}$ .

The three parameters that could reasonably be assumed constant for a subject during all tasks and repetitions were  $I_{seg}$ ,  $f_o$  and  $k_{tend}$ . They were estimated during the classical tasks, and kept constant during the car-following tasks.

The remaining six variable parameters ( $b_{int}$ ,  $k_{int}$ ,  $b_{con}$ ,  $k_{con}$ ,  $k_{vel}$ ,  $k_f$ ) were allowed to vary between tasks and repetitions.

Parameters were estimated by least-squares minimization of a frequency domain error criterion:

$$E_{nms} = \sum_{k=n_1}^{n_2} ln(\frac{\hat{H}_{adm}^{bj}(f_{t_k})}{H_{adm}^{nms}(f_{t_k})})^2$$
(6.9)

with k denoting the index of frequency samples. The accuracy of each parameter estimation was checked by the standard error of the mean, a measure of the variance of the parameter distribution (Ljung, 1999, De Vlugt and Van der Helm, 2006). Generally, parameters that have little contribution to the prediction error, will show large variances. Additionally, the variability of the fit for each repetition in the time-domain was checked. If the parameter variance is large, it should also result in variability over each repetition.

**Validation of the NMS parameterization steps** Entering the model parameters in a NMS model in SIMULINK yielded simulated signals (e.g.  $\theta_c^{nms}$ ). A common metric for validation is the variance accounted for (VAF), a measure of how well the variance of a measured signal x is approximated by its simulated counterpart  $\hat{x}$ , according to:

$$VAF = \frac{\sum_{n} |x(t_n) - \hat{x}(t_n)|^2}{\sum_{n} |x(t_n)|^2}$$
 (6.10)

For the classical tasks the variance is only the result of  $T_{dist}$ . The measured signals should therefore have mainly power at frequencies  $f_t$ . However, for driving tasks a substantial part of the variance is also due to a response to  $v_{lead}$  at  $f_v$ . When comparing the measured torque to the torque simulated with a Box Jenkins model with only input  $T_{dist}$ , the VAF will be low, even if the response to  $T_{dist}$  is perfectly described by the model. Therefore, to better judge the goodness of fit with VAFs, a frequency separation was done in the time domain. This was accomplished by an anti-causal filtering method, here called FFT/FFT. In order to produce only the linear response to  $T_{dist}$  a signal was

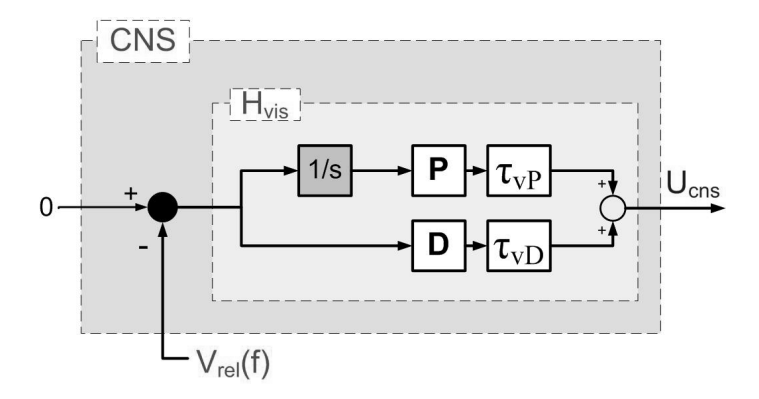


**Figure 6.4:** Parameters describing the output of the Central Nervous System (CNS) to the input of  $v_{rel}$ . The visual controller  $H_{vis}$  is modeled as a PD controller with time delays (see text), and produces the supra-spinal input  $U_{cns}$ .

transformed with FFT to the frequency domain, subsequently the power at all frequencies except  $f_t$  was set to zero, and finally the signal was transformed back to the time domain with iFFT. This yielded  $T_c^{f_t}(t)$  and  $\theta_c^{f_t}(t)$ , signals that only contained power at  $f_t$ . The same was done for frequencies  $f_v$ , and also for  $f_r$ , the remaining set of frequencies at which no power was applied. The three filtered signals together constitute the measured signal:

$$T_c(t) = T_c^{f_t}(t) + T_c^{f_v}(t) + T_c^{f_r}(t)$$
(6.11)

$$\theta_c(t) = \theta_c^{f_t}(t) + \theta_c^{f_v}(t) + \theta_c^{f_v}(t) \tag{6.12}$$

All VAFs for the NMS parameters were calculated with respect to the filtered signals  $T_c^{f_t}(t)$  and  $\theta_c^{f_t}(t)$ .

A disadvantage of the VAF metric is its insensitivity to fitting errors at high frequencies (because then the amplitudes are smaller, and contribute less to the variance). Therefore, another validation was done in the frequency domain, by comparing the FRFs of  $H_{adm}^{nms}(f_t)$  to  $\hat{H}_{adm}^{bj}(f_t)$  and the non-parametric FRF estimated from spectral densities,  $\hat{H}_{adm}(f_t)$ .

#### 6.2.3 Visual Controller Parameterization

The visual controller  $H_{vis}$  was parameterized as follows (see Figure 6.4):

$$H_{vis}(s) = \frac{U_{cns}}{v_{rel}} = \left[\frac{P}{s}\right] e^{-s\tau_{vP}} + [D] e^{-s\tau_{vD}}$$
(6.13)

84 CHAPTER 6

with P being a gain relating to  $x_{rel}$ , D a gain relating to  $v_{rel}$ , and  $\tau_{visP}$  and  $\tau_{visD}$  the corresponding time delays, respectively. This controller assumes that the driver tries to keep the relative velocity to zero, and simultaneously keep the  $x_{rel}$  at a desired value.

**SIMULINK model** Once the admittance parameters had been estimated, they were entered into a SIMULINK model which was modeled according to Figure 6.1. The car dynamics  $H_{car}$  were described by a realistic car model, kindly provided by Nissan Motor Company. It was the same model that was used in the driving simulator.

The visual model was implemented as shown in Figure 6.4. The NMS model  $H_{adm}$  was implemented as shown in Figure 6.3, containing the estimated values for the NMS parameters.  $H_{dss}$  was described by a non-linear relationship from inputs THW and iTTC to output  $\Delta K$ , being the added stiffness generated by the DSS. The exact formula can be found in previous literature (Mulder et al., 2005b).  $H_{ped}$  was parameterized by the inertia of the pedal, and its total stiffness (the sum of the constant spring stiffness and  $\Delta K$ ).

**Parameter fit and validation** Given  $v_{lead}$  and a set of visual parameters, the SIMULINK model generated driver control inputs (e.g.  $\theta_c^{vis}(t)$ ) but also resultant  $x_{rel}(t)$  and  $v_{rel}(t)$ . The four visual parameters were estimated by minimizing the following quadratic error criterion in the time domain, using data averaged over all repetitions:

$$E_{vis} = \sum_{k=n_1}^{n_2} (|\theta_c^{f_v}(t_k) - \theta_c^{vis}(t_k)|)^2$$
(6.14)

with k indexing the time samples,  $\theta_c^{f_v}$  being the filtered  $\theta_c$  (containing power only at  $f_v$ ), and  $\theta_c^{vis}$  being the simulated gas pedal position.

Validation was done with VAFs between  $\theta_c^{vis}$  and  $\theta_c^{fv}$  of the second 40 seconds. Note that this VAF measure also incorporates contributions by the NMS parameters.

**Total Driver Model Validation** Finally, all estimated parameters (NMS and visual) were entered in the SIMULINK model, which was subsequently run with both inputs  $T_{dist}$  and  $v_{lead}$ . Subsequently, for each condition (V, VH, H) the simulated outputs of  $\theta_c$ ,  $T_c$ ,  $x_{rel}$ ,  $v_{rel}$ ,

#### 6.3 Results

#### 6.3.1 NMS parameters

**Classical Tasks** The NMS parameters were estimated first for the classical tasks PT, RT and FT and are shown for a typical subject in Figure 6.5. The parameters were consistently estimated over the two repetitions, and the standard error of the mean (shown

**Table 6.2:** NMS parameters describing inertia  $I_{seg}$  ( $gm^2$ ), tendon stiffness  $k_{tend}$  (Nm/rad), and eigen-frequency of muscle activation dynamics  $f_0$  (Hz). The parameters were estimated for each subject (S1-S8) during the classical tasks, and kept constant for all repetitions and tasks.

Parameter	S1	S2	S3	S4	S5	S6	S7	S8
$I_{seg}$	105.4	220.0	146.9	99.0	139.2	105.9	127.8	154.4
k <sub>tend</sub>	1799	2420	3815	3117	2212	2933	1419	3998
$f_o$	1.1	1.0	1.2	1.8	1.0	1.1	1.4	1.2

in the error bars) is relatively small for each parameter. Moreover, VAFs for position and torque were over 90%, and the fits described the frequency domain characteristics well (shown in Figure 6.6) for all tasks and subjects. An intriguing result is the important role of GTO gain  $k_f$  in changing the admittance: the gain was positive (inhibitory) during FT, but negative (excitory) during PT. A NMS model without GTO activity did not fit well in the frequency domain, and resulted in reduced VAFs. The admittance during FT was further increased by reduced muscle co-contraction ( $k_{int}$  and  $b_{int}$ ) and more slack contact stiffness ( $k_{con}$ ). Muscle spindle feedback gain  $k_v$  was estimated consistently at relatively small values (usually excitory). The values of three constant parameters  $I_{seg}$ ,  $f_0$  and  $k_{tend}$  were determined (see Table 6.2), and used for the parameter fit during driving tasks.

Car-following Tasks The NMS parameters during the car-following conditions V,VH and H are shown for a typical subject in Figure 6.7. Again the standard error of the mean is small for all parameters. The VAFs for position and torque were less than during the more defined classical tasks, but still ranged between 60-80%, and the frequency domain fit was good (see Figure 6.8). The estimated NMS parameters during all tasks are shown for each subject in Table 6.3. The table also contains the means and standard deviation over all subjects. The increase in admittance when the DSS is activated is shown to be mainly brought about by an increased  $k_f$  (inhibiting GTO activity) and a decrease in  $k_{int}$  (muscle co-contraction); and to a lesser extent by decreased  $k_{con}$  (contact stiffness). Condition H was the least defined condition, with sometimes large drifts (for subjects 5 and 8 this condition was therefore discarded from further analysis). However, the admittance was even larger than during VH, which was usually fitted with increased  $k_f$ , and sometimes with reduced  $k_{int}$ . All NMS parameters are shown in Table 6.2.

A noteworthy result from the noise analysis done with the FFT/iFFT filtering, was that the remnant at  $f_r$  was smallest during VH (< 13% for V, < 9% for VH and < 21% for H). This indicates that subjects introduce less noise (at frequencies where the two perturbations did not contain power).

#### 6.3.2 Visual Parameters

The four visual parameters were fitted over the first or second half (determined randomly) of the time-averaged signals (a time period of  $\pm 40s$ ). For the conditions V

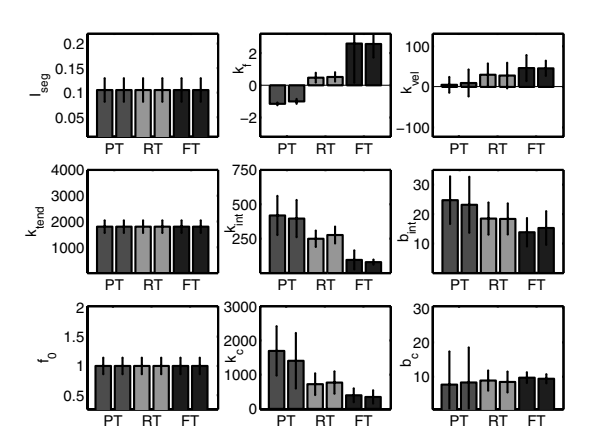


**Figure 6.5:** The estimated admittance parameters of a typical subject (S1) during classical tasks. Each of the nine graphs show first both repetitions of PT, then both repetitions of RT, and then both repetitions of FT. All parameters are discussed in the text. The error bars denote the standard error of the mean of each estimated parameter.

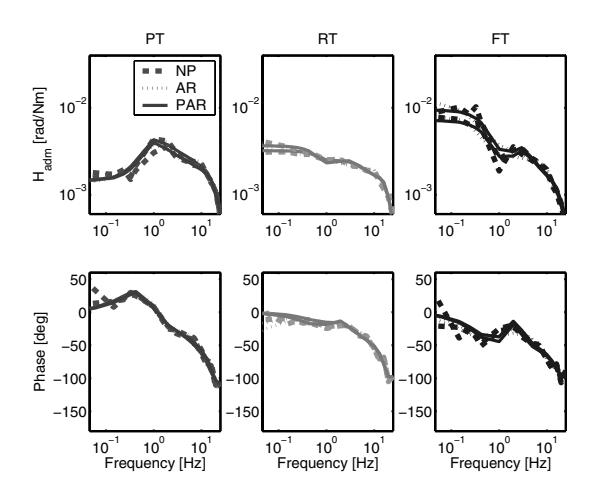


**Figure 6.6:** Gain and phase of the estimated admittances of a typical subject (S1) during both repetitions of each classical task. The left graphs show the maintain position task (PT), the middle the relax task (RT) and the right the maintain force tasks (FT). The thick dashed lines (NP) are the estimated non-parametric FRFs. The thin dotted lines (AR) are the FRF of the ARMAX model. The solid lines (PAR) are the FRF of the parameterized model.

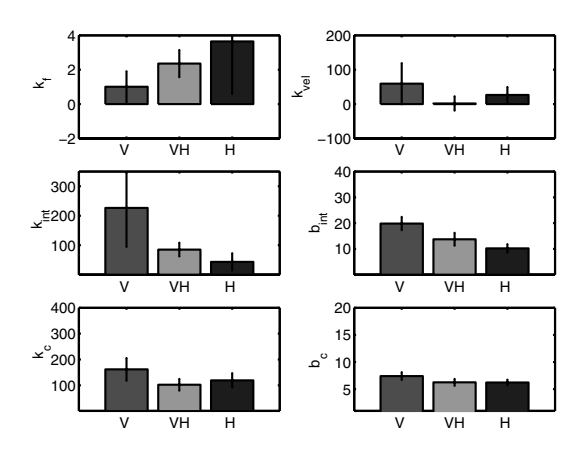


**Figure 6.7:** The estimated admittance parameters of a typical subject (S1) during car-following tasks. Each of the six graphs show the results of the parameter fit on the time-averaged trials of V, VH, and H. All parameters are discussed in the text. The error bars denote the standard error of the mean of each estimated parameter.  $k_f$ ,  $k_{int}$ ,  $k_{con}$  are in Nm/rad, and  $k_v$ ,  $b_{int}$  and  $b_{con}$  are in Nms/rad.

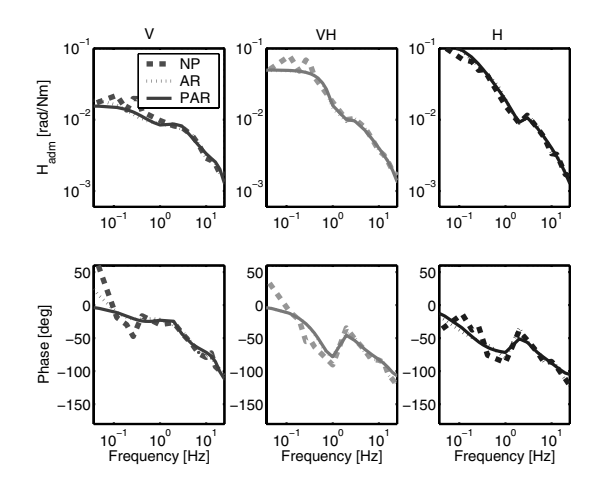


**Figure 6.8:** Gain and phase of the estimated admittance of a typical subject (S1) during carfollowing tasks. The left, middle and right graphs show the driving conditions V, VH and H, respectively. The thick dashed lines (NP) are the estimated non-parametric FRFs. The thin dotted line (AR) is the FRF of the ARMAX model. The solid line (PAR) is the FRF of the parameterized model.

**Table 6.3:** Admittance parameters during the classical tasks and car-following tasks, for each subject. The values for the classical tasks are the average of the two parameter fits over both repetitions. The values for the car-following tasks were estimated on the time-average over all repetitions of the driving trials. The parameters are described in section 6.2.2.  $k_f$ ,  $k_{int}$ ,  $k_{con}$  are in Nm/rad, and  $k_v$ ,  $b_{int}$  and  $b_{con}$  are in Nms/rad.

		S1	S2	S3	S4	S5	S6	S7	S8	Mean	STD
$k_f$	PT	-1.08	-0.5	-1.01	-0.2	-0.95	-0.97	-0.91	-0.86	-0.81	0.30
	RT	0.49	0.58	1.3	0.24	0.42	0.53	0.51	0.42	0.56	0.32
	FT	2.58	1.95	0.71	1.18	1.32	2.44	2.74	1.35	1.78	0.75
	V	1.01	-0.03	-1.83	0.86	0.42	0.14	0.28	-1.01	-0.01	0.96
	VH	2.36	1.8	-0.06	2.27	0.51	0.81	1.82	0.47	1.24	0.92
	Н	3.64	0.78	2.88	2.33	-	2.89	0.9	-	2.24	1.16
$k_v$	PT	7.4	19.5	1.8	-14.3	-11.6	24.5	-18.1	-12.4	-0.40	16.4
	RT	29	13.3	76.5	2.2	18.9	32.1	12	59.1	30.4	25.4
	FT	46.1	50.7	84.3	24.2	44.6	71.9	39.8	27	48.6	20.6
	V	59.4	-12.2	31.6	27.1	72.7	111.6	7.6	-8.9	36.1	42.9
	VH	1.8	22.4	-5.1	39.5	-9.3	16.5	11.3	-2.4	9.3	16.4
	Н	26.5	2.7	60.2	35.1	-	66	-0.5	-	31.7	27.9
k <sub>int</sub>	PT	407	859	647	477	518	449	342	339	505	175
	RT	263	808	783	542	596	398	340	334	508	209
	FT	87.4	128	704	87.2	328	110	56.9	27.3	191	226
	V	227	161	32.3	28.5	350	239	70.9	2.3	139	125
	VH	85.1	78	87.9	8.7	283	96.8	54.3	129	103	80.7
	Н	43.4	2.2	23.5	7.1	-	28.5	6.4	-	18.5	16.0
$b_{int}$	PT	23.9	27.5	19.8	14.2	20.8	21.9	13.8	13.1	19.4	5.2
	RT	18.4	27.4	14.9	23.3	24.3	19.8	17.2	31.9	22.2	5.7
	FT	14.6	22.2	15	15.9	18.8	17	10.5	14.5	16.0	3.4
	V	19.8	11	18.5	17.1	26.2	23.8	7.8	16.3	17.6	6.08
	VH	13.7	11.4	9.5	14.7	24.8	18.9	5.5	8.3	13.4	6.21
	Н	10.2	13.7	13.3	12.6	-	17.9	8.7	-	12.7	3.18
$k_{con}$	PT	1550	1247	677	1124	1105	1282	1361	799	1143	288
	RT	745	1251	430	813	1658	1889	1704	555	1130	569
	FT	372	492	421	416	1588	945	358	329	615	439
	V	162	279	129	244	400	377	177	285	257	98.6
	VH	102	260	226	240	391	301	221	391	268	97.1
	Н	119	136	230	202	-	330	86	-	184	89.3
$b_{con}$	PT	8	12.2	12.4	10.6	12.1	10.3	6.8	12.1	10.6	2.12
	RT	8.7	10.5	13.8	16.9	8	8.5	8.2	14.9	11.2	3.50
	FT	9.6	13.2	13	10.7	8.4	16.2	10.4	12.7	11.7	2.48
	V	7.4	7	7.7	6.9	8.5	8.6	6.8	8.5	7.68	0.76
	VH	6.3	7.4	9.3	6.7	9.9	9.8	7.7	6.2	7.91	1.55
	Н	6.2	7.6	8.3	6.2	-	11.2	6.8	-	7.72	1.89

			-				_			
Parameter	Unit	Task	S1	S2	S3	S4	S5	S6	S7	S8
P	[-]	V	0.9	1.68	1.2	0.16	1.11	2.1	0.82	0.36
		VH	0.84	1.36	0.55	0.16	1.04	0.89	0.99	0.24
D	[-]	V	1.87	1.22	1.09	0.52	1.95	1.7	1.56	1.21
		VH	0.62	1.07	0.98	0.17	1.5	0.69	1.21	0.89
$ au_{vP}$	[s]	V	0.23	0.71	0.26	0.45	0.22	0.3	0.65	0.92
		VH	0.62	0.51	0.41	1.22	0.69	0.51	0.52	0.87
$ au_{vD}$	[s]	V	0.71	0.23	0.24	0.93	0.97	0.47	0.63	0.81
		VH	0.35	0.36	0.24	0.46	0.68	0.37	0.76	0.76

**Table 6.4:** Visual parameters during car-following tasks, estimated for each subject. These values were estimated on the time-average over all repetitions of the driving trials.

and VH, the results for each subject are shown in Table 6.4. The results show interindividual differences in control strategies: some drivers opt for large gains (meaning large pedal deviations in response to changes in  $x_{rel}$  and  $v_{rel}$ ), others for smaller, and some react fast and others slower. The influence of the DSS on the visual gains was the same for all subjects: the P and D gains both decreased.

The parameters all had a small standard error of the mean, and the fitting procedure was robust to different initial values. For all conditions and all subjects, the VAFS for position were between 70%-85%, and for torque between 65%-85%, indicating a good fit at the control inputs.

The parameter fits during the H condition yielded very low visual gains: P and D usually smaller than 0.2 (not shown). Low visual gains were expected since no visual feedback was present, but the low gains also caused the simulated signals to drift away from the operating point, with resulting low VAFs. This modeling result suggests that drivers need visual feedback to prevent drift and accurately control low frequency perturbations.

In the experiment, during H, drivers showed more drift compared to VH or V. But even without visual feedback they could generally prevent the drift from escalating. Subjects generated time-variant corrective actions, probably when they had been feeling very large or small torques for a while and deduced they were not at the operating point anymore. Such non-linear cognitive processes are not captured by the current model (nor were they intended to be).

#### 6.3.3 Total Driver Model Validation

Figure 6.9 shows the simulated outputs of the parameterized model plotted against the measurement data of a typical subject car-following with only visual feedback. Not only the control inputs ( $\theta_c$  and  $T_c$ ) are predicted well (VAFs> 70%), but also car-following metrics such as  $x_{rel}$ ,  $v_{rel}$ , THW and iTTC (VAFs> 85%). During VH the VAFs were usually slightly better than during V.

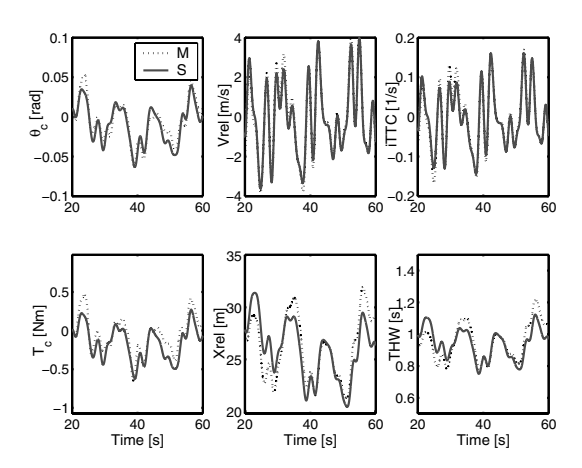


**Figure 6.9:** Several measured signals (dotted line, M) plotted against the simulated outputs (solid line, S) of the parameterized model for subject 2.

#### 6.4 Discussion

#### 6.4.1 NMS model structure and parameter fit procedure

When choosing a model structure, one has to balance fitting accuracy on one hand and over-parameterization on the other. A NMS model with only a three parameters (a simple mass-spring-damper model) for example did not capture all dynamics accurately. A model with too many parameters can lead to a very accurate fit, but the interpretability may be left wanting. There will probably also be substantial parameter interaction, leading to several solutions of parameters with a comparable goodness of fit. The repeatability of the parameter fits (see Figure 6.6), the small standard error of the mean for each parameter and the robustness to different initial values suggest that the current model structure offers good insight in the physiological parameters it describes, without falling into the pitfall of over-parameterization.

In future research, the parameter fit procedure could be further improved by adding more information to the error criterion, for example EMG FRFs (Schouten, 2004). In the current study, EMG was too noisy to use for parameter fitting, but better EMG measurement techniques might improve the accuracy of the fitting. Additionally, several parameters could perhaps be validated by separate measurements before the main experiment (inertia by measuring the response to very high bandwidth perturbations, reflexive time delays by measuring the EMG onset times in response to transient position perturbations).

Note that some caution needs to be taken when comparing the estimated NMS parameters to other studies where pure ankle rotations are applied. The current parameters describe the ankle-foot complex in a driving situation with the heel on the ground, and torque perturbations at the ball of the foot.

#### 6.4.2 Effects of the haptic DSS on car-following behaviour

When comparing drivers' response with and without the haptic DSS, three main effects are apparent. First of all, the DSS provokes an increased admittance, resembling the characteristics of a classical force task (Abbink et al., submitted). Drivers change their NMS properties in order to keep the pedal torque constant. As a result – by giving way to the continuous feedback torques – they already execute part of the pedal displacements necessary to accomplish the car-following task. The results of the current model study show that such a control strategy is realized by increased GTO gains and decreased muscle co-contractions, as hypothesized. Evidence for decreased muscle co-contraction was corroborated by reduced EMG activity for all muscles (Abbink et al., submitted).

Second, car-following with the DSS results in a decrease in visual gains. Indications for the reduction of the visual load were also found in previous research (Mulder et al., 2004a). The DSS causes a shift in control behaviour, made possible by the fact that information that was previously available only visually, was now also available haptically. Generally speaking, subjects also showed more linear behaviour during VH, as indicated by larger VAFs, better coherences, and reduced power of the remnant (at frequencies  $f_r$ , where neither of the perturbations had power). The DSS provokes less pedal deviations that had no linear relationship to the disturbances; or – in other words – enabled a better coupling between perception and action.

Third, the effect of DSS on car-following performance metrics (e.g. THW, iTTC) are negligible or marginally positive (Abbink et al., submitted; Mulder et al., 2005a,b). Apparently, drivers use the DSS to relieve their workload, not to increase performance. This is in accordance to the theory that drivers do not optimize performance, but satisfice it (Boer and Hoedemaeker, 1998; Boer, 2000).

Car-following without visual feedback The main results of this study were found when visual feedback was present. An important additional advantage of the haptic DSS lies in the fact that when visual feedback is absent (in periods of inattention) drivers will still have haptic feedback about the separation to the lead vehicle. Where normally the continuous control loop is interrupted when visual feedback is absent, the haptic feedback allows the loop to remain closed. Therefore, the consequences of a moment of visual inattention when the lead vehicle is braking will be less severe. The H condition represented an extreme case of lack of visual feedback. Even though drivers did not report this to be a relaxed driving experience (preferring to drive with combined visual and haptic feedback) they could maintain reasonable performance for most repetitions without crashing or drifting far behind the lead vehicle.

Drift was substantially larger when compared to V or VH, which suggests that visual feedback is necessary for low-frequent control. This may be caused by the fact that force perception deteriorates at low frequencies (Abbink and Van der Helm, 2004), whereas the visual channel is well-suited to compare steady-state differences. Most likely, the design of the DSS also contributes to the drift: the haptic feedback was not directly related to THW, but instead to changes in TTC (that were scaled by THW). Therefore a

different operating point of THW did not result in a different steady-state torque, complicating the judging of absolute THW, and the amount of drift. This notion is also shown by the fact that the haptic feedback entailed more reduction in visual D-actions (relating to changes in  $v_{rel}$ ) than in the P-actions (relating to changes in  $x_{rel}$ ).

The current haptic DSS supports the driver in car-following mainly by mitigating TTC variations, and leaves the choice of the THW up to the driver, and consequentially also the low-frequent drift correction. Although a different DSS could be designed to incorporate static THW feedback, in order to better support drift correction, such a DSS will not leave the THW choice up to the driver, and – more dangerously – might induce drivers to reduce visual attention even more.

Although the results of the DSS are promising indeed, the experimental data and modeling validations should be extended to capture driving behaviour during a variety of driving conditions, in order to fully understand the impact of the haptic driver support system.

#### 6.4.3 Model Assumptions

The current research assumes that the relatively simple simulator induces realistic car following behaviour. Driver response is not only dependent on simulator fidelity, but also on the perturbations provided to the subjects (i.e. amplitude and bandwidth of  $v_{lead}(t)$ ), the operating point (THW), average velocity) and — most importantly — the driver state: task interpretation, preferences and motivation. The data compares very well to data gathered with the same subjects under the same experimental conditions in a more advanced driving simulator (Mulder et al., 2005a,b). Also, the required operating point  $(THW=1\ [s])$  relates well to the 'naturally' preferred THW deduced from data gathered in the real world (Fang et al., 2001).

Another model assumption is that drivers can perceive newtonian variables like  $x_{rel}$ and  $v_{rel}$ . More realistic variables would perhaps be THW and TTC. However, for the given experimental conditions the difference is merely a scaling factor (see Figure 6.9). Note that different visual controllers (e.g. employing visual angles and Weber ratios) can easily be implemented and compared in the SIMULINK model. This was out of the scope for the current paper. It was also assumed that the driver's response would be linear during the given experimental conditions, which was confirmed by high coherences and VAFs. However, it must be noted that the experiment was designed to provoke a linear response: time-variant behaviour was minimized by a careful selection of experimental conditions. Drivers were motivated to perform their task as well as possible. The THW operating point was constant for all subjects, with calibrations between each trial to prevent drift. The lead vehicle speed profile was relatively high frequent, provoking continuous reactions from the drivers. The influence of disturbance bandwidth and THW operating points on car-following behaviour was shown previously (Mulder et al., 2005a,b) and their influence on the driver model parameters should be investigated in future research. The approach works well for the current experimental conditions, but is expected to lose its strength when time-variant actions dominate the control behaviour (e.g. sudden corrections after drifting away due to inattention or lack of motivation). The inability to describe higher level processes (therefore assuming them to be either zero or time-invariant), is exactly why control theoretic modeling may be inadequate for capturing inter- and intra-individual driver differences in real traffic situations (Boer, 2000, Brackstone and McDonald, 1999). In reality, driving is not a continuous application of a single control law. Drivers are usually engaged in several tasks at the same time, giving only intermittent attention to the car-following task. True as this may be, developing predictive models that also address time-variant behaviour is out of the scope of the current research. Suffice it to say that driver inattention is the main reason for rear-end collisions (Knipling et al., 1993), and that continuous haptic feedback may very well be a comfortable way of ensuring that the driver remains in the control loop.

#### 6.5 Conclusions

For the experimental conditions studied, the following conclusions can be drawn:

- A linear driver model consisting of a spinal (neuromuscular model) part and a visual (PD controller) part, can accurately describe car-following behaviour in a driving simulator, with and without haptic feedback. This was shown by high VAFs for pedal position and torque (65-80%), as well as for relative position and velocities (75-95%). All NMS and visual parameters can be estimated accurately, shown by a good repeatability for different repetitions, a small standard error of the mean, and a good fit in the frequency domain.
- Using haptic feedback while car following causes two main changes in the estimated parameters of the driver model:
  - 1. increased gain of the GTO reflexes and decreased muscle co-contraction
  - 2. decreased visual gains (mainly the derivative gain)
- The increased admittance during haptic feedback resembled the admittance shown during a classical force task, which also entailed increased GTO gains reflexes and decreased muscle co-contractions. On the other hand, during classical position tasks the admittance was decreased substantially, which was effected by increased co-contractions but also by the GTO turning into an excitory feedback loop. It is concluded that the GTO reflex is an important mechanism to adapt low-frequent motion control of the ankle-foot complex.
- In case of visual inattention, the haptic feedback allows control actions on a spinal level to replace the visual control actions temporarily (92 seconds). However, visual feedback remains necessary to keep the drift from escalating after longer periods of car-following.
- The designed haptic driver support systems is beneficial to drivers. It results in car-following behaviour with the same performance but with a reduced control effort, by allowing the driver's spinal reflexes to contribute to control actions.

## Do Gas Pedal Feedback Torques Influence Driver's Response to a Braking Lead Vehicle?

David A. Abbink, Frans C.T. van der Helm, Erwin R. Boer Submitted to: *Biological Cybernetics* 

Only two things are infinite: the universe and human stupidity.

And i'm not sure about the former.

Albert Einstein

Several studies have investigated the influence of a haptic driver support system on continuous car following behaviour, indicating beneficial results. However, its effect on driver response to sudden and prolonged braking of a lead vehicle is unknown. The high feedback torques might provoke an undesired stretch-reflex, that depresses the gas pedal when it should be released.

The purpose of the study is to experimentally determine whether the DSS influences the driver's response to a braking lead vehicle. Subjects (n=5) participated in a driving simulator study, where they were instructed to follow the lead vehicle at a time-headway of 0.5 seconds. At the end of each trial the lead vehicle braked hard and the driver's response was measured, including the electromyographic (EMG) activity of calf and shin muscles. Car following behaviour before the onset of the braking was characterized by the amplitude of a continuous lead vehicle perturbation (large/small), and by the state of the haptic feedback (on/off). Several time-domain and frequency-domain metrics were chosen to quantify task performance, safety performance and control effort.

EMG results showed no significant stretch reflex in response to the large feedback torque due to braking. The reaction of the driver was not influenced significantly by either the haptic feedback or amplitude. During continuous car following, haptic feedback caused a decrease in control effort and an increase in safety performance for the large amplitude, although these benefits were not found for the small amplitude.

It is concluded that when drivers are visually attentive, they may benefit from the haptic feedback during continuous (non-critical) car following. But when responding to heavy braking of the lead vehicle, haptic feedback improves nor degrades the performance when visual feedback is also present: the latter dominates the response.

#### 7.1 Introduction

In recent years, the design of various driver support systems (DSS) has received much attention. In previous studies (Mulder et al., 2004a), a haptic DSS was designed that translates changes in separation to the lead vehicle *continuously* to changes in gas pedal torque. Effectively, the visual feedback loop is now supported by a continuous haptic feedback loop. The effect of the DSS on continuous car following behaviour has been shown to be beneficial (Abbink et al., submitted; Mulder et al., 2004b, 2005a,b). Generally speaking, the same car-following performance is reached with reduced control effort. It was shown that drivers give way to the feedback torques, and use increased GTO activity and reduced muscle contractions to do so (Abbink et al., submitted).

However, all these studies looked at driver response to continuous perturbations of a lead vehicle. Whether the haptic DSS is still beneficial when the lead vehicle brakes heavily remains largely uninvestigated.

**Effect of sudden large feedback torques** A braking lead vehicle results in a rapid decrease in separation, and therefore a rapidly increasing feedback torque. The DSS thereby informs the driver that it will be safer to quickly remove his foot from the gas pedal, but possibly the torque could also provoke a stretch reflex in the calf muscles (see e.g., Mirbagheri et al., 2000). Depending on the strength of the stretch reflex, it could induce either an increase in the time it takes the driver to remove his foot from the gas pedal, or even cause him to press down the gas pedal: exactly the opposite to the desired response.

However, this study hypothesizes that DSS torques are unlikely to evoke undesired response. Stretch reflex activity is largest when the frequency content of the transient perturbation is high (a hammer tap to the knee tendon causes the leg to kick up, slow pressure to the tendon does not). The DSS torques are the result from changes in relative position and velocity of two cars with relatively sluggish longitudinal dynamics, and can therefore not have a very high bandwidth. Moreover, during haptic feedback, the whole neuromuscular system is set to give way (Abbink et al., submitted), not to resist. High muscle spindle stretch-reflex gains are therefore not likely.

Since no literature or data is available to back up the hypothesis, an experimental study is proposed.

**Goal and Approach** The aim of the study is to determine whether DSS torques influence the driver's response when a lead vehicle is braking heavily. In order to test this, drivers will be subjected to a scenario of car following at a close following distance, where an unexpectedly braking lead vehicle will entail the highest feedback torque that the DSS is capable of delivering. To investigate whether preceding car-following behaviour influences the response, the amplitude of the continuous lead vehicle perturbation will be varied.

The effect of the experimental conditions on EMG activity, pedal force and pedal position will be examined, as well as on overall car-following metrics such as relative position and velocity.

## 7.2 Method

## 7.2.1 Subjects and Setup

Five subjects (of which one female) participated in the experiment. All were young (19-22 years old) and had their drivers license for at least one year. They were seated in a simplified driving simulator (see Abbink et al., 2004a, submitted for full description) of which the gas pedal was actuated by a high-fidelity force-controlled robot manipulator. The manipulator was set to behave like a normal gas pedal (a bias force of 20 [N] and pedal stiffness of 0.16 [N/% pedal depression]). A haptic feedback system could be simulated, that generated an additional pedal stiffness  $\Delta K$ , depending on changes in time-to-contact (TTC) to the lead vehicle. No steering wheel or brake pedal was available in this setup.

A 17-inch computer screen (resolution  $1024 \times 768$ ) placed at approximately 1.5 m in front of the subject's eyes showed a realistic representation of a straight road and a lead vehicle, updated at 50 Hz. Audio feedback was available in the form of engine sounds.

## 7.2.2 Experiment Protocol

**Task Instruction** The subjects were instructed to maintain a constant time-headway (THW) of 0.5 second to the lead vehicle, as well as possible. They were told that after a random period of car following the lead vehicle could sometimes brake heavily, and that in that case they should do all they could to avoid a collision or – if unavoidable – to at least reduce the impact of the collision. Since no brake pedal was available in the simulator, this meant releasing the gas pedal quickly.

**Lead vehicle speed profile** To define the driver behaviour before the onset of the braking, two different continuous lead vehicle velocity perturbations ( $v_{lead}$ ) were used. In the top row of Figure 7.1 the two amplitudes of  $v_{lead}$  can be seen: the small amplitude of  $v_{lead}$  S and the larger L, with maximal amplitude of 0.4 and 0.88 m/s, respectively. The left plot shows  $v_{lead}(t)$ , the middle plot shows the resulting lead vehicle accelerations, and the right plot shows the auto-spectral density of  $v_{lead}$ . It can be seen that both perturbations contain power only at certain frequencies points (bandwidth 0.02-0.3 Hz), and that the  $v_{lead}$  with amplitude S contains less power than with L. The  $v_{lead}$  was designed as a multi-sine with random phase, resulting in an unpredictable signal. The perturbation design yielded good signal-to-noise ratio's at the frequencies where power was added  $(f_v)$ , but also enabled noise analysis at remnant frequencies ( $f_r$ ) where no power was present in  $v_{lead}$ . Note that in contrast to previous studies (Abbink et al., submitted,s) the power at higher frequencies was filtered to better resemble real highway traffic (Boer et al., 2005).

The perturbations yielded car-following behaviour that can be seen in the bottom row of Figure 7.1 for unsupported car following. As a baseline, the results were simulated when no control actions would have been taken.

98 Chapter 7

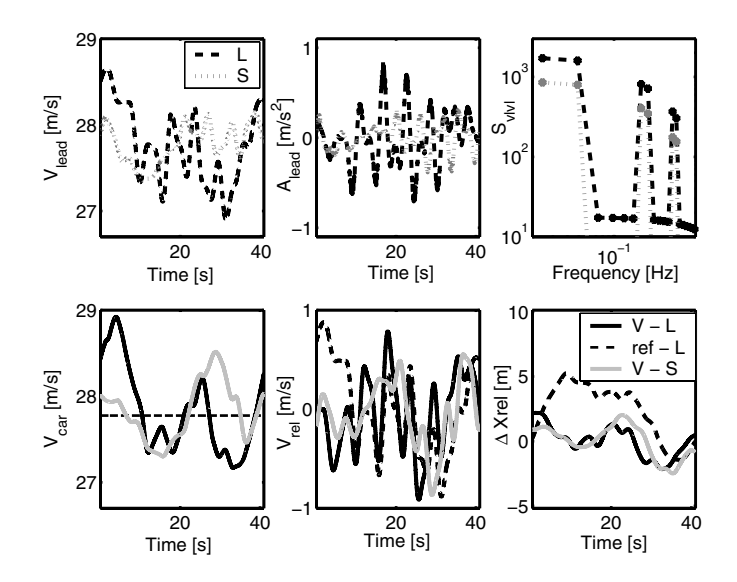


**Figure 7.1:** Time domain and frequency domain properties of the two  $v_{lead}$  perturbations: with large (L, black dashed lines) and small amplitude (S, gray dotted lines). The top row shows the time domain signals of velocity and acceleration, and at the right the power spectral density of both  $v_{lead}$ 's. The bottom row shows the  $v_{car}$ ,  $v_{rel}$  and  $x_{rel}$  for three different conditions: a simulated baseline condition where no control actions are done (for L, dashed); and typical experimental results measured during normal car following (condition V), for both large (L, black) and small (S, gray)  $v_{lead}$  amplitudes.

**Trials** A full trial consisted of six randomized repetitions where both amplitudes of  $v_{lead}$  were used, and a seventh repetition where at the end – instead of  $v_{brake}$  – a strong torque step  $T_{dist}$  was presented at the gas pedal, with an amplitude of 3.75 Nm ( $\approx 50$ N at the contact point with the foot). A trial lasted approximately 10 minutes, and was done for two DSS conditions in random order: normal car following with visual feedback (V), and car following with the haptic feedback from the DSS in addition to visual feedback (VH). The experimental conditions are summarized in Table 7.1.

Subjects were explained about the lead vehicle decelerations, but not about the torque transient. Therefore, the first time the transient came totally unexpected. Afterwards the subject was told that it was a single event to catch them unaware and that it would not happen again. It was therefore assumed that subjects were again not expecting the torque transient during the second trial.

In order to visualize the car-following task, a red square was shown in front of the car at the start of each repetition: if it touched the rear bumper of the lead vehicle, subjects knew their THW was exactly 0.5 second. Upon reaching that THW at a constant operating point ( $v_{car} \approx 28m/s$ ;  $\theta_c \approx 25\%$  pedal depression) the red calibration square disappeared and after a random amount of seconds the lead vehicle's speed was perturbed.

repetition with raist which was always last.						
	DSS condition	Perturbations	Repetitions			
		Continuous	Transient			
	V,VH	L	$v_{brake}$	3		
	V,VH	S	$v_{brake}$	3		
	V.VH	S	$T_{dict}$	1		

**Table 7.1:** All repetitions contained in a single trial of V or VH. The repetitions were randomized, except the repetition with  $T_{dist}$  which was always last.

After 42-50 seconds (randomized to prevent predictability) the transient perturbation  $v_{brake}$  was presented to the subject. The transient was the same for each condition, a deceleration that started at 5  $m/s^2$  until  $v_{lead}$  reached approximately 20 m/s. At such a close separation a crash could not be avoided, only the impact of the crash could be influenced by releasing the gas pedal as soon as possible.

# 7.2.3 Signals

While performing each trial, the following signals were measured at 200 Hz: the pedal depression  $\theta_c(t)$  [%], the contact torque  $T_c(t)$  [Nm] and the torque perturbation  $T_{dist}(t)$  [Nm]. For ease of interpretation, the torques are translated to forces at the ball of the foot. Car following data was also measured at 200 Hz: the lead vehicle perturbation  $v_{lead}(t)$  [m/s], the own vehicle speed  $v_{car}(t)$  [m/s], and the relative separation  $x_{rel}(t)$  [m]. From the car following signals the relative velocity  $v_{rel}(t)$  was calculated, as well as time-headway THW(t) and inverse time-to-contact iTTC(t):

$$THW(t) = \frac{x_{rel}(t)}{v_{car}(t)},\tag{7.1}$$

$$iTTC(t) = \frac{v_{rel}(t)}{x_{rel}(t)},\tag{7.2}$$

with  $v_{rel}(t)$  defined as:

$$v_{rel}(t) = v_{lead}(t) - v_{car}(t)$$
(7.3)

Additionally, the electromyographic (EMG) activity of four relevant lower leg muscles was measured. Disc-shaped ( $\oslash$ 30 mm) differential (34 mm interspacing) electrodes (Ag/AgCl) were placed over the soleus (SO), the gastrocnemius lateralis (GL) and medialis (GM), and the tibialis anterior (TA). Skin conduction was improved by using hydrogel, local shaving of the skin, abrasion with sandpaper and cleaning with alcohol. The EMG signals were pre-amplified, low-pass filtered (analogue, 3rd order Butterworth, cut-off frequency at 450 Hz, 18 dB/oct) to prevent aliasing, sampled at 1200 Hz, and digitally stored for off-line analysis. The stored signals were subsequently high-pass filtered (analogue, 3rd order Butterworth, cut-off frequency at 20 Hz, 18 dB/oct) to prevent

any motion artifacts, rectified, and finally resampled at 200 Hz (after low pass filtering at 100 Hz), to speed up the analysis.

The EMG(t) measured during each trial was scaled by  $EMG_{max}$  for each muscle.  $EMG_{max}$  is the maximal EMG measured during the trials, which was determined for each muscle by averaging the 100 samples with the highest value. The scaling yielded  $EMG_{rel}(t)$ , a relative measure of the EMG activity, that allowed a better comparison of inter- and intra-individual differences in EMG activity.

## 7.2.4 Analysis

Each repetition was cut into two parts that were separately analyzed. The first part was the 50 seconds of continuous response to  $v_{lead}$  and the second part contained the six seconds after the transient  $v_{brake}$ , as well as one preceding second.

#### **Transient Response**

The response to  $v_{brake}$  was averaged over the three repetitions to reduce noise. The response to  $T_{dist}$  could not be averaged, since there was only a single repetition per DSS setting.  $EMG_{rel}$  of all four muscles was examined for peaks of reflexive activity after the onset of the transients.

In order to quantify how well drivers responded to  $v_{brake}$ , two performance metrics were employed. The first is  $\Delta t_{release}$ , the time it took drivers to fully release the gas pedal after the onset of the transient. The second was  $v_{rel}(t_{crash})$ , the relative velocity at the time of the impact, a measure of crash severity. Note that both metrics depend on the initial conditions  $(x_{rel},\,v_{rel},\,\theta_c)$ , so there will be a natural inter– and intra-subject variability. An analysis of variance (ANOVA) was done ( $\alpha$ =0.05) on the two metrics. The independent variables were the two amplitudes of  $v_{lead}$  (L and S), and the driving condition (V or VH).

#### **Continuous Response**

The first seconds of each measured signal were discarded to reduce onset effects, leaving 8192 samples ( $=2^{13}$ ), convenient for fast Fourier transforms) for further identification. A variety of objective car-following metrics were used to describe control effort, task performance, safety performance, and how well the drivers remained at the operating point.

**Time Domain Metrics** The standard deviations of THW and  $x_{rel}$  were used as, respectively, a perceptual and a newtonian metric for task performance. If these metrics are large, it means there are large fluctuations in the separation: an indication of decreased performance of the task. Likewise, the standard deviation of iTTC and  $v_{rel}$  were used to describe safety performance: large values mean a decreased success in matching the lead vehicle's speed, resulting in hazardous closing velocities. These metrics are shown in Table 7.2. The mean of THW was checked to see if subjects remained close to the operating point of THW=0.5 s.

An ANOVA was done on these metrics, similar to the transient metrics.

	· ·		
Metric for	Time Domain		Frequency Domain
	Newtonian	Perceptual	
Task Performance	$STD(x_{rel})$	STD(THW)	-
Safety Performance	$STD(v_{rel})$	STD(iTTC)	$H_{perf}(f)$
Control Effort	$STD(\theta_c)$	-	$H_{control}(f)$
Operating point	-	mean(THW)	-

Table 7.2: Metrics in time and frequency domain that describe continuous car-following behaviour.

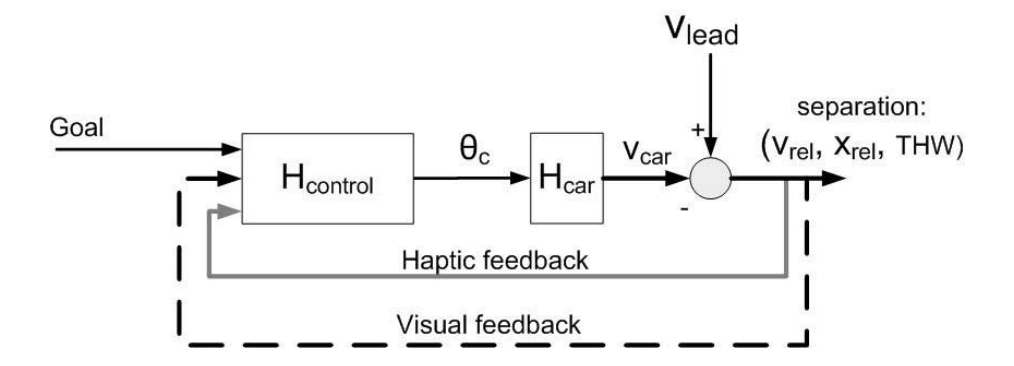


**Figure 7.2:** Frequency domain block diagram describing a closed-loop car-following situation. The driver uses gas pedal deviations  $(\theta_c)$  to change the speed  $(v_{car})$  of his car  $(H_{car})$ . Lead vehicle perturbations  $(v_{lead})$  cause a relative velocity  $v_{rel}$  that the driver aims to control back to zero.  $H_{control}$  describes the total response to  $v_{rel}$ , either using only visual feedback (V), or combined with haptic feedback (VH).

**Frequency Domain Metrics** The mean and standard deviation of a signal cannot describe its differences in frequency content. For example, the standard deviation of a single sine depends solely on its amplitude, not on its frequency. Therefore, a radically different control strategy might show 'no statistical difference' when solely looking at means and standard deviations.

A more rich way of describing signal properties is by analyzing the frequency domain characteristics, something which is rarely done in car-following literature. Furthermore, if the experiment is set up well, closed-loop system identification can be done, which shows the causal dynamic relationship between the input and output of a (sub)system. In such a way, properties are revealed that cannot be seen from analysis of separate signals. In the current study the standard time-domain metrics will be supplemented by frequency-domain metrics.

Figure 7.2 shows the frequency-domain block diagram of the closed-loop car-following task. The driver receives information about  $v_{rel}$  (either only visually V or with added DSS feedback VH) and exerts control actions on the gas pedal. The frequency response function (FRF) that describes the dynamics between input  $v_{rel}$  and output  $\theta_{c}$  is called

 $H_{control}$ . It is a metric for control effort: if it's small, the pedal control actions with which the driver responds to a perceived relative velocity are small. The FRF was estimated according to:

$$\hat{H}_{control}(f_v) = \frac{\hat{S}_{v_{lead}\theta_c}(f_v)}{\hat{S}_{v_{lead}v_{vol}}(f_v)}$$
(7.4)

where  $\hat{S}_{xy}(f_v)$  describes the estimated cross-spectral density between signals x and y (e.g.,  $\hat{S}_{v_{lead}v_{rel}}$  between  $v_{lead}$  and  $v_{rel}$ ). The cross-spectral densities were averaged over two adjacent frequency bands to reduce variance.

A second interesting FRF is  $H_{perf}$ , which describes the dynamics between input  $v_{lead}$  and output  $v_{rel}$ . It is a measure of how much relative velocity is the result of the lead vehicle disturbance. If it is smaller than one, then the impact of  $v_{lead}$  on  $v_{rel}$  is reduced, resulting in less hazardous situations. The FRF is estimated according to:

$$\hat{H}_{perf}(f_v) = \frac{\hat{S}_{v_{lead}v_{rel}}(f_v)}{\hat{S}_{v_{lead}v_{lead}}(f_v)}$$

$$(7.5)$$

The two frequency-domain metrics are shown in relationship to the time-domain metrics in Table 7.2. The usage of system identification techniques assumes linear responses around an operating point, and to verify this assumption the (squared) coherence is estimated according to:

$$\hat{\Gamma}^{2}(f_{v}) = \frac{|\hat{S}_{v_{lead}v_{car}}(f_{v})|^{2}}{\hat{S}_{v_{lead}v_{lead}}(f_{v})\hat{S}_{v_{car}v_{car}}(f_{v})}$$
(7.6)

For a linear system, the coherence function equals one when there is no noise (either linearization or measurement noise), and equals zero in the worst case.

# 7.3 Results

#### 7.3.1 Transient Perturbations

The EMG response of all muscles to the torques can be seen in Figure 7.3, in the right column. If a stretch reflex would occur, the plantar flexors (SO, GM, GL) would show increased EMG activity, approximately 50 ms after the onset of the perturbation. The additional DSS stiffness  $\Delta K$  reached its maximum value after 400 ms, and in this period no peaks in EMG activity were found. The response to the transient  $T_{dist}$  is shown in Figure 7.4, and is – for ease of interpretation – translated to an endpoint force at the foot  $F_{dist}$ . Even with this large and sharp transient no significant increase in EMG activity of the spinal reflexes can be seen.

The response of a typical subject to the braking lead vehicle is shown in Figure 7.5, for lead vehicle perturbations with large amplitudes L (left column) and small amplitudes

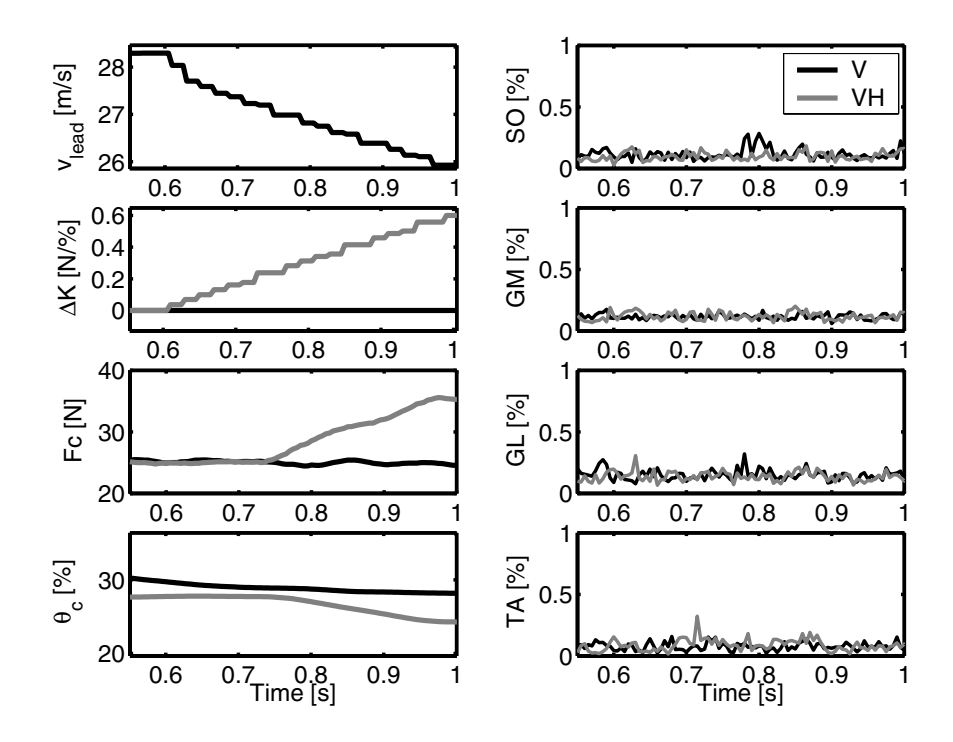


**Figure 7.3:** Time domain response of a typical subject to the transient braking  $v_{lead}$ . In the left column the mechanical response is shown: the  $v_{lead}$  results in an increase in pedal stiffness  $\Delta K$  when the DSS is active, which influences  $F_c$  and  $\theta_c$ . In the right column the  $EMG_{rel}$  of each muscle is shown.

S (right column). The braking lead vehicle causes a rapid increase in pedal stiffness  $\Delta K$ , which causes an extra torque on the gas pedal (re-calculated to a force at the ball of the foot, for ease of interpretation). Performance metrics  $v_{rel}(t_{brake})$  and  $\Delta t_{release}$  were not significantly influenced by either the DSS or amplitude of  $v_{lead}$ . Only a separate analysis of the effect of DSS during S showed that  $v_{rel}(t_{brake})$  was significantly smaller (p=0.03), indicating a decreased crash velocity as a result of the haptic feedback. The same trend could be seen during L, but it was not significant (p=0.18).

It must be noted that the results were influenced by a considerable inter- and intrasubject variability of initial conditions at  $t_{brake}$ : the  $THW(t_{brake})$ ,  $v_{rel}(t_{brake})$  and  $\theta_c(t_{brake})$ . This is logical since the experiment was chosen to have drivers actively participating before responding to the braking situation; thereby allowing natural variability in carfollowing behaviour.

104 Chapter 7

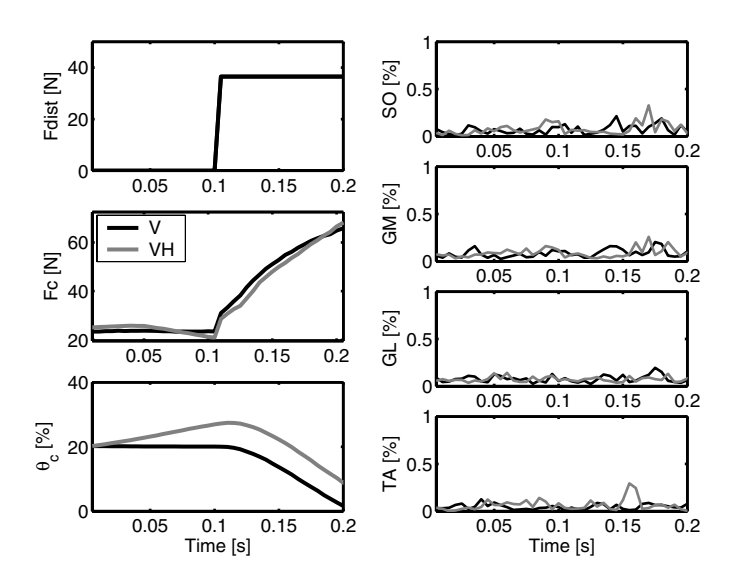


**Figure 7.4:** EMG response of a typical subject to the transient perturbation  $F_{dist}$ , during V (black lines) and VH (gray lines). In the left column the mechanical response is shown, in the right column the EMG response.

#### 7.3.2 Continuous Perturbations

#### **Time Domain Analysis**

All subjects remained at the operating point with relatively little drift: neither the amplitude of  $v_{lead}$  or the DSS provoked significant differences in mean THW or mean  $\theta_c$ . The results of the metrics are shown in Figure 7.6, averaged over all subjects. The black bars in the middle of each group show the baseline condition: what the metric would have been if the driver would have kept a constant velocity at the operating point, without reacting to the lead vehicle perturbations. It can be seen that both amplitude and DSS influence the performance metrics.

Surprisingly the control actions of the driver did not improve all metrics. The  $STD(v_{rel})$  did not change significantly, and the STD(iTTC)) actually increased for both amplitudes, with and without haptic feedback. Apparently, at this operating point, driver's control actions are not optimal for velocity-related metrics, but are more focused at reducing changes in  $x_{rel}$  and THW (which are better compared to the baseline condition).

**Influence of Amplitude** Statistical analysis showed that a smaller amplitude S of  $v_{lead}$  evoked substantial changes in driving behaviour. The changes were characterized by increased safety performance (smaller  $STD(v_{rel})$ , p=0.01; and smaller STD(iTTC), p=0.02) and less control effort (smaller  $STD(\theta_c)$ , p=0.003). The same task performance was reached: there was no significant difference for  $x_{rel}$  and THW.

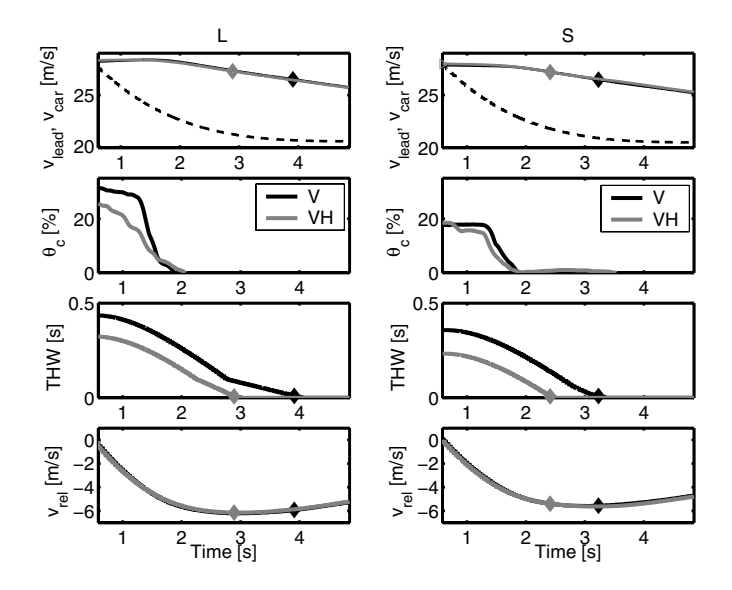


**Figure 7.5:** Averaged time domain response of a single subject to the transient braking  $v_{lead}$ , for both amplitudes of  $v_{lead}$ : L (left column) and S (right column). In each plot the response during V (black) and VH (gray) is shown. In the top plots also the  $v_{lead}$  perturbation is shown (dashed line), which drops to nearly 20 m/s. The point of the crash is denoted with a diamond.

Influence of DSS — The effect of the DSS on car following metrics were not significant for both amplitudes. However, a significant interaction was observed for the amplitude and DSS, showing that the influence of the DSS was dependent on the  $v_{lead}$  amplitude. A separate test showed significant effects of DSS for L: namely, reduced  $STD(\theta_{\rm c})$  and  $STD(v_{rel})$  during VH. The standard deviations of the other metrics also were smaller, but not significantly so. For the small amplitude S the effect of DSS was not significant for any of the metrics.

#### **Frequency Domain Analysis**

In Figure 7.7 the FRFs of  $H_{control}$  (left column) and  $H_{perf}$  (middle column) are shown during L, with phase and coherence. Coherences were generally high ( $\Gamma^2>0.8$ ) for L. For small amplitudes of  $v_{lead}$  the coherence was substantially smaller ( $\Gamma^2>0.6$ ). Additionally, the remnant of  $\theta_c$  at frequencies  $f_r$  (where  $v_{lead}$  contained no power) was significantly larger (not shown), indicating that the smaller amplitude evoked control behaviour that was less linearly related to the perturbation.

Figure 7.7 shows the FRFs of both  $H_{control}$  and  $H_{perf}$  for L. Both were smaller when the haptic DSS was activated. The results are shown for a typical subject, but similar trends were found for all subjects. In the right column the time domain plots of  $\theta_c$ , THW and iTTC are shown for the same subject. The decreased FRFs for control effort and

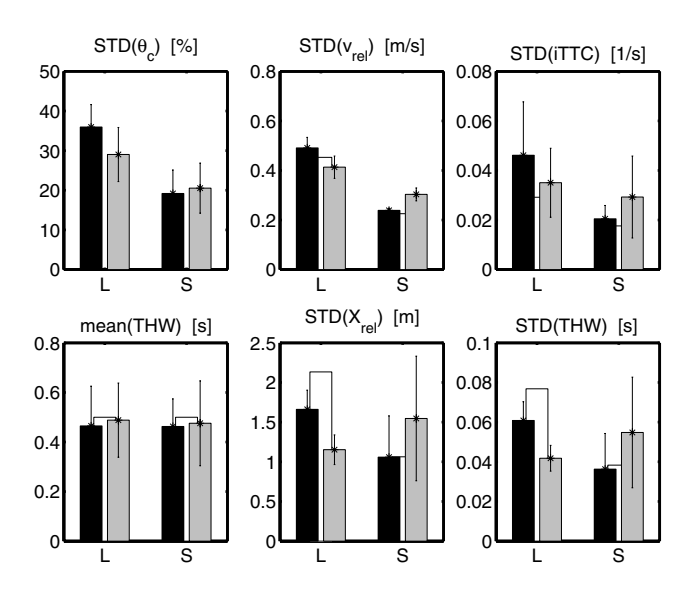


**Figure 7.6:** Time domain metrics during continuous car following, averaged over all subjects. At the left side of each graph, the metrics for the large amplitude L are shown, at the right side for the small amplitude S. The error bars denote the standard deviation over the metric. At either side of a graph, a group of bars is shown. The left bar shows the results during V (black), the right bar during V (gray). The white bar in the middle denotes the simulated results when a driver would not have reacted to  $v_{lead}$  but rather maintained a constant speed.

safety performance correspond to the time domain metrics.

The main increase in safety performance occurs at low frequencies:  $H_{perf}$  is larger than 1 for higher frequencies, indicating a decreased safety performance compared to the 'no control actions' baseline condition. This corresponds to the time-domain results shown in Figure 7.6.

# 7.4 Discussion

# 7.4.1 Transient Response

The experimental results showed that the sharpest increasing torque that the DSS could realistically deliver was not enough to evoke EMG response in the calf muscles, let alone cause a response to press down on the gas pedal instead of releasing it. A reflexive response was not even seen after  $T_{dist}$ , which reached a much higher torque much more rapidly than would be possible with the DSS in real traffic.

A possible cause for the absence of the stretch reflex could be that the forces at the foot do not directly cause the calf muscles to be stretched, due to a compliant force transfer (e.g., soft tissue of the foot sole). A second reason could be that the stretch

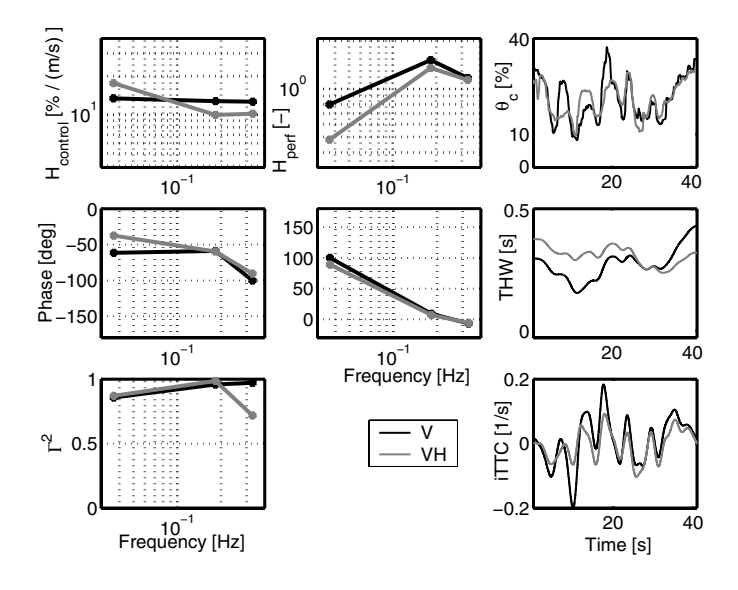


**Figure 7.7:** Response of a typical subject in the frequency domain (left and middle column) and time domain (right column). The results are shown in response to  $v_{lead}$  with L, for both DSS conditions.

reflex is inhibited, because the driver is not attempting to maintain a fixed ankle position. Previous studies for the upper extremity (Doemges and Rack, 1992a,b) report that the reflexive response to transients is much smaller during force tasks compared to position tasks. The response to transients for a leg in a driving position has not been reported in literature. However, during continuous torque perturbations, drivers have been shown to adopt a force task strategy while car following with the DSS (Abbink et al., submitted). In other words, drivers become more slack when interacting with the haptic feedback, choosing to give way to the informational torques instead of resisting them. Drivers adapt their reflexive gains accordingly: less muscle stretch and stretch velocity feedback, and more muscle force feedback from the Golgi Tendon Organs (Abbink et al., submitted). This may be the reason for the absence of the stretch reflex even during  $T_{dist}$ : drivers were not aiming to resist pedal torques just before the onset of the transient, but tried to give way to them.

Regardless of the explanation, the DSS did not negatively influence the response to a hard-braking lead vehicle. It did not cause drivers to react faster either. The lack of influence that any preceding condition had on the braking response, suggests that the salient visual feedback dominates the braking response at this close distance.

# 7.4.2 Continuous Response

The result of the DSS on continuous car following behaviour corresponds well to that described in previous literature (Abbink et al., submitted; Mulder et al., 2004b,a, 2005b,a):

the same task performance, but with a reduced control effort and increased safety performance. The current experimental results also show that the benefits of the DSS were not present for a amplitude S. The explanation of this effect may be that during small amplitudes of  $v_{lead}$  the limits of perception are reached, or – perhaps more likely – the limits of motivation: why would one do one's best to minimize  $v_{rel}$  when it is already small? Drivers are not optimal controllers: they don't spend all their resources to optimize performance, rather they satisfice it (Boer, 2000; Boer and Ward, 2003; Boer et al., 2005). Therefore, the control behaviour was less attuned to the  $v_{lead}$  (which is supported by the found results of an increased remnant and decreased coherence), and the information of the DSS was less valuable.

The results also yielded a surprising fact, namely that according to safety metrics (diminishing variations in  $v_{rel}$  and iTTC) it would have been even better if drivers had not responded to  $v_{lead}$  at all. However, task performance (diminishing variations in  $x_{rel}$  and THW) was increased by the driver's control actions. The frequency domain metric  $H_{perf}$  clearly showed this focus: it was smaller than one (= improved) at low frequencies, and larger than one (= deteriorated) at high frequencies. This implies that driver's response is triggered by velocity-related cues, even if the control efforts do not improve the performance.

# 7.5 Conclusions

For the experimental conditions studied, the following conclusions were drawn:

- An unexpected torque transient (imposed by changes in pedal stiffness produced
  by the haptic DSS due to braking of the lead vehicle) did not provoke a stretch
  reflex of the calf muscles. Even an unrealistically large and sharply increasing
  torque transient did not provoke a stretch reflex.
- Driver response to the braking lead vehicle did not change with conditions preceding the braking: the DSS neither improved or deteriorated the driver's control actions. Apparently the visual feedback during hard braking situations is dominant.
- The DSS positively influenced driver car following behavior in response to a continuous lead vehicle perturbation  $v_{lead}$ , as shown by:
  - 1. an improvement in safety performance metrics. The standard deviation of the relative velocity  $v_{rel}$  was significantly smaller. The corresponding frequency domain metric  $H_{perf}$  also decreased, which indicated less impact of  $v_{lead}$  on  $v_{rel}$ .
  - 2. an improvement in control effort metrics. The standard deviation of pedal rotations decreased, as well as the corresponding frequency domain metric  $H_{control}$ , indicating decreased pedal displacement in response to  $v_{rel}$ .
- ullet For the smaller amplitude of  $v_{lead}$  the benefits of the DSS were not found. However, due to the smaller changes in velocities, safety performance increased significantly independent of the DSS. The drivers showed reduced control effort, but

also a reduced linear response to the  $v_{lead}$ , indicating that they were either not as able or as motivated to match their control actions to  $v_{lead}$ .

# **Chapter 8**

# **General Discussion of the Results**

David A. Abbink

Sometimes I've believed as many as six impossible things before breakfast. – Lewis Carroll

The research contained within this thesis has culminated in the design of a prototype for a haptic driver support system (DSS), its experimental validation in a driving simulator, and a parameterized detailed driver model that captures the impact of the DSS on visual and spinal contribution to car-following control.

In this chapter the main research results are discussed and put into perspective. The conclusions can be summarized as follows: the DSS provides drivers with an additional fast haptic feedback loop that allows useful control behaviour at a spinal level, thereby reducing the need to respond to all changes in separation through visual feedback. This effect allows drivers to realize the same (or an even better) car-following performance with reduced control effort.

Furthermore the limitations of the used approach are addressed, and recommendations are given for future research and applications.

## 8.1 Introduction

The research described in the current thesis was part of a larger research project, which aimed to develop and evaluate a continuous haptic driver support system (DSS) for car following on highways, which that could be implemented in an actual car.

The aim of this thesis is to analyze the impact of continuous haptic feedback from such a DSS on driver behaviour during car following, both at the level of car-following behaviour and at the level of neuromuscular motion control behaviour. The goal was met by experimental and theoretical studies, and the resulting knowledge was applied in the design and evaluation of prototypes of the support system.

Contributions to the design of a final DSS prototype were made on theoretical grounds (see Chapter 2) and experimentally, by determining force perception limits (Chapter 3) and muscle use while manipulating a gas pedal (Chapter 4). In cooperation with other members of the research project, the translation from separation to haptic information was designed as a stiffness feedback algorithm, based on the time-to-collision (TTC) scaled by time-headway (THW) (Mulder, 2007).

The evaluation of the final DSS prototype was combined with detailed driver identification (Chapter 5) and modeling (Chapter 6), aiming to understand how drivers respond to the haptic feedback, with a special emphasis on neuromuscular contributions to the gas pedal control. The data for this experiment was gathered in a simplified driving simulator. Drivers were asked to follow at car at a fixed THW, while the lead vehicle speed was perturbed. Metrics for car-following performance (safety) and workload (comfort) were established and measured while following a lead vehicle with and without the haptic DSS.

The system was designed to mainly provide support during non-critical highway situations, emphasizing controllability during relatively low-frequent interaction with traffic. In order to investigate the effect of the haptic feedback during more critical situations a final experiment was done (Chapter 7), in which driver response to a strongly braking lead vehicle was measured.

The experiments yielded results that could be analyzed statistically in the time-domain, and related to other car-following studies in the project and in literature. However, the strength of the cybernetic approach used throughout this thesis lies in the fact that the data was gathered so that frequency-domain system identification techniques could be used. The techniques have led to additional understanding of the control strategies of the driver, complementing and enhancing the insights gained from looking at the data in the time-domain. However, in order study the complex changes in driver behaviour as a result of the DSS, two new techniques needed to be developed.

**Developed Techniques** The first technique is a method to estimate the dynamic response to pedal forces of the ankle-foot complex, while it is actively engaged in a carfollowing task. Existing literature uses classical tasks such as 'maintain position', during which the dynamic response to perturbations is estimated as an admittance. The admittance is a non-parametric frequency response function (FRF) that describes the

response of the rotations that result from the pedal torques. An external torque perturbation at the foot is necessary to reliably estimate the admittance through closed-loop identification techniques. The new technique consists of a special perturbation design: the torque perturbations contain power only at the frequencies where the lead vehicle speed perturbation does not contain power and vice versa. The frequency separation of the two perturbation signals allows the estimation of the admittance while car following, and simultaneously the estimation of the dynamic response to lead vehicle velocity perturbations. The technique results in two descriptions of driver control behaviour: one of motion control and one of car following. The power of the torque perturbations was much smaller than those of the haptic feedback, and was shown to have no significant effect on car-following behaviour.

The second technique consists of a new driver model that, in addition to a visual control part, contains a spinal neuromusculoskeletal part. The spinal part was described with several physiological parameters, including intrinsic muscle visco-elasticity due to co-contraction, reflexive feedback by Golgi tendon organs (GTO's) and muscle spindles, neural time delays and the total inertia of the moving parts. The visual part was modeled as a simple PD controller with time-delays.

The parameters of this detailed driver model were estimated by a fit to the FRFs obtained with the new admittance estimation technique, and the entire model was validated on experimental data in the time and frequency domain.

**Goal** The goal of this chapter is to discuss the combined results and conclusions from all chapters of this thesis, and to view them in light of findings from other researchers in the project and available literature. The limitations of the used approach are discussed, and recommendations for improvements will be given as well as how to use these analysis results in the synthesis of the final design. The chapter will finish with some predictions of the possible use of haptic interfaces in cars.

### 8.2 Results and Conclusions

When all results and conclusion of this thesis are recapitulated, seven main statements can be made concerning the impact of the driver support system on car-following. They are stated and discussed in the following paragraphs.

# 8.2.1 Driver's physical control effort decreases when the DSS is active

The amount of effort that drivers spent on maintaining a certain car-following performance was described by various metrics, all of which decreased when the DSS was active.

The first metric is the standard deviation of gas pedal displacements, which was shown to decrease significantly (Chapter 5 and Chapter 7), indicating that drivers changed their gas pedal depression less often and with smaller amplitudes.

The second metric is a frequency-domain metric, obtained through cybernetic identification: the frequency response function (FRF) of the total controller (combining driver and pedal). The FRF quantifies the estimated total dynamic response of pedal depression (output) to changes in relative velocity (input). It was shown to decrease in Chapters 5 and 7, indicating reduced pedal activity. The FRF decreased mainly at relatively low frequencies (below 0.1 Hz) when following a lead vehicle at a THW of 1, whose speed was perturbed with high frequencies (uniform power until 0.5 Hz, see Chapter 5). It was shown to decrease mainly at high frequencies (larger than 0.1 Hz) while following at a THW of 0.5 Hz a vehicle whose velocity was perturbed with lower frequencies (see Chapter 7). The latter situation was more critical and required a tight high-frequent response, in which the DSS aided the drivers.

The third metric was used in Chapter 5: the electromyographic (EMG) activity of all relevant lower leg muscles. For all muscles the EMG activity decreased, meaning that less energy was spent during a trial to realize changes in pedal deviations.

All findings support the same conclusion: drivers displayed less control effort when the DSS was active. This was also found in other studies (see Mulder, 2007), where it was suggested that without the DSS, drivers tend to overshoot in accelerating or decelerating, for which they need to compensate again in the next seconds. Apparently, most drivers did not have a good grasp of the longitudinal vehicle dynamics (some of the effect might be the result of the lack of motion cues in the simulators). The haptic feedback from the DSS caused drivers to display less of this 'bang-bang' control behaviour. The DSS allows for a better coupling between perception and action, which is supported by the fact that with the DSS the pedal responses contained less noise (Chapter 5).

The stiffness feedback algorithm is likely to be the main cause for this beneficial effect: in a hazardous situation the pedal stiffness will be high, resulting in increased difficulty to fully depress the pedal, and immediate and salient information that the driver is doing the wrong control action. Therefore, the beneficial influence on control effort is expected to be less with a force feedback algorithm.

# 8.2.2 Driver's car-following performance increases or remains similar with the DSS

The standard deviations of several time-domain signals were used as metrics to describe safety performance and task performance in car following. The signals to describe task performance were the standard deviations of distance-related metrics: relative position  $(x_{rel})$  and time headway (THW). The metrics for safety performance were the standard deviations of velocity-related signals, relative velocity  $(v_{rel})$  and the inverse of time-to-contact (iTTC). Even though the control effort decreased, the DSS never had an adverse effect on the safety and task performance metrics. Moreover, for safety performance metrics a beneficial effect was measured: for the experimental conditions in Chapters 5-6 the standard deviations of  $v_{rel}$  and iTTC, for the conditions in Chapter 7 only  $v_{rel}$ . Frequency domain metrics showed a similar result (Chapter 7): the performance FRF (with input  $v_{lead}$  and output  $v_{rel}$ ) was lower, indicating a reduced impact of the lead vehicle velocity on the relative velocity. Apparently, the DSS enabled drivers to

better control potentially hazardous changes in relative velocity to zero.

The beneficial effect on safety performance (velocity-related measures) is expected to be due to the mapping from the DSS: a mapping that related pedal stiffness to changes in iTTC, which were furthermore weighed by THW (stronger cues at close following distances). By keeping the pedal force constant drivers could easily minimize the impact of lead vehicle perturbations on changes in  $v_{rel}$  and iTTC.

The mapping also suggests that the beneficial effect of the DSS is expected to be larger at close following distance than at large ones, which is supported by other experiments (Mulder et al., 2005b). At larger following distances the haptic feedback is less salient, and additionally drivers can accept larger variations in iTTC and  $v_{rel}$ , resulting in a reduced need for control.

Increased criticality did not change this conclusion. It was shown that the response to sudden hard braking of the lead vehicle was not influenced by the haptic DSS (Chapter 7). The relatively large feedback force resulting from the braking vehicle did not provoke a 'kick-back' reflex (depressing the gas pedal when it should be released). This corresponds to the fact that the continuous DSS provokes a force task, where the whole neuromuscular system is set to give way to forces instead of resisting them. An improperly designed DSS would not evoke a force task, and could therefore be susceptible to an unwanted reflexive 'kick-backt' in the same situation.

## 8.2.3 Haptic feedback can temporarily replace visual feedback

The continuous haptic feedback provides drivers with an additional channel for maintaining situation awareness, supplementing the visual feedback. The mentioned benefits of the DSS were obtained while drivers were already paying visual attention. The haptic feedback was expected to contribute to safety performance especially in situations where visual attention was (temporarily) absent. This was experimentally tested using an extreme form of visual inattention: simply offering no visual information during the whole trial (Chapters 5 and 6).

Without the DSS, drivers now had no feedback of the separation states, and no trials could be completed: subjects usually crashed or sometimes lagged behind the lead vehicle at increasing distances. However, when aided by the DSS drivers were able to perform the car-following task within reasonable boundaries for the entire trial duration ( $\pm 80$  seconds); thereby proving the saliency of the haptic information.

Still, most subjects showed increased drift in the THW compared to driving with visual feedback. This can be explained by the fact that the DSS did not communicate THW directly: it was designed to convey changes in iTTC, which were scaled by the THW. Giving way to such haptic feedback results in decreased changes in  $v_{rel}$  and iTTC, reducing the role of visual feedback to choosing the desired separation (THW). This was also shown by the effect of the DSS on estimated gains of the visual controller: the derivative gains decreased most when the DSS was used, indicating that most of the velocity-related control actions were done on a spinal level, leaving the proportional actions (related to distance) for visual control.

Another interesting fact is that when drift occurred, it was usually away from the lead ve-

hicle, which is beneficial, but also logical: at close distances the changes in lead vehicle velocity are felt very well, but at larger distances the information becomes less salient, reducing the (need for) control.

These results also indicate that when a control action is required during a moment of visual inattention, haptic feedback can temporarily replace the visual feedback loop. In such a situation the safety performance is expected to be improved substantially. The DSS will not only redirect visual attention back to the car-following situation, but also allows immediate and adequate response, even before the visual loop is closed again, resulting in less severe consequences of a critical situation. This was shown by driving simulator evaluation studies (not published yet) at another university that participated in the Nissan project.

It is not expected that the haptic feedback loop will inadvertently increase visual inattention: car-following with only haptic information required concentration, and informal interviews revealed that drivers were slightly uneasy when visual feedback was absent for such a prolonged time: they preferred to see what they were doing.

### 8.2.4 The DSS evokes a force task

Normally, when drivers perceive a change in separation they may adjust their pedal position (a position task) in order to maintain a safe separation. In case of the designed haptic DSS, the pedal stiffness – and therefore the pedal force – is changed as a function of the separation. The DSS was hypothesized to change the driver's position task into a force task: by continuously keeping the total pedal force constant, the separation is kept constant.

A force task strategy can be shown by means of the estimated endpoint admittance (a dynamic measure of the amount of displacement due to a force). As discussed in Chapter 1, humans can adapt their admittance by changing muscle activity and reflexive activity. Test subjects were shown to adapt their admittance during tasks commonly used in literature (dubbed 'classical tasks'): the largest admittance was found during force tasks, followed by the relax task; the position task entailed the smallest admittance.

Through the novel techniques described in Chapter 5, the admittance could also be estimated while car following. It was shown that the DSS evoked an increase in the admittance compared to unassisted driving, and resembled a classical force task. This increased admittance signifies an increased tendency to give way to the pedal force, and can be viewed as a sign that drivers follow the advice of the haptic information. If a decreased admittance would have been found, it would have meant that the drivers resisted the feedback forces: a sign of distrust.

Essentially, the DSS simplified the car-following task, a more simple task: keeping the pedal force constant, by giving way to the feedback forces. Thereby it reduced the influence of an imperfect internal model of the dynamics of the car-following task, which explains why subjects reported the system to be comfortable and easy to use. This is supported by the fact that a better coupling between perception and action was found, that resulted in a reduced control effort to reach the same performance.

# 8.2.5 Golgi Tendon Organ reflex is a main contributor to admittance adaptation

It is difficult to separate the individual contributions of reflexes and muscle co-contractions to motion control. Their combined effect can only be separated by either eliminating mechanisms and see what remains (decerebration in cats, or using medicines that inhibit reflexive activity) or by a modeling approach. Chapter 6 describes how a validated, physiologically-based model was be used to identify the separate contributions of the Golgi tendon organ (GTO) reflex, the muscle spindle reflex, and muscle co-contractions. The force feedback gain of the GTO reflex was consistently and accurately estimated. The increased admittance during haptic feedback was mainly the result of an increased GTO gain, combined with reduced muscle contraction (which was supported by the reduced EMG activity).

The GTO reflex was shown to have a major contribution to the endpoint admittance, more so than the muscle spindle reflex (commonly regarded as the most important reflexive pathway). For example, during the classical position task – when trying to maximally resist forces – the GTO gain even changed sign, thereby contributing to a decreased admittance. The role of GTO as an excitory pathway was previously predicted (Prochaska et al., 1997a) in literature, but never supported by experiments and detailed modeling.

# 8.2.6 The DSS allows control actions to be done partly on a spinal level

The fact that the reflexive contribution to driver's response could be estimated (Chapter 6), provided support for another hypothesis: that the haptic DSS allows drivers to use their fast reflexes while car-following. The DSS causes a shift in the control strategies of drivers: a larger part of the control actions arise from spinal control, and a smaller part through visual feedback.

Chapter 5 already provided qualitative support for the hypothesis. The total controller FRF – consisting of both visual and spinal control actions – was equal or even smaller (see also Mulder (2007)), but the admittance (describing only spinal contributions) was larger. This implies a decreased contribution of visual control actions.

The parameterized model results of Chapter 6 show this effect quantitatively. On the one hand, increased GTO activity and reduced muscle contractions were estimated, explaining the increased admittance. On the other hand, smaller visual gains of the PD controller were estimated. Apparently, the DSS provokes behaviour that favours reflexes over visual feedback to perform the car-following task.

The analysis also explains the reduced time-delay during haptic feedback that was found using a cross-over analysis (Mulder et al., 2005b): response with spinal reflexes is substantially faster than response to visual information (40 milliseconds and 200-500 milliseconds, respectively).

118 Chapter 8

## 8.2.7 The design of the DSS is essential for the measured benefits

The found beneficial results strongly depend on the design characteristics of the final prototype. The most important choice has been to use continuous feedback instead of binary warnings (e.g., vibrations or transient forces). Binary warnings do not provide continuous haptic information, and will therefore not induce drivers to increase their admittance. It is expected that binary haptic feedback will not yield the benefits of the fast reflexive contributions to gas pedal control (i.e., decreased control activity, and faster response to changes in separation).

Although the detailed identification methods described in Chapters 5 and 6 were not used to investigate other feedback algorithms, the choice for a stiffness feedback algorithm based on THW and TTC information is thought to have been crucial for the found results. In other research in the project (Mulder, 2007) additional feedback algorithms were investigated: stiffness feedback based on changes in THW and force feedback based on changes in THW and TTC. The additional benefit of stiffness feedback is that drivers immediately and strongly felt the inappropriateness of accelerating in a hazardous situation, thereby contributing to reduced pedal depressions. Using TTC introduces relative velocity information in the haptic feedback, effectively providing derivative information to the separation control, thereby allowing for improved control. The final prototype combined the two benefits: increasing pedal stiffness increased as TTC became more critical, and this increase was further exaggerated at small THWs. This final algorithm yielded the best results in terms of reduced control effort, increased safety performance, and reduced overall time delay (Mulder, 2007).

Another contribution to the final prototype design was achieved with the results gained from the force perception experiments (Chapter 3). They contributed to the scaling of the stiffness, to ensure proper transfer of haptic information. Note that feedback forces that are below the conscious perception threshold may still cause pedal deviations, either as a result from passive properties or through subconscious reflexive mechanisms. Footwear reduced the effectiveness of conscious haptic perception: socks were found to provide the lowest perception limits. All experiments were done while subjects wore their socks, however, similar DSS benefits were found in experiments where drivers wore their own shoes (Mulder et al., 2005b).

The experiments were all done with on actuated gas pedal, which behaved like a standard gas pedal when no haptic feedback was present. Results from Chapter 4 show that current passive gas pedal characteristics are not optimized for minimal muscle activity. When relaxed, passive properties of the ankle-foot complex cause the gas pedal to be pressed down to  $\pm 50\%$ , while car-following at highways requires a pedal depression of only  $\pm 25\%$ . Consequently, muscle activity is needed to pull the foot up (explaining why cramp in the shin muscle occurs after a long drive). A heavier gas pedal would compensate the foot's weight at a lower pedal depression level, resulting in less muscle activity at highway conditions. This effect is thought to be partly responsible for the reduced EMG activity found while car-following with DSS: the continuous feedback increased the average pedal force.

#### 8.2.8 Summarized Conclusions

The conclusions can be summarized as follows: the additional continuous haptic feed-back loop allows useful control behaviour at spinal level, thereby reducing the need to respond to all perturbations through visual feedback. This effect allows drivers to realize the same, or an even better, car-following performance with reduced control effort.

## 8.3 Limitations and Recommendations

# 8.3.1 Analysis Limitations: Used System Identification Techniques

The cybernetic approach is based on system identification techniques that can only be applied to linear time-invariant systems. Through careful experimental design, behaviour was evoked around a constant operating point, behaviour that was more-or-less constant during the experiment trial. FRF's of car-following behaviour and spinal motion control behaviour were estimated with high coherences, confirming that the driver indeed behaved linearly, and justifying the application of the techniques.

However, these linear techniques cannot cope with higher-level aspects of driver behaviour such as inattention, planning, motivation, or preferences. Such aspects result in non-linear, time-variant control actions, that with the employed techniques are all regarded as noise. Whether the noise originates from a moment of inattention or a general lack of motivation to respond cannot be learned from the used techniques. However, when a low amount of noise is present, it is a clear indication that non-linear effects are negligible (which was the case during the experiments described in this thesis).

Behaviour during sudden emergency actions is not well-suited to the used techniques for similar reasons. For example, the fast shift from steady-state control to maximal braking, cannot be understood well with the current models.

More advanced (non-linear) time domain analyses and modeling are necessary to address such issues, for example the relatively new technique of wavelet analysis.

# 8.3.2 Analysis Limitations: Used Experimental Conditions

The measured impact of DSS on driver behaviour depends on a variety of conditions, such as the driving simulator fidelity, the frequency and amplitude of used perturbations, the operating point (average velocity and mean THW) and the task instruction. They are discussed in the following paragraphs.

**Simplified driving simulator** The research assumed that the simplified driving simulator evoked realistic car-following behaviour. The absence of a steering wheel, a brake pedal and high-fidelity visual, audio and motion cues, did not cause statistically significant differences in the performance and workload metrics that were obtained from the same subjects during the same conditions in the more realistic driving simulator at Aerospace Engineering (Mulder, 2007). Apparently the behaviour was dominated by gas pedal control during visual and haptic feedback; exactly what the simulator was built to study.

The lack of motion feedback in the driving simulations may have been the cause of the 'bang-bang'-like gas-pedal control behaviour during unsupported driving mentioned earlier. In reality drivers may very well mitigate their accelerations for reasons of comfort.

**Lead vehicle speed profile** The lead vehicle speed profile used in Chapters 5 and 6 provokes linear car following behaviour. The signal was designed to induce maximal effort and therefore contained uniformly distributed power up 0.5 Hz, whereas during real life car-following, the power already drops steadily at lower frequencies. Without braking the drivers could not match the designed speed profile, but at the operating point (THW=1 [s]) the separation to the lead vehicle was large enough that braking was not necessary to prevent a crash. Driver response to the speed profile may therefore be characterized by an exaggerated response to high-frequent velocity changes, and a diminished need for low-frequent control actions necessary to prevent a crash. In real traffic, most drivers would probably overtake a lead vehicle accelerating and decelerating like this, or would keep some extra distance.

In a subsequent study, (see Chapter 7 for details) the speed profile was designed to better reflect average highway traffic (it contained power until 0.3 Hz and the velocity amplitudes were scaled so that the speed profile could be better matched by the driver without braking) and also to cause more hazardous situations that require low-frequent corrective actions.

The effect of the frequency and amplitude of lead vehicle perturbation was found to be substantial, as was established for exactly the same subjects in the realistic driving simulator at Aerospace Engineering (see Mulder et al., 2005b).

Note that in all cases, the lead vehicle speed profile was unpredictable, thereby excluding effects of anticipation. In reality, drivers are likely able to better anticipate the changes in lead vehicle speed, by previewing road and traffic conditions.

Operating point and task instruction Two other factors that influence car-following behaviour are the operating point and the task instruction. All car-following studies by DUT were done at an average velocity of 100 km/h, a common average highway speed in the United States and Europe. The effects of average velocity were not investigated. The influence of different THW separation on car-following behaviour was investigated in simulator experiments (Mulder et al., 2005b), and found to be highly significant. At a THW of 0.5 seconds the DSS entailed increased beneficial effect on safety and control effort, compared to a THW of 1 or 1.5 seconds. This can be explained by the fact that at larger THWs the feedback forces are smaller, which leads to reduced haptic perception of the changes in separation (analogue to the reduced visual perception). Additionally, there is less need for control actions at such a large distance. The two effects contribute to more time-variant behaviour and reduced benefits of the DSS at larger THWs.

The task instruction for subjects who participated in the experiments was to maintain a THW of 1 second as well as possible. In between trials the correct THW was shown to recalibrate the subjects. The task instruction ensured drivers remained in the operating point, so that the application of linear cybernetic analyses was valid. However, drift in THW may occur in reality, especially in case of inattention.

# 8.3.3 Application Limitations: Operational domain

The proposed haptic feedback systems was designed for highways, and the main benefits are for situations with relatively low-frequent changes in separation. By increasing the safety performance during these conditions, the chance of a critical situation is reduced. If one occurs regardless, it was shown that the DSS did not result in increased safety (Chapter 7). Other systems might be better suited to assist the driver in such critical situations, perhaps automation when it is really clear what the correct evasive actions are.

In that sense, the operational domain (longitudinal highway situations of low and medium criticality) compares well to that of cruise control and ACC, and the DSS will be a competitor to these systems in its current design. Since both cruise control and ACC are based on the idea of relinquishing control of the gas pedal, and the DSS is based on controlling as much situations as possible with the gas pedal, additional research is needed when the combination of both types of systems is desired.

## 8.3.4 Recommendations: Improve Analysis Cycle

#### Improve and Extend the Identification Techniques

The used identification techniques might be enhanced and further developed. In previous research (Schouten, 2004) the reflexive impedance (the FRF with input position, and output EMG activity) was used to improve the parameter identification. In the current study the EMG proved to be too noisy to be successfully used, but better EMG measurement techniques might allow for a more reliable parameter estimation.

As mentioned earlier, identification techniques that do not assume time-invariant linear behaviour (e.g., Kirsch and Kearney (1997)) could be applied to analyze the more complex aspects of driver behaviour. Such techniques will open the scope of experimental situations that can be analyzed.

Yet even without such (possible) improvements, the developed techniques have led to novel insights into human motion control, which may be applied to different research areas. Especially the found role of GTO feedback on the dynamics of the ankle-foot complex (Chapter 6) is expected to have consequences in the field of neuromuscular study. In most motion control studies the GTO reflex is neglected, and reflexive adaptations in the control dynamics are attributed solely to the muscle spindles, which may not always be correct. Future studies need to take this into account, and previous studies reassessed with respect to their conclusions about muscle spindles.

Furthermore, the new task-centered approach and frequency-separation of perturbations may be applied in new experiments, on other joints or for other tasks. The ability of the techniques to quantify spinal control actions and visual control actions while the subject is engaged in a daily-life control task, will surely lead to a better understanding of the human motion control system.

#### Improve and Extend the Driver Model

The model used relative velocity and distance as relevant separation states for visual feedback. However, drivers do not perceive the world in newtonian variables, but in terms of looming, visual angles, optical flow and Weber ratios. Available knowledge on visual perception was not included in the model and might provide a better description and therefore better fits.

An additional issue of the current driver model is the lack of a feedback loop about the average velocity of the lead vehicle. This is not a problem when explaining behaviour around a fixed operating point as is the case in the current study. However, when different speeds and THWs are traversed the model will not predict low-frequent driver behaviour well. A simple feedback loop that describes how (with what gain and timedelay) drivers match the average speed of a lead vehicle will suffice. The input to the driver should be the error between estimated average velocity of the lead vehicle compared to that of the own car (see Boer et al., 2005).

## 8.3.5 Recommendations: Use the Analysis to Improve the DSS

Based on the results of this thesis, that of Mark Mulder (Mulder, 2007) and the work of others in the research project it can be concluded that the concept of haptic driver support system is very promising. The designed prototype yields beneficial results, even though it may not yet be the optimal system. The knowledge gained from the analysis described in this thesis can be used to further optimize the design. Criterions to which the system may be optimized could include safety performance metrics, control effort, or the admittance. The developed driver model is expected to greatly facilitate the optimization.

#### Improve Passive Gas Pedal Design

Based on the experimental findings in Chapter 4, the gas pedal can be optimized to minimize muscle activation during car-following, by increasing the passive pedal characteristics to match the weight of the foot at pedal depressions of  $\pm 25\%$ . Such a pedal will result in decreased muscle activity, thereby reducing fatigue, increasing comfort and entailing a larger admittance, which will increase the effectiveness of the haptic feedback.

### Improve Haptic Feedback Algorithm

Two other feedback algorithms were tested in related research (Mulder, 2007), and both did not result in the overall benefits associated with the prototype DSS (reduced control effort to realize the same performance). These – and other – haptic feedback algorithms may be evaluated with respect to the admittance that evoke: a larger admittance means that the driver responds better to the haptic feedback. If haptic feedback is not designed well, the admittance will be lower. In that the case the visual and reflexive parameters are not expected to change substantially: the benefits of tapping into the spinal reflexes

will disappear. Optimizing the DSS for maximal admittance and GTO gains is expected to lead to the best DSS.

### **Improve Nature of Haptic Information**

Another place where further optimization could be valuable is in the translation from hazard level to haptics. The found stiffness feedback concept has greatly increased the beneficial effects of the DSS, but perhaps mappings can be found that further improve the DSS. Options could include other tunings of the stiffness and force to the hazard; different magnitudes of the haptic information; or even a non-linear increase of the pedal damping, only in the way of pedal depression to better inform about a dangerous situation, while further discouraging acceleration in such a case.

#### **Further DSS Evaluation**

The effect of the THW operating point, task instruction, lead vehicle speed profile and average speed on overall car-following behaviour has been investigated to some degree, but not at the level of spinal and visual parameters. The developed driver model may be used to predict driver response. Additional experiments could be used to validate these predictions, leading to more insight concerning the impact of the DSS on spinal and visual contributions to car-following behaviour in different conditions.

More experiments concerning driving distraction are also necessary. In Chapters 5 and 6, the effect of driver distraction was studied by means of a prolonged period of visual occlusion, with subjects receiving only haptic feedback. This method is excellent for investigating the characteristics of the information transfer through the DSS, but provides a purely visual distraction: drivers were still focusing on the car-following task, but through the haptic modality instead of the visual.

The driver can also be distracted cognitively, for example by being engaged in a mobile phone conversation. The effect of DSS on this kind of distraction remains largely uninvestigated, although Mulder (Mulder, 2007) describes one experiment, where the DSS did not significantly improve driver's car- following behaviour during cognitive distraction. Finally, extensive evaluations (with a large amount of subjects and a variety of traffic situations) were not done for the developed prototype. Long term effects such as fatigue, nuisance, risk homeostasis<sup>1</sup> and driver acceptance need to be studied in simulators and on test tracks before the designed system could be introduced on the market.

# 8.4 Future Directions

Continuous haptic feedback can also be used to support lateral driving tasks such as lane-keeping and curve negotiation. The same design cycle can be applied that was used in this thesis to ensure an in-depth understanding of the impact of the system on driver behaviour, with an emphasis on neuromuscular dynamics. Additionally, it may be combined with the haptic gas pedal in order to support situations where both lateral

<sup>&</sup>lt;sup>1</sup>The effect that improving safety leads to more reckless driving, finally resulting in the same hazards

and longitudinal control are required: entering sharp curves, overtaking and evasive manoevres.

In a world of increasing traffic density and in-vehicle distractions, the prevailing tendency seems to be to automate driving tasks more and more. However, some drivers will prefer to remain in control of their car, and responsibly enjoy driving. Continuous haptic feedback on the gas pedal is a promising alternative, both for them and for society.

# References

- Abbink DA, van der Helm FCT, Boer ER (2004). Admittance Measurements of the Foot during 'Maintain Position' and 'Relax' Tasks on a Gas Pedal. Proceedings of the IEEE International Conference on Systems, Man, and Cybernetics, Den Haag, the Netherlands, October 2004
- Abbink DA, van der Helm FCT (2004b). Force Perception Measurements at the Foot. Proceedings of the IEEE International Conference on Systems, Man, and Cybernetics, Den Haag, the Netherlands, October 2004
- Abbink DA, Mulder M, Van der Helm FCT, Mulder M, Boer ER (submitted). Measuring the effect of Haptic Feedback on Neuromuscular Control and Car-Following Behaviour. Biological Cybernetics (submitted)
- Abbink DA, Mulder M, Van der Helm FCT, Mulder M, Boer ER (submitted). Modeling the effect of Haptic Feedback on Neuromuscular Control and Car-Following Behaviour. Biological Cybernetics (submitted)
- Agarwal GC, Gottlieb CL (1977b). Compliance of the human ankle joint. Journal of Biomechanical Engineering 1977b; 99:166-170
- Arampatzis A, Karamanidis K, Stafilidis S, Morey-Klapsing G, DeMonte G, Brüggemann G (2006). Effect of different ankle- and knee-joint positions on gastrocnemius medialis fascicle length and EMG activity during isometric plantar flexion. Journal of Biomechanics.
- Bengtsson J, Johansson R, Sjogren A (2001). Modeling of Drivers Longitudinal Behavior. IEEE/ASME International Conference on Advanced Intelligent Mechatronics Proceedings 8-12 July 2001, Como, Italy.
- Billing CE, Woods DD (1994). Concerns about Adaptive Automation in Aviation Systems. Human Performance in Automated Systems: Current Research and Trends, pp 264-269, Hillsdale NJ.
- Bliss J, Gilson R, Deaton J (1995). Human probability matching behavior in response to alarms of varying reliability. Ergonomics, 38, 2300-2312.
- Boer ER, Hoedemaeker M (1998). Modeling Driver Behavior with Different Degrees of Automation: A Hierarchical Decision Framework of Interacting Mental Models. In Proceedings if the XVII-th European Annual Conference on Human Decision making and Manual Control, Valenciennes, France, Dec. 14-16

- Boer ER (2000). Car Following from a Driver's Perspective. Transportation Research, Part F: Traffic Psychology and Behaviour, 2, 201-206
- Boer ER, Ward N (2003). Event-Based Driver Performance Assessment. Proceedings of the Second International Driving Symposium on Human Factors in Driver Assessment, Training and Vehicle Design.
- Boer ER, Ward N, Manser M, Yamamura T, Kuge N (2005). Driver Performance Assessment with a Car Following Model. Proceedings of the Third International Driving Symposium on Human Factors in Driver Assessment, Training and Vehicle Design.
- Bobet J, Norman RW (1990). Least-squares identification of the dynamic relation between the electromyogram and joint moment. J Biomech 23:1275-1276.
- Brackstone M, McDonald M (1999). Car-Following: A Historical Review. Transportation Research F, Vol.2, No.4, pp. 181-196.
- Brackstone M, McDonald M (1999). What is the answer? And come to that, what are the questions? Transportation Research F, Vol.2, No.4, pp. 221-224
- Breznitz S (1983). Cry Wolf: the psychology of false alarms. Hillsdale, NJ: Erlbaum.
- Cathers I, O'Dwyer N, Neilson P (1999). Dependance of stretch reflexes on amplitude and bandwidth of stretch in human wrist muscle. Experimental Brain Research 129:278-287.
- Carsten OMJ, Nilsson L (2001). Safety assessment of Driver Assistance Systems. EJTIR, 1, no.3, pp 225-243.
- Commission of European Communities (2001). European transport policy for 2010, time to decide.
  - (http://ec.europa.eu/transport/roadsafety/index en.htm)
- De Vlugt E, Schouten AC, Van der Helm FCT (2003a). Closed-loop multivariable system identification for the characterization of the dynamic arm compliance using continuous force disturbances: a model study. Journal of Neuroscience Methods 122:123-140.
- De Vlugt E (2004). Identification of Spinal Reflexes. PhD thesis, Delft University of Technology. Delft University Press.
- De Vlugt E, Van der Helm FCT (2006). Intrinsic and reflexive properties during a multijoint posture task. Accepted in Journal of Neurophysiology.
- Doemges F, Rack PMH (1992a). Changes in the stretch reflex of the human first dorsal interosseous muscle during different tasks. Journal of Physiology 447, 563-573
- Doemges F, Rack PMH (1992b). Task-dependent changes in the response of the human wrist joints to mechanical disturbance. Journal of Physiology 447 pp 575-585.

- Endsley MR, Kiris EO (1994). The Out-of-the-loop performance problem: Impact of Level of Automation and Situation Awareness. Human Performance in Automated Systems: Current Research and Trends, pp 8-14, Hillsdale NJ.
- Fancher P, Ervin R (1998). Adaptive cruise control field operational test. UNMTRI Research Review, 29 (4): 1-17
- Fang X, Pham H, Kobayashi M (2001). PD controller for Car-Following Models based on Real Data. Proceedings of the 1st Human-Centered Transportation Simulation Conference, Iowa City, IA, 2001
- Gibson JJ, Crooks LE (1938) A theoretical field analysis of automobile driving. Journal of Psychology, Vol. 51, No. 3, pp. 453-471.
- Godthelp J, Schumann J (1993). Intelligent Accelerator: an Element of Driver Support. In: Driving future vehicles. Parkes AM, Franzén S (Eds.), pp 265-275. London: Taylor & Francis.
- Hale AR, Stoop J, Hommels J (1990). Human error models as predictors of accident scenarios for designers in road transport systems. Ergonomics, 33, pp 1377-1388.
- Hjälmdahl M, Almqvist S, Várhelyi A (2002). Speed regulation by in-car active accelerator pedal effects on speed and distribution. IATSS Research, Vol. 26(2), pp. 60-67.
- Hoedemaeker M (1999). Driving with intelligent vehicles: driving behaviour with adaptive cruise control and the acceptance by individual drivers. PhD thesis, Delft Technical University. TRAIL Thesis Series 99/6, Delft University Press.
- Janssen W (1995). An extended evaluation of driving a prototype intelligent vehicle. Proceedings 2nd world congres Intelligent Transport Systems, Yokohama. VERTIS, Tokyo. pp 1771-1776.
- Jones LA (1989). Matching forces: Constant Errors and differential Thresholds. Perception, Vol.18, pp 681-687, 1989
- Kandel ER, Schwartz JH, Jessel TM (2000). Principles of neural science, fourth edition. McGraw-Hill, New York, USA.
- Kirsch R, Kearney R (1997). Identification of time-varying stiffness dynamics of the human ankle joint during an imposed movement. Exp Brain Res (1997) 114:71-85
- Knipling RR, Mironer M, Hendricks DL, Tijerina L, Everson J, Allen JC, and Wilson C (1993). Assessment of IVHS countermeasures for collision avoidance: rear-end crashes. National Highway Traffic Safety Administration (NHTSA), U.S. Dept. Transp., Washington, DC, DOTHS-807-995, 1993.
- Lee JD, McGehee DV, Brown TL, Reyes ML (2002). Collision Warning Timing, Driver Distraction, and Driver Response to Imminent Rear-End Collisions in a High-Fidelity Driving Simulator. Human Factors, 44 (2), pp 314-334.

- Lee JD, Hoffman JD, Hayes E (2004). Collision warning design to mitigate driver distraction. In Proceedings of CHI (pp. 65-72): ACM, New York.
- Ljung L. (1999). System Identification Theory for the User. Second edition PTR Prentice Hall: Upper Saddle River, N.J., 1999
- Mademli L, Arampatzis A, Morey-Klapsing G, Brüggemann GP. Effect of ankle joint position and electrode placement on the estimation of the antagonistic moment during maximal plantar flexion. Journal of Electromyography and Kinesiology 2004; Volume 14, Issue 5, 591-597
- McRuer DT, Weir DH, Klein RH (1971). A Pilot-Vehicle Systems Approach to Longitudinal Flight Director Design. Journal of Aircraft, Vol. 8, No. 11, pp 890-897.
- Meyer J, Bitan Y (2002). Why Better Operators Receive Worse Warnings. Human Factors, 44 (3), 343-353.
- Michon JA (1985). A critical view of driver behavior models: what do we know, what should we do? In: Evans L and Schwing R.C. (Eds.) 'Human behavior and traffic safetyt'. New York: Plenum Press. pp 485-524
- Michon JA (1993). Generic Intelligent Driver Support. London: Taylor & Francis.
- Mirbagheri MM, Barbeau H, Kearney RE. Intrinsic and reflex contributions to human ankle stiffness: variation with activation level and position. Experimental Brain Research 2000; 135:423-436.
- Mulder M, Mulder M, van Paassen MM, Kitazaki S, Hijikata S, Boer ER. Car-Following Support with Haptic Gas Pedal Feedback. Proceedings of IFAC HMS Symposium 2004, Georgia, Atlanta, September 7-9.
- Mulder M, Mulder M, van Paassen MM, Kitazaki S, Hijikata S, Boer ER (2004). Reaction— Time Task During Car-Following with an Active Gas Pedal. Proceedings of the IEEE International Conference on Systems, Man, and Cybernetics, Den Haag, the Netherlands, October 2004.
- Mulder M, Mulder M, van Paassen MM, Abbink DA (2005). Identification of Driver Car-Following Behaviour. Proceedings of the IEEE International Conference on Systems, Man, and Cybernetics, Hawaii, USA, October 10-12 2005.
- Mulder M, Mulder M, van Paassen MM, Abbink DA (2005). Effects of Lead Vehicle Speed and Separation Distance on Driver Car-Following Behaviour. Proceedings of the IEEE International Conference on Systems, Man, and Cybernetics, Hawaii, USA, October 10-12 2005.
- Mulder M (2007). Haptic Gas Pedal Feedback for Active Car-Following Support. PhD thesis, Delft University of Technology. Delft University Press.

- Olney SJ, Winter DA (1985). Predictions of knee and ankle moments of force in walking from EMG and kinematic data. J Biomech 18:9-20
- van Paassen, MM (1994). Biophysics in aircraft control. PhD thesis, Delft University of Technology. Delft University Press.
- Pang XD, Tan HZ and Durlach NI (1991). Manual Discrimination of force using active finger motion. Perception and Psychophysics, 49(6), 531-540, 1991
- Paul C, Belotti M, Jezernik S, Curt A (2005). Development of a human neuro-musculo-skeletal model for investigation of spinal cord injury. Biol Cybern (2005) 93:153-170.
- Pintelon R, Schoukens J (2001). System identification: a frequency domain approach. IEEE Press, New York, USA.
- Pritchett AR (2001). Reviewing the Roles of Cockpit Alerting Systems. Human Factors in Aerospace Safety, Vol. 1, No. 1, pp. 5-38, 2001
- Prochaska A, Gillard D, Bennet DJ (1997a). Positive force feedback for control of muscles. J Neurophysiol 73(6):2578-83
- Ranjitkar P, Nakatsuji T, Kawamua A (2005). Car-Following Models: an experiment based benchmarking. Journal of the Eastern Asia Society for Transportation Studies, Vol 6, pp 1582-1596, 2005
- Rasmussen, J. (1983). Skills, rules, knowledge; signals, signs, and symbols, and other distinctions in human performance models. IEEE Transactions on Systems, Man and Cybernetics, 13, 257-266.
- Riley V (1994). A theory of Operator Reliance on Automation. Human Performance in Automated Systems: Current Research and Trends, pp 8-14, Hillsdale NJ.
- Schouten AC (2004). Proprioceptive reflexes and neurological disorders. PhD thesis, Delft University of Technology. Delft University Press.
- SENIAM (Hermens CJ, Freriks B). European Recommendations for Surface ElectroMyoGraphy. Roessingh Research and Development, Enschede, the Netherlands, 1999, ISBN 90-75452-14-4
- Sheridan, TB (1992) Telerobotics, automation and human supervisory control. Cambridge, MA: MIT Press
- Srinivasan R, Jovanis PP (1997). Effect of in-vehicle route guidance systems on driver workload and choice of vehicle speed: Findings from a driving simulator experiment. In Y.I. Noy (Ed.), Ergonomics and Safety of Intelligent Driver Interfaces (pp. 97-114). Mahwah, NJ: Lawrence Erlbaum Associates.
- Tan HZ, Pang XD and Durlach NI (1992). Manual Resolution of length, force and compliance. In Proceedings of ASME Winter Annual Meeting: Advances in Robotics, Mechatronics and Haptic Interfaces, volume 42, pages 13-18, 1992

- Tan HZ, Srinivisan MA, Eberman B, Cheng B (1994). Human factors for the design of force-reflecting haptic interfaces. Dynamic Systems and Control, Vol. 1, Ed: C.J.Rdcliffe, DSC-Vol.55-1, pp. 353-359, ASME, 1994.
- Toft E, Sinkjaer T, Andreassen S, Larsen K. Mechanical and electromyographic responses to stretch of the human ankle extensors. Journal of Neurophysiology 1991; 65:1402-1410.
- Van der Helm FCT, Schouten AC, De Vlugt E, Brouwn GG (2002). Identification of intrinsic and reflexive components of human arm dynamics during postural control. Journal of Neuroscience Methods 119:1-14
- Van Winsum W, Heino A (1996). Choice of time-headway in car-following and the role of time-to-collision information in braking. Ergonomics, Apr;39(4):579-92.
- Várhelyi A (2002). Speed Management via in-car devices: effects, implications, perspectives. Transportation, Vol.29, pp. 237-252. Kluwer Academic Publishers.
- Verwey WB, Alm H, Groeger JA, Jansen WH, Kuiken MJ, Schraagen JM, Schumann J, van Winsum W, Wantorra H (1993). GIDS functions. In: Generic Intelligent Driver Support, Michon JA (Ed.), pp. 113-146. London: Taylor & Francis.
- Wang X, Mick F, Vernet M, Freigneau F (1996). Experimental investigation of the relationship between the sensation and force applied to a pedal. Advances in Applied Ergonomics 1996; 572-575
- West R, Elander J, French D (1992). Decision making, personality and driving style as correlates of individual risk. Contractor Report 309, Transport Research Laboratory, Crowthorne, UK.
- Wickens CD and Hollands JG (2000). Engineering Psychology and Human Performance. Third Edition, Prentice-Hall International.
- de Winter J, van Paassen MM, Mulder M., Abbink DA, Wieringa P (2006). A twodimensional weighting function for a driver assistance system. Proceedings of the IEEE International Conference on Systems, Man, and Cybernetics, 2006.
- de Winter JCF, Mulder M, de Groot S, Wieringa PA. Factor analysis for driving assessment. applied to car following in a simulator. In: Proceedings of the 9th TRAIL congress, Rotterdam, The Netherlands, november 2006, accepted for publication.
- Woods DD (1994) Automation: Apperent Simplicity, Real Complexity. Human Performance in Automated Systems: Current Research and Trends, pp 8-14, Hillsdale NJ.

# **Summary**

Over the last decades, the increase in road mobility has stimulated both governmental organizations and the automotive industry to come up with various measures to reduce the number of traffic accidents and their impact on human lives. A fairly recent direction is that of designing intelligent systems that aim to aid drivers in the execution of their driving tasks. In spring 2002 Nissan Motor Company initiated a three-year research project, with the goal to explore the possibilities of a car-following driver support system based on haptic feedback. A thorough understanding of the neuromuscular properties of the ankle-foot complex while manipulating the gas pedal is important, which is why the BioMechanical Engineering department of Delft University of Technology was asked to participate.

The aim of this thesis is to provide an analysis of the impact of continuous haptic feedback from a haptic driver support system (DSS) on driver behaviour during car following, both at the level of car-following behaviour and at the level of neuromuscular motion control behaviour. The goal was met by experimental, theoretical and modeling studies.

In a theoretical study, the motivation for designing the haptic DSS was argued. There are many issues with existing driver assistance system that aim to aid in car-following: automation systems such as Advanced Cruise Control have been shown to induce unwanted behavioral adaptation (e.g. inattention, riskier lane-changing, complacency) and collision warning systems often result in nuisance. A task analysis showed that current systems do not offer continuous support in assessing the criticality of the separation, nor do they support drivers in their own control of the gas pedal.

These opportunities for support are realized by a support system, which uses haptic feedback applied directly at the gas pedal in order to continuously communicate the criticality of the car-following situation. The driver remains in the direct control loop, avoiding issues with automation. Expected benefits compared to existing systems include: better situation awareness (even during periods of visual inattention) and faster responses (the haptic feedback is available directly at the gas pedal, allowing the use of fast reflexes). It was concluded that such benefits can best be realized through a design that is based on a thorough understanding of neuromuscular response to feedback forces.

One of the design requirements is that the feedback forces should be large enough that drivers can feel them, but not so large that they provoke nuisance or fatigue. No literature was available on force perception at the foot, so experiments were done to determine the effect of amplitude and frequency of force sinusoids. It was found that increasing the frequency of a pedal force stimulus decreased the just noticeable difference, and

footwear was shown to have a substantial impact on the force perception at all frequencies. The measured perception limits were used in the design of the prototype.

A better understanding of muscle use during gas pedal manipulation was attained by analyzing electromyographic activity of relevant muscles, over a range of forces and pedal positions. It was hypothesized that a minimum of activity for all relevant muscles will be found when the pedal force is equal to the weight of the foot, and that co-contraction will not occur when pushing or pulling. The first hypotheses was proved experimentally, but co-contraction was found when the foot's weight needed to be pulled up. This is the case while maintaining a highway speed with most standard gas pedals. It is argued that a higher gas pedal force will lead to less muscle activity during gas pedal manipulation.

The knowledge gained in the previously described studies aided in the design of a prototype of a haptic feedback algorithm. To evaluate the prototype, and to provide data for a neuromuscular analysis, an experiment was conducted in a simplified driving simulator. Subjects (n=10) were required to follow a lead vehicle – with and without the aid of the haptic DSS – at a constant time headway of 1 second, during which the lead vehicle speed was perturbed. The dynamic neuromuscular response to forces was described as an admittance, estimated by applying small torque perturbations to the pedal, separated in the frequency domain from the lead vehicle perturbations. The main hypothesis of the experiment was that the DSS would provoke drivers to adopt a force task, resulting in a larger admittance compared to other tasks; and that drivers would need less control effort to realize the same performance. Time and frequency domain analyses supported these hypotheses, and also showed that the haptic feedback entailed less electromyographic activity. Additionally, it was shown that the haptic feedback was good enough to replace the visual feedback temporarily.

Although the experiment showed a beneficial effect of the DSS on car-following, it remained unclear to what extent visual feedback and reflexive activity contributed to the observed behaviour. To investigate this, a computational linear driver model was developed that contained a neuromusculoskeletal (NMS) part in addition to a visual control part. Model parameters describing a variety of physiological phenomena (e.g., reflexive feedback on force and position, muscle co-contraction, visual PD controller) were quantified on the car-following data obtained in the driving simulator experiment. The parameter fit procedure was repeatable and yielded a validated driver model that predicts car-following metrics, pedal positions and forces accurately (both in time and frequency domain). The parameters showed that drivers gave way to the haptic feedback torques through increased Golgi tendon organ activity and decreased muscle co-contraction; and the visual gains were found to decrease for all subjects. It is concluded that the DSS allows some part of the necessary control actions to be done by spinal reflexes, thereby resulting in faster responses and a reduction of the visual workload of the drivers.

Although the experiment showed that the DSS was beneficial during non-critical carfollowing, its effect on driver response to a more critical situation remained unknown. The high feedback torques might provoke an undesired stretch-reflex, that depresses the gas pedal when it should be released. An experimental study was performed to investigate whether the DSS influences the driver's response to a heavily braking lead

vehicle, as well as the behaviour during a preceding car-following task at a close separation (THW=0.5). It is concluded that drivers benefit from the haptic feedback during the non-critical car-following task. However, when responding to the heavy braking of the lead vehicle haptic feedback does not improve the response, but neither does it degrade it: no undesired stretch-reflex was found.

The research described in this thesis has culminated in a thorough analysis of the effect of haptic feedback on neuromuscular properties and its implications for car-following with a haptic DSS. The analysis contributed to the design of a prototype, its experimental validation in a driving simulator, and a parameterized detailed driver model that captures the impact of the DSS on visual and spinal contributions to car-following control.

The conclusions can be summarized as follows: the developed DSS provides drivers with an additional fast haptic feedback loop that allows useful control behaviour at a spinal level, thereby reducing the need to respond to all changes in separation through visual feedback. As a consequence, the DSS allows drivers to realize the same (or an even better) car-following performance with reduced control effort, and is informative enough to replace visual feedback for short periods.

# Samenvatting

In de laatste decennia heeft de toegenomen mobiliteit op de weg ervoor gezorgd dat zowel de overheid als de voertuigindustrie zich hebben bezig gehouden met de ontwikkeling van maatregelen om het aantal ongelukken te reduceren. Een recente richting daarin is het ontwerpen van intelligente systemen die de bestuurder helpen met het uitvoeren van rij-taken. In het voorjaar van 2002 startte Nissan Motor Company een 3-jarig project, met als doel de mogelijkheden te onderzoeken van een ondersteuningssysteem gebaseerd op haptische feedback. Daarvoor is een goed begrip nodig van neuromusculaire eigenschappen van het voet-enkel complex in interactie met een gaspedaal, en daarom werd de Biomechanische afdeling van de Technische Universiteit Delft bij het project gevraagd.

Het doel van dit proefschrift is om een analyse te geven van de impact van een continu haptisch ondersteuningssysteem (DSS) op het regelgedrag van bestuurders, zowel op het niveau van volggedrag op de snelweg, als op het niveau van neuromusculaire bewegingssturing. Dit doel werd nagestreefd door theoretische, experimentele en model studies.

In een theoretische studie werd de motivatie voor het ontwerp van een haptisch feedback systeem beargumenteerd. Er kleven verschillende nadelen aan de bestaande assistentiesystemen voor volggedrag op de snelweg: automatische systemen zoals de Advanced Cruise Control leiden tot ongewenste aanpassing van gedrag (bv. onoplettendheid, meer van baan wisselen), en waarschuwingssystemen leiden vaak tot irritaties. Een taakanalyse laat zien dat de huidige systemen geen ondersteuning bieden in het continue beoordelen van veranderend gevaar van een volg situatie, en de bestuurder ook niet helpen bij het regelen met het gas pedaal.

Deze ondersteuningsmogelijkheden worden benut door een systeem dat met behulp van continue haptische feedback op het gaspedaal het gevaar van de volgsituatie communiceert. De bestuurder blijft 'in de loopt', zodat de problemen met automatisering worden voorkomen. De verwachte voordelen van het systeem zijn o.a.: betere 'situational awarenesst' (ook tijdens momenten van visuele afleiding) en snellere reacties (de haptische feedback maakt reacties d.m.v. reflexen mogelijk). Zulke voordelen kunnen alleen gerealiseerd worden door een ontwerp dat gebaseerd is op een goed begrip van de neuromusculaire respons op de feedback krachten.

Een van de ontwerpeisen is dat de feedback krachten groot genoeg zijn dat bestuurders er op kunnen reageren, maar niet zo groot dat ze leiden tot vermoeiing en irritatie. Er was geen literatuur beschikbaar over krachtsperceptie van de voet, dus is experiment gedaan dat de invloed van amplitude en frequentie van krachten op de perceptie onderzocht. Een van de resultaten was dat de perceptie beter was voor krachten met een hogere frequentie, en dat schoeisel een forse invloed had op de krachtsperceptie bij alle gemeten frequenties. De gemeten perceptiegrenzen werden gebruikt in het ontwerp van een DSS prototype.

Om het gebruik van spieren tijdens het manipuleren van een gaspedaal te begrijpen, werd een experiment gedaan dat de electromyografische activiteit van relevante spieren bestudeerde over uiteenlopende pedaalkrachten en posities. De hypothese was dat er een minimum van activiteit is als de pedaalkracht overeenkomt met de kracht die de voet in rust uitoefent op het pedaal, en dat er geen co-contractie optreedt wanneer het pedaal wordt ingedrukt of losgelaten. De experimentele data bevestigde de eerste hypothese, maar er werd co-contractie gemeten wanneer het gewicht van de voet moest worden gecompenseerd. Dit is het geval wanneer op een snelweg een vaste snelheid wordt aangehouden. De conclusie was dat een hogere pedaalkracht tot minder spieractiviteit kan leiden.

De kennis die werd opgedaan uit deze studies heeft bijgedragen aan het uiteindelijke ontwerp van een DSS prototype. Om het prototype te evalueren en data te verzamelen voor een gedetailleerde neuromusculaire studie, werd een experiment gedaan in een vereenvoudigde rij-simulator. Proefpersonen moesten een auto volgen op een time-headway van 1 seconde, terwijl de auto continue van snelheid veranderde. Daarbij werd de respons met en zonder de haptische feedback gemeten. De dynamische neuromusculaire respons op krachten werd beschreven als een admittantie, die kon worden bepaald met behulp van een kleine krachtperturbatie. De belangrijkste hypotheses waren dat de DSS zou leiden tot een krachttaak, die terug te zien is een verhoogde admittantie; en dat bestuurders met minder inspanning de zelfde volgprestatie zouden kunnen leveren. Analyses in het tijdsdomein en frequentiedomein bevestigden deze hypotheses, en lieten ook zien dat de DSS tot minder electromyografische activiteit leidde. Bovendien was de haptische feedback goed genoeg om visuele feedback tijdelijk te vervangen.

Hoewel het experiment liet zien dat de DSS een voordelig effect had op volggedrag, bleef het onduidelijk in welke mate visuele en reflexieve stuuracties bijdroegen tot het gemeten gedrag. Om dat te onderzoeken werd er een linear bestuurdersmodel ontwikkeld, dat naast een beschrijving van een visuele regelaar ook een neuromusculair gedeelte bevat. De model parameters beschreven een aantal fysiologische eigenschappen (zoals reflexieve kracht- en positie-feedback, spier co-contractie, visuele PD-regelaar), en werden gekwantificeerd door middel van een fit op de simulatordata. De parameterfit procedure was herhaalbaar en leverde een gevalideerd bestuurdersmodel op dat zowel autovolg gedrag als pedaal posities en krachten voorspelde (zowel in tijddomein als frequentiedomein). De parameters lieten zien dat bestuurders meegaven met de haptische feedback door middel van een vergrote activiteit van de Golgi peesorgaan krachtreflex, en door middel van minder spier (co-)contractie. Ook werden er lagere visuele gains geschat voor alle proefpersonen. De conclusie was dat de DSS het mogelijk maakt om een gedeelte van de stuuracties op spinaal niveau te doen, waar-

door de reactietijd sneller is en de visuele werkbelasting lager is.

Deze studies demonstreerden dat de DSS een positief effect had op het volgen van een auto in een niet-kritieke situatie, maar het effect op de respons van de bestuurder tijdens meer kritieke situaties bleef onbekend. Wellicht kunnen de hoge feedback krachten die optreden in zo'n situatie een ongewenste stretch-reflex veroorzaken, waardoor het pedaal ingetrapt wordt terwijl het losgelaten zou moeten worden. Daarom werd een nieuw experiment gedaan, waarbij het effect van de DSS op de respons van de bestuurder liet zien, zowel tijdens autovolgen op een kleine afstand (THW=0.5 s) als tijdens hard remmen van de voorligger. De conclusie was dat de DSS weer zorgde voor verbetering (zelfde of verbeterde performance-maten bij minder regelinspanning) tijdens het autovolgen. Echter, de respons op de hard remmende voorligger werd niet beter door de DSS, maar ook niet slechter: er werd geen ongewenste rek-reflex gevonden.

Het onderzoek dat dit proefschrift beschrijft heeft geleid tot een gedetailleerde analyse van het effect van haptische feedback op neuromusculaire eigenschappen van de bestuurder, en de implicaties daarvan op volggedrag. De analyse heeft bijgedragen aan het ontwerp van een prototype van de DSS, de experimentele validatie daarvan in een rij-simulator, en een geparameteriseerd bestuurdersmodel dat de impact van de DSS op visuele en spinale contributies aan volggedrag kan beschrijven.

De conclusies kunnen als volgt worden samengevat: het ontwikkelde support systeem verschaft bestuurders een extra haptische terugkoppelbaan, dat het mogelijk maakt om een gedeelte van het regelgedrag op spinaal niveau kan doen in plaats van via visuele terugkoppeling. Als gevolg daarvan maakt de DSS het mogelijk om dezelfde (of zelfs een betere) volgprestatie te leveren met minder regelinspanning. Bovendien is het systeem informatief genoeg om gedurende een korte periode de visuele feedback te vervangen.

# **Dankwoord**

Vier jaar geleden, nee zelfs nog twee jaar geleden, had ik iedereen uitgelachen die had gezegd dat er nu een proefschrift zou liggen met mijn naam op de kaft. Een flink aantal mensen heeft ervoor gezorgd dat deze onwaarschijnlijke gebeurtenis werkelijkheid is geworden, en dat ik er zelfs een beetje trots op ben geworden. Die personen wil ik hier graag speciaal bedanken.

Als eerste, mijn promotor Frans van der Helm. Het is heel simpel: zonder jou was dit proefschrift er nooit geweest. Mijn wetenschappelijke carrière was ongetwijfeld snel geëindigd als je me niet enkele maanden na mijn afstuderen gevraagd had voor een project met Nissan, me terloops reddend van mijn tijdelijke bestaan als pindakaaspotten stapelaar. Je bood me een promotieplek aan, die ik in eerste instantie weigerde: ik had net mijn eerste buitenlandse tour met mijn band gedaan, en wou nu vooral tijd hebben om muziek te maken en op te treden! De vrijheid die je me vervolgens bood om vier dagen in de week te werken en buitenlandse tours te doen wanneer dat zo uitkwam, heeft me overgehaald om het maar eens een jaartje te proberen. De combinatie onderzoeker/muzikant bleek een perfecte te zijn voor me: het jaar vloog voorbij en werd een volgende en een volgende, en na 3 jaar onderzoek was de stap niet zo groot meer om toch maar die promotie te doen... Frans, met je humor, grenzeloze enthousiasme, scherpe kritiek, inlevingsvermogen en het vertrouwen dat je me gaf om op mijn manier te werken, heb je een van de belangrijkste bijdragen geleverd aan het feit dat ik met veel plezier vier jaren op de universiteit heb gewerkt. Bedankt!

Frans en ik waren niet de enige Delftenaren in het Nissan project: we hebben nauw samengewerkt met collega's van Lucht en Ruimtevaart. Verreweg de meeste tijd heb ik doorgebracht met Mark Mulder. Tussen alle flauwe grappen en drinkavondjes door werden we langzaam aan goede vrienden, en mede dankzij jou bleef het project leuk en uitdagend. Yokohama, San Diego, Minnesota, Vancouver, en Budapest zullen nooit meer hetzelfde zijn!

Bij de besprekingen met Frans en Mark waren ook altijd Mark's begeleiders Max Mulder en René van Paassen aanwezig. Beiden hebben een wezenlijk aandeel gehad in de kwaliteit van het geleverde werk. Max, ik wil je graag bedanken voor je stimulerende rol als co-promotor, voor het vele kritische commentaar op dit proefschrift, voor de goede gespreken over alles wat echt belangrijk is in het leven, en voor de vele uren slappe lach in Vancouver. René, je hebt een enorme bijdrage geleverd aan het project, op een manier die kenmerkend voor je is: bescheiden, to-the-point, intelligent, maar ook heel erg hartelijk.

Verder werkten er nog veel meer mensen mee aan dit project: vanuit Nissan Motor Company in Japan (Kitazaki-san, Hijikata-san, Yamamura-san, Doi-san, Akatsu-san, Kuge-san) zonder wiens sponsoring en intellectuele input we dit onderzoek nooit hadden kunnen doen. Ook collega's vanuit diverse universiteiten in USA en Canada hebben meegewerkt aan het totale project, en de psychonautische avonturen met David Wipf en Jonathan Levi in Amsterdam, de kleine roadtrip door het midwesten met Bobbi Seppelt en Mark, en het goede gezelschap van Nic Ward, Mike Manser, Mike Goodrich, Deborah Forster, John Lee en alle andere collega's hebben allemaal bijgedragen aan de goede sfeer en het uiteindelijke goede resultaat.

Dat in deze groep met totaal verschillende karakters, wetenschappelijke achtergrond, taal en cultuur niet alleen zo'n goede sfeer ontstond, maar ook nog eens goed onderzoek werd afgeleverd is in hoge mate te danken aan het onvolprezen leiderschap van Erwin Boer. Ik heb met verbazing gekeken hoe jij onze regeltechnische bevindingen moeiteloos herformuleerde in psychologische termen, en hoe je probleemloos de soms cryptische vragen van Japanse collega's vertaalde. Je kritische vragen, enthousiasme, enorme achtergrondkennis, en vooral de zestienmaal overgeschreven whiteboards hebben een blijvende indruk op me gemaakt.

Alle internationale samenwerking en reizen ten spijt deed ik het meeste werk natuurlijk gewoon op de faculteit Werktuigbouwkunde in Delft. Daar was het goed toeven met mijn Delftse collega's. Sommige verdienen een speciale vermelding hier.

Erwin de Vlugt en Alfred Schouten hebben me tijdens mijn afstuderen begeleid, en zijn ook later altijd beschikbaar geweest voor vragen, advies, feedback of flauwe grappen. Richard van der Linde heeft in het begin veel geholpen aan het project, met name met het realiseren van de meetopstelling. Esther Blom was er altijd om mee te lachen, uit te gaan en thee te drinken, Joost de Winter voor goede discussies en commentaar op papers, Dineke voor persoonlijke en organisatorische ondersteuning, en Magda, Ruben, Sander, Jasper, Erica, Valentina, Dimitra, John, Martijn, Daan, Dirk-Jan, Edward en alle andere collega's waren altijd beschikbaar voor wat afleiding als we weer eens gek werd van dat beeldscherm voor onze neus.

Tijdens mijn werk heb ik ook een aantal studenten begeleid. Vier groepen bachelor studenten hebben experimenten uitgevoerd die te maken hadden met mijn project, en daar was het plezierig mee samenwerken. Het kostte tijd maar sommig onderzoek was goed genoeg om een publicatie op te schrijven (zie o.a. Hoofdstuk 3 en 7).

Ook heb ik Winfred Mugge mogen begeleiden met zijn afstuderen. Je hebt me goed van de straat weten te houden met je vele discussies over het onderzoek, en over de zin van wetenschap, kunst en het leven in zijn algemeen. We hebben samen vele nieuw inzichten verkregen in de taak-afhankelijkheid van de menselijke admittantie, en de rol van het (vaak vergeten maar o zo belangrijke) Golgi peesorgaan. Ik vind het heel leuk dat je na je afstuderen een collega bent geworden: en nu op naar dat Nature artikel! En natuurlijk is ook een woord van dank op zijn plaats voor alle proefpersonen aan de experimenten, die zich lang moesten concentreren om mij van data te voorzien. Bedankt!

Ik had nooit blij kunnen zijn met mijn leventje als onderzoeker als ik niet de tijd had gehad om daarnaast veel bezig te kunnen zijn met de dingen die het leven voor mij de moeite waard maken: vrienden, familie, en natuurlijk muziek maken. In de afgelopen vier jaar heb ik enorm veel plezier gehad met de bands waar ik mee opgetreden, opgenomen en getourd heb: Fettalacrack, Until We Bleed, Fat Chance en natuurlijk Cheesy. Met name met Cheesy heb ik veel meegemaakt, meer dan ik ooit had kunnen dromen: zeven tours door elf landen, CD-opnames, een videoclip op MTV, grote festivals en TV-optredens... Coen, Rick, Wouter, Michel, Ohad, Chicha, Annemieke, Justin, Chiel en alle bands en boekers: bedankt voor alle goede ervaringen! Jammer genoeg komt aan alle goede dingen een eind: afgelopen zomer stopte Cheesy voor mij, maar inmiddels ben ik weer bezig met nieuwe muzikanten. Met Alejandro, Juan-Manuel en Marcel is er voor mij een nieuwe wereld opengegaan met veel inspiratie, goede etentjes en bovenal fantastische muziek. Ik hoop dat we met Cultura Tres daar nog veel meer van kunnen maken!

Een speciaal woord van dank gaat uit naar mijn ouders, zus, Rodrigo, Fix, Wouter en Harry. In een van de moeilijkste periodes van mijn leven hebben jullie me dubbel en dwars gesteund met advies, een luisterend oor, of door simpelweg leuke dingen met me te gaan doen.

En zoals dat gebruikelijk is in een dankwoord: als laatste de belangrijkste persoon. Voor mij is dat mijn Anduska, die het geduld had om van me te houden en de moed om haar thuis op te geven voor ons, en met wie het leven nog leuker is dan het al was.. Nagyon hulye vagyok beléd!

David Abbink Amsterdam, October 2006

# **Curriculum vitae**

#### 19 september 1977

Born in Purmerend, the Netherlands.

#### 1989-1995

Atheneum at college Hageveld in Heemstede.

#### 1995-2002

Master of Science study at Delft University of Technology, faculty of Mechanical Engineering. During one year the studies in Delft were combined with a study in Philosophy at the University of Amsterdam.

Part of the MsC study was a three-month internship with prof. Kirsch at Case Western Reserve University, USA. The final project concerned the effect of position and force tasks on human arm admittance.

#### 2002-2005

Research engineer at Delft University of Technology, faculty of Mechanical Engineering. The work was done in an international team sponsored by Nissan Motor Company. Team members included Nissan Research Center and several universities in USA and Canada. The project concerned the design and evaluation of a continuous haptic driver support system.

In the meantime David pursued another path: that of a drummer in the crossover band Cheesy, recording a full-length album (mastered at Abbey Road, London), appearing in a videoclip on MTV, and performing over a hundred shows in 11 countries.

#### 2005-2006

PhD study at Delft University of Technology, faculty of Mechanical Engineering. The title of the thesis is 'Neuromuscular Analysis of Haptic Gas Pedal Feedback during Car Following'.

#### 2006-present

Research engineer at Delft University of Technology, faculty of Mechanical Engineering. The project concerns a new assignment for Nissan Motor Company.